

Abstract

Murrell, Rachel Nichole. Gene Expression Profiling in Surrogate Tissues to Identify Biomarkers Following Conazole Exposure. (Under the direction of John C. Rockett).

Conazoles are a class ofazole fungicides which are used for agricultural and pharmaceutical applications. This study examined two conazoles that possess a range of reproductive, carcinogenic, and neurodevelopmental effects. Sprague-Dawley rats were dosed daily by oral gavage for 14 days with triadimefon (5 or 115 mg/kg/day) or myclobutanil (10 or 150 mg/kg/day). Relative liver weight increased following high dose triadimefon and myclobutanil exposure. Weight changes were not observed in testes, nor were there significant changes in serum testosterone levels. Microarray analysis of 4,370 genes yielded forty-eight differentially expressed genes in blood. Of these, nine genes were found to be concordant with liver and testis gene expression data.

**Gene Expression Profiling in Surrogate Tissues to Identify Biomarkers Following
Conazole Exposure**

By

Rachel N. Murrell

A thesis submitted to the Graduate Faculty of
North Carolina State University
In partial fulfillment of the
Requirements for the Degree of
Master of Science

Toxicology

Raleigh

2004

APPROVED BY:

Dr. Ernest Hodgson
Chair of Committee

Dr. John C. Rockett

Dr. David J. Dix

DEDICATION

This thesis and all the work that has led up to this finished project are dedicated to my parents, Bill and Cathy Murrell, and Paul Zigas, who have been relentless in their encouragement and support.

PERSONAL BIOGRAPHY

I was born in Wilmington, North Carolina as the eldest of two children to Bill and Cathy Murrell. My early years were spent actively exploring outdoors, capturing small bugs and frogs, which I would observe through mason jars and then release. My love of animals was encouraged by my interactions with the family horses, dogs and cats. I was riding horses with my father by age six months. At age eighteen months my parents got me a pony and my father began leading me all around the pasture. I quickly began competing in horse riding lead line events and won several trophies. I started taking English style horse riding lessons at age three.

In addition to horse riding, I spent time with my father at the family business on tugboats, barges and all around the shipyard. As my school career progressed I excelled at English and History, and while I did well in science, I did not have a strong interest in the subject. Towards the end of high school I began to participate in a science-oriented job, working at the family business, which in addition to tugboats and barges involved environmental response and remediation. I became a certified HAZWOPER technician and worked on several spill remediations in the summer after high school and during the summers in college.

My love of animals and newfound interest in science led me to pursue a degree in Zoology at North Carolina State University. While the material in Zoology was interesting, I came away with the knowledge that I did not have the desire to go to Veterinary or Medical School. I felt I was destined for a different path. A background in life sciences and in environmental response and remediation led me to pursue a career in Toxicology.

I began my toxicological studies in the master of toxicology program. During the summer of 2001 I volunteered in the laboratory of Dr. Robert Smart to gain laboratory experience. I also was a teacher's assistant in biochemistry for the third time; the two previous times being during my

undergraduate studies. By the summer of 2002 I had transferred into the Masters program and had secured a position in the laboratory of Dr. John C. Rockett at the U.S.Environmental Protection Agency (EPA). I participated in reproductive toxicology studies that involved cutting-edge microarray technology and gave me the opportunity to learn many other molecular biology techniques. My experiences at the E.P.A. have equipped me with the skills and knowledge that will help me to succeed in the field of toxicology, be it in academia, industry or government.

ACKNOWLEDGEMENTS

I would like to thank Dr. John C. Rockett for accepting me as a graduate student in his laboratory at the US E.P.A. Dr. Rockett was a driving force in my education in animal work and molecular techniques that are an integral part of the study of Reproductive Toxicology.

I would like to thank Dr. David Dix for serving as a member of my graduate committee. Dr. Dix was an important influence on my work at the US E. P. A. His advice, input and support shaped my project, my research and my thesis.

I would like to thank Judy Schmid for her tremendous contribution to my project. Judy performed the statistical analysis of the microarray data and helped with the analysis of body and organ weights, as well as hormone data. Judy not only performed the analysis, but also explained the process in a clear and logical manner.

I would like to thank several additional people at the US E. P. A. Dr. Hongzu Ren taught me how to prepare the microarrays. Carmen Wood performed the qRT-PCR assays. Debbie Best taught me how to perform T-RIAs. Indira Thillainadarajah helped me to perform the T-RIAs. Dr. Tammy stoker permitted the use of her laboratory and gamma counter for the T-RIAs. Dr. Douglas Tully provided reference RNA and rat liver and testis microarray data for comparison to blood microarray data.

I would also like to thank Dr. Ernest Hodgson, who served as my graduate advisor from my beginning in the Toxicology program at North Carolina State University and then became a member of my committee. Dr. Hodgson's support and encouragement have allowed me to succeed in the toxicology program. My work was supported by the US E.P.A./NCSU Cooperative Training Agreement # CT826512010.

Table of Contents

List of Figures.....	vii
List of Tables.....	viii
Introduction.....	1
Materials and Methods.....	15
Results.....	22
Discussion.....	25
Figures.....	39
Tables.....	56
References.....	86
Appendix.....	97

List of Figures

1. Structures of 1, 2, 4-N substituted azole ring conazoles.....	39
2. Ergosterol biosynthesis.....	40
3. Ergosterol biosynthetic pathway from squalene to ergosterol.....	41
4. Biosynthesis of phytosterols, ergosterol and mammalian sex steroid hormones.....	42
5. Biosynthesis of MAS.....	43
6. Process of sample preparation for microarrays and subsequent analysis.....	44
7. Bioanalyzer results showing gel and graph for analyzed samples.....	45
8. Analysis of covariance of triadimefon and myclobutanil treated male rat body weights	46
9. Analysis of covariance of triadimefon and myclobutanil treated liver in male Sprague-dawley rats.....	47
10. Analysis of covariance of triadimefon and myclobutanil treated left testes in male Sprague-dawley rats.....	48
11. Analysis of covariance of triadimefon and myclobutanil treated right testes in male Sprague-dawley rats.....	49
12. Testosterone Radioimmunoassay Results.....	50
13. Example of Blood RNA Microarray slide.....	51
14. Prenormalization of two hundred fourteen genes for Hi Myc and Hi Tri.....	52
15. Loess normalization of two hundred fourteen genes for Hi Myc and Hi Tri.....	53
16. Quantile normalization of two hundred fourteen genes for Hi Myc and Hi Tri.....	54
17. Biomarkers of myclobutanil, triadimefon and for both conazoles.....	55

List of Tables

1. Multiple conazoles-scientific names, trade names and uses.....	56
2. Differentially expressed genes identified in microarray data that encode enzymes..	59
3. Differentially expressed genes identified in microarray data that encode G protein coupled receptors and G proteins.....	63
4. Differentially expressed genes identified in microarray data that encode proteins involved in nucleic acid binding and that act as transcription factors.....	65
5. Differentially expressed genes identified in microarray data that encode binding and transport proteins.....	66
6. Differentially expressed genes identified in microarray data that encode immune related proteins.....	67
7. Differentially expressed genes identified in microarray data that encode for peptide hormones.....	68
8. Differentially expressed genes identified in microarray data that encode ion channels.....	69
9. Differentially expressed genes identified in microarray data that encode proteins that suppress or promote tumorigenesis.....	70
10. Differentially expressed genes identified in microarray data that encode proteins with various proteins.....	71
11. Genes from microarray data that show significant ($p \leq 0.05$) gene expression change in blood.....	72
12. Genes from microarray data that show significant ($p \leq 0.05$) gene expression change in blood and in liver and testis target tissues.....	77
13. Cytochromes previously identified in blood, liver and testis microarray data following conazole exposure.....	80
14. Genes selected for qRT-PCR.....	81
15. qRT-PCR results.....	82
16. Ten myclobutanil blood biomarkers of conazole effect.....	83
17. Six triadimefon blood biomarkers of conazole effect.....	84
18. Twenty-one conazole blood biomarkers of effect.....	85

INTRODUCTION

The conazoles, a family ofazole derivative fungicides were discovered in the 1960's. They are completely synthetic, and are the most rapidly expanding family of anti-fungal compounds (Fromtling, 1988). The conazoles are fungistatic with a broad spectrum of activity against most yeasts and filamentous fungi (Georgopapadakou et al., 1996).

The conazoles have been proposed for study because they are used extensively in the agricultural and pharmaceutical sectors, resulting in diverse and widespread human exposures. Agriculturally, conazoles are used for fungal control on fruits, vegetables, grains, and seeds. Conazoles are used pharmaceutically for the treatment of candidiasis, cryptococcosis, and coccidiomycosis (see Table 1).

Pharmacology of Conazoles

The conazoles are divided into two classes, imidazoles and triazoles, which have two or three nitrogens in the five-membered azole ring. The imidazoles have a 1, 3 nitrogen substituted azole ring (Georgopapadakou et al., 1996). Myclobutanil and triadimefon, the conazoles selected for this study, are both triazoles with 1, 2, 4 nitrogen substituted azole rings (Figure 1).

Conazole fungicides interact with lanosterol 14 α -demethylase, which is involved in the synthesis of ergosterol from squalene (White et al.1998). Ergosterol is critical for fungi, as it serves as the predominant sterol in fungal plasma membranes. Trace amounts of ergosterol are also necessary for the cells to progress through the cell cycle (White et al. 1998). Ergosterol serves as a bio-regulator of membrane fluidity and asymmetry and consequently of membrane integrity (Ghannoum et al. 1999) (Figures 2 and 3).

Lanosterol 14 α -demethylase catalyzes the oxidative removal of the 14 α -methyl group (C32) of lanosterol and 24-methylene-24, 25-dihydrolanosterol in fungi, lanosterol and 24, 25-

dihydrolanosterol in mammals, and obtusifoliol in plants. Demethylation of substrates proceeds through three monooxygenation steps that do not release intermediates. The methyl group is first converted to alcohol, then aldehyde and in the last step is removed as formic acid. Each step in this process requires one molecule of oxygen and one molecule of NADPH (Rozman et al 1998). Lanosterol 14 α -demethylase is a class II enzyme that requires the FAD/FMN-containing NADPH-cytochrome P450 reductase as a redox partner. This complex sterol 14-demethylation reaction is one of the key steps in sterol biosynthesis, an essential metabolic pathway that produces ergosterol in fungi, phytosterol in plants, and cholesterol in animals (Lamb et al. 1998) (Figure 4).

Lanosterol 14 α - demethylase is a cytochrome P450 (CYP) enzyme that contains a heme moiety in its active site. The conazoles bind to the iron atom of the heme through an unhindered nitrogen, which prevents activation of oxygen that is necessary for the demethylation of lanosterol (White et al 1998). The second nitrogen of the conazoles is also thought to interact with the apoprotein of lanosterol demethylase. The position of this second nitrogen in relation to the apoprotein may determine the differences in specificity of the conazoles for the enzyme (White et al 1998).

Inhibition of lanosterol 14 α -demethylase (CYP 51) leads to depletion of ergosterol and accumulation of sterol precursors including 14 α -methylated sterols (lanosterol, 4, 14-dimethylzymosterol, and 24-methylene-24, 25-dihydrolanosterol) resulting in the formation of a plasma membrane with altered structure and function (Debeljak et al. 2003). Ergosterol depletion and the accumulation of lanosterol and other sterols interfere with the functions of ergosterol as a membrane component; disruption of plasma membrane structure increases vulnerability to more damage and alters the activity of several membrane bound enzymes, like those associated with nutrient transport and chitin synthesis (White et al 1998).

At high concentrations, the conazoles may also interact directly with lipids in the membranes. Clotrimazole and miconazole, which are imidazoles, have a very rapid fungicidal action due to direct membrane damage (Sud et al., 1981). Two additional imidazoles, tioconazole and ketoconazole also cause direct membrane damage. Imidazoles damage fungal membranes by causing very rapid and extensive leakage of ATP. This damage occurs at different concentrations for each imidazole (Ansehn et al., 1984).

Lanosterol 14 α -demethylase belongs to the cytochrome P450 family number 51 and is thus also named CYP51. Because CYP51 was first classified in yeast, it has a nomenclature number that was reserved for fungal P450s. It is the only cytochrome P450 family that is present in all biological kingdoms and is thought to be the ancestor of all other P450 families (Kelly et al. 2001; Nelson et al. 1999; Yoshida et al. 2000; Yoshida et al. 1997). A comparison of rat and yeast CYP51 showed they both possessed the 14 α -demethylase function, supporting orthologous P450s occurring in distinct kingdoms (Aoyama et al. 1996). CYP51 also has a role in meiosis-activating sterols (MAS) in mammalian germ cells (Byskov et al. 1995).

In animals, the CYP51 reaction is part of the pathway leading to the biosynthesis of cholesterol. Cholesterol in turn is the substrate for the production of the sex steroid hormones (Ronis et al., 1994). More specifically, C14 demethylation of lanosterol in animals produces the follicle fluid meiosis-activating sterol (FF-MAS), which is further metabolized to the testis meiosis-activating sterol (T-MAS). If lanosterol is reduced by the sterol δ 24-reductase to 24, 25-dihydrolanosterol prior to demethylation, the resulting metabolites are MAS-412 and MAS-414 (Figure 5). These MAS cholesterol precursors have recently been shown to modulate male and female germ cell development (Zarn et al 2003).

The ability of the conazoles to inhibit the cytochrome P450 enzymes involved in the biosynthesis of steroid hormones in mammalian cells has lead to endocrine-related side effects,

such as depletion of testosterone and glucocorticoids, resulting in gynecomastia and adrenal insufficiency (Georgopapadakou et al 1996; Barret-Bee et al 1988; Hanger et al.1988).

In the liver, conazoles affect the activity and expression of a number of P450s. For example, the pesticide propiconazole induces the activities of CYP1A2, CYP2B1, CYP3A1 and CYP3A2 in rat liver. In mouse liver, propiconazole induces CYP2B10 and CYP3A11. (Sun et al., in press). Triadimefon inhibits aromatase *in vitro* in human placental microsomes (Vinggaard et al., 2000). A study of five imidazole fungicides in human lymphoblastoid cells and human liver microsomes yielded alteration of many cytochrome P450s. Ketoconazole inhibited CYP3A4 and CYP2C9; clotrimazole inhibited CYP3A4; miconazole inhibited CYP2B6, CYP2C19, CYP2D6 and CYP3A4; sulconazole inhibited CYP1A2, CYP2B6, CYP2C19, CYP2C9 and CYP2D6 and tioconazole inhibited CYP1A2, CYP 2C19, CYP2E1 and CYP3A4 (Zhang et al., 2002).

Exposure of rodents to conazole fungicides has resulted in multiple toxic endpoints including carcinogenic, neurological, reproductive, and endocrinological effects. Many of the conazoles are hepatotoxic and hepatocarcinogenic in mice (Hunter et al., unpublished, submitted to WHO by Ciba-Geigy Ltd., Basle, Switzerland 1982). Some conazoles induce thyroid follicular cell tumors in rats and several are hepatotoxic in humans (Loser et al., 1984). These effects may be due to the fact that conazole fungicides affect the activity and expression of a number of cytochrome P450 enzymes. Conazoles can act as both inducers and inhibitors of CYP450s, dependent on the tissue and specific conazole being considered (EPA 2001). Some conazoles have also been developed to selectively inhibit CYP19 aromatase for the treatment of breast and prostate cancer (Millos-Santos et al., 2004; Kelloff et al., 1998).

The widespread use of the conazoles makes them an ideal choice for study because humans have the potential for clinical and environmental exposure. The conazoles that have been chosen for this study were selected based on their availability, interest by regulators, and possible

steroidogenic disruption in the vertebrate system. The two conazoles chosen, triadimefon and myclobutanil, have a range of adverse effects including liver tumors in mice, thyroid tumors in rats, spermatogenic abnormalities, and steroidogenic disruption.

The Joint Food and Agriculture organization/ World Health Organization Meeting on Pesticide Residues (JMPR) evaluated triadimefon in 1981 and 1985 (FAO/WHO, 1982, 1986). An acceptable daily intake for humans of 0-0.3 mg/kg body weight was set based on a NOEL of 2.5 mg/kg and body weight effects and reduced hematopoiesis at greater than or equal to 25 mg/kg established during a two year rat study. A rat reproductive study demonstrated a reduced female/male sex ratio in F₂ at 77 mg/kg and that the female fertility index was one third that of the control group. In a supplementary study, males treated with 77 mg/kg were mated with untreated females. This resulted in a significantly reduced pregnancy rate, but the ratio of pregnant to inseminated females was not affected. The conclusion of the study was that triadimefon impaired the sexual behavior of the male rats and their testosterone level was doubled (FAO/WHO 1982, 1986). A recent study by Goetz et al. (submitted) indicates that the cause of the reduced pregnancy rate appears to be ejaculation failure.

JMPR also evaluated myclobutanil in 1992 (FAO/WHO 1993). An acceptable daily intake for humans of 0-0.03 mg/kg was set based on a NOEL of 2.5 mg/kg in a two-year rat study and many effects on the male reproductive system at greater than or equal to 10 mg/kg. Reduced testis weight, testis atrophy, reduced or absent spermatid production, necrotic epididymis, and atrophy of the prostate were observed with increasing doses (FAO/WHO 1993).

The doses of triadimefon and myclobutanil selected for this study are based on two-year cancer bioassays and multigenerational reproductive experiments. The use of these doses will allow for comparison of blood gene expression profiles with the reproductive and cancer data.

Surrogate Tissue Analysis

Humans worldwide are exposed to wide variety of environmental toxicants on a daily basis. Exposure to such toxicants may be occupational or domestic in nature and can produce acute or chronic effects depending on the specific chemical and exposure scenarios. Furthermore, many compounds are bioaccumulative and have delayed toxicity, which is only detected at the point of clinical manifestation.

Unfortunately, at the present time, exposure to toxicants is usually only assessed once the effects are clinically manifested. However, it is thought that many toxicants may cause changes in gene and protein expression prior to clinical manifestation, which provides a mechanism for early detection of biomarkers of exposure (Rockett 2002). The problem is that it is not feasible to biopsy inaccessible target tissues, like testis, from outwardly healthy individuals for biomarker evaluation. An emerging alternative may be to use surrogate tissue analysis (STA). STA could be used to measure molecular changes as a means to monitor and/or diagnose exposure to environmental toxicants at an early stage of development, when clinical symptoms have not yet manifested (Rockett 2002).

In STA, an accessible tissue takes the place of an inaccessible target tissue. Surrogate “tissue” is a convenient, but somewhat misleading term. Though “tissue” is specified, the term is in fact used broadly to refer to any biologically derived material used to report on events in a specific target tissue. Bodily fluids like urine, blood, saliva, feces, milk, and semen may be categorized as surrogate tissues. Specific cell populations derived from bodily fluids like epithelial cells from milk and urine, buccal cells from saliva, and sperm from semen can also be seen as surrogate tissues. More typical tissues like placenta and hair follicles might also be used as surrogate tissues (Rockett 2002).

STA could provide an effective tool to monitor and diagnose environmental toxicant exposure early in the pathogenesis of disease, thus facilitating more informed policy and risk assessment and allowing intervention at pre-clinical stages of disease (Rockett 2002).

Proof of the Utility of Surrogate Tissue Analysis

STA analysis incorporating gene expression profiling is a new approach to analyzing the impact of pharmaceutical agents and toxicants on molecular events in inaccessible tissues, but the principle of STA is not new. Indeed, a number of published studies have demonstrated that lymphocytes can be used as surrogate tissues. For example, in a study of DNA-carcinogen adduct formation in rats administered polycyclic aromatic hydrocarbons, benzo [a] pyrene DNA adducts in both liver and lung tissue could be predicted by peripheral blood lymphocyte (PBL) DNA adduct levels. These results suggested that PBL adduct-based dosimetry might reflect patterns of adduction in less accessible tissues (Nesnow et al., 1993). In a cross sectional study of thirty-three workers exposed to benzidine and benzidine dyes and fifteen non-exposed controls, exposure status and internal dose of benzidine metabolites were strongly correlated with the levels of specific benzidine-DNA adducts in exfoliated urothelial cells. DNA adduct levels in peripheral white blood cells (WBCs) were evaluated in a subset of eighteen exposed workers and seven controls selected to represent a wide range of adducts in exfoliated urothelial cells. A strong correlation was found between WBC and exfoliated urothelial cell adduct levels among exposed subjects. Additionally, the sum of urinary benzidine, N-acetylbenzidine and N, N'-diacetylbenzidine correlated with the levels of this adduct in both tissues. The results illustrated the relationship between specific carcinogen adduct in a surrogate tissue and in urothelial cells, which are the target for urinary bladder cancer (Zhou et al., 1997).

STA has also been used to study the impact of different environmental exposures, such as radiation. In a study of human exposure to ionizing radiation, human blood from normal healthy donors was obtained and the components were separated. PBLs were cultured and then irradiated. Using DNA microarrays, genes expressed at increased levels in human PBLs following *ex vivo* irradiation were identified. The results suggest that relative levels of gene expression in PBLs may provide estimates of environmental radiation exposures (Amundson et al., 2000).

STA has also been used to examine the effects of steroid hormones. In a study of 17 β -estradiol exposure, gene expression changes were compared for rat blood and uterus. One hundred ninety three genes were expressed in common between the PBL and uterus. Eighteen were changed significantly in both tissues, nine of which were treatment specific, but not tissue specific. The results demonstrated that many genes are co-expressed in PBL and uterus, and that some are co-regulated by estradiol (Rockett et al., 2002).

STA has also been used to monitor endometrial receptivity in women. The expression of integrin (ITG) cell adhesion molecules on PBLs and their correlation with endometrial cell ITG expression in fertile and infertile women during peak uterine receptive period (day 19/20) was examined. The expression of ITGs was significantly decreased in the endometrial cells of infertile women compared to fertile women, and correlated well with the data obtained from PBL-ITG expression. These results suggest that endometrial receptivity could be measured by frequent blood sampling instead of repeated endometrial biopsies, which would be advantageous as endometrial biopsies are traumatic and can cause intra-uterine infections (Reddy et al., 2001).

In another study designed to determine the validity of STA, microarray technology was used to investigate whether gene expression profiling in white blood cells could be used as a fingerprint of various disease states. Researchers subjected adult rats to ischemic strokes,

hemorrhagic strokes, sham surgeries, kainite-induced seizures, hypoxia and insulin induced hypoglycemia and were then compared with controls. The white blood cell RNA expression profiles were assessed twenty-four hours later. Results showed that many genes were up regulated or down regulated at least two fold in the white blood cells after the experimentally induced disease states and that blood gene expression profiles were different for each condition (Tang et al., 2001).

Thus, initial research indicates that STA may prove to be a very useful biomonitoring tool that will facilitate identification of pre-clinical manifestations of toxicant exposure in at risk populations or other physiological conditions.

Biomarkers

Appropriate biomarkers are the key to the success of STA. A biomarker is considered to be any biological index capable of being measured, which is associated with or indicative of, a defined biological endpoint such as a developmental or disease stage. Numerous cellular, molecular and biochemical indexes have been described. These include the presence of a parent compound or metabolite; proliferation and differentiation indices; apoptotic endpoints; changes in membrane permeability; formation of DNA adducts or damage; chromosomal abnormalities; micronuclei formation; receptor activation; change in gene expression profile (single or multiple genes); measurement of enzyme activity and others (Rockett et al., 2003).

Any of these endpoints can be used in STA providing that their presence or activity is related to a toxic endpoint or level of exposure in the target tissue, and the measured change is somehow co-ordinate in surrogate tissue. The ideal situation is that regulation of the measured change in both surrogate and target tissue occurs by the same mechanism, to the same degree, and over a wide dose and time response range.

In this study, genetic biomarkers of conazole exposure were identified in surrogate tissues (blood). Biomarkers of exposure are measurable changes in biological appearance or function that indicate exposure to a particular stimulus, which may be chemical, biological or physical in nature. Such biomarkers may be useful in identifying potentially toxic exposures. Biomarkers of exposure need not be a direct result of the exposure, although in many examples this is the case. In this study, biomarkers were specific patterns of gene expression changes, and the primary tool for identifying the biomarkers was DNA microarrays.

DNA Microarrays

DNA microarrays allow the expression of hundreds or thousands of genes to be monitored at the same time. This technology is useful in quantifying the expression of genes and obtaining information about the transcriptome profile of a cell, tissue, organ, or organism. The utility of transcriptional profiling as a sensitive method to classify cells, identify mechanisms of action for compounds and determine the function of previously unidentified genes has been demonstrated (Waring et al., 2001). Gene expression signatures derived from microarrays were recently used to cluster acute myeloid leukemia (AML) and acute lymphoblastic leukemia (ALL) cells. In this study, twenty-nine of thirty-four bone marrow or peripheral blood samples were classified as ALL or AML with one-hundred percent accuracy (Golub et al., 1999). This data demonstrates that different leukemia subtypes can be differentiated based on gene expression profile.

Steroidogenic Cytochrome P450s Found in the Blood

Many of the cytochrome P450 enzymes that are involved in the production of sex steroid hormones, including aromatase, have been found to be present in the blood. CYP activity in the

blood was first described 30 years ago (Kellerman et al., 1973). It has been difficult in the past to accurately monitor biotransformation systems in extra-hepatic cell types because the typically low levels of expression required highly sensitive and specific assays to enable their detection. However, advances in molecular techniques have now made it possible. For example, CYP51 was investigated in human liver tissue, kidney tissue, and lymphocytes by using a radio-HPLC assay to detect the 4, 4-dimethyl-5 α -cholesta-8, 14-dien-3 β -ol (diene) metabolite, one of three sequential products that have been identified during the conversion of lanosterol to cholesterol. CYP51 activity was detected in microsomes isolated from human lymphocytes. The lymphocyte enzyme was capable of converting dihydrolanosterol to both aldehyde and the demethylated product and is most likely very similar to the liver CYP51 (Raucy et al., 1991).

In addition to CYP51, several other steroidogenic CYPs have been detected in blood lymphocytes. In one study, steroid metabolism was investigated in cultured human B-lymphoblastoid cells (B-LCL), and peripheral blood T- and B-cells. Appropriate sized transcripts were detected in both cultured and fresh peripheral lymphocytes for CYP11A and CYP17. B-LCL, but not T- and B-cells, expressed CYP11B. From this study it was concluded that sex hormone metabolism, including androgen synthesis, occurs in lymphocytes, and may modulate immune response (Zhou et al., 1998).

In another study CYP19 expression was demonstrated in human lymphocytes. Lymphocytes were isolated from 11 surgical samples of breast cancer and mononuclear cells were separated from the blood of 15 female volunteers. Expression of CYP19 gene was readily demonstrated by standard RT-PCR in blood mononuclear cells. In the tumor-infiltrating lymphocytes (TIL) of breast cancer patients, CYP19 expression was discovered only with the aid of nested PCR (Berstein et al., 2002).

CYP21 has also been detected in human blood lymphocytes. A novel source of CYP21 expression in normal human cultured B-lymphocytes was found in a study of patients with congenital adrenal hyperplasia (CAH). The quantity of 21-hydroxylase transcripts was reduced in B-cell lines of CAH subjects compared with that in normal B-lymphoblastoid cells. No CYP21 transcript was detected in lymphocytes from a CAH patient with homozygous CYP21 deletion. Cultured lymphoid cells, including those carrying homozygous CYP21 deletion, and peripheral blood lymphocytes converted both 17-hydroxyprogesterone to 11-deoxycortisol and progesterone to deoxycorticosterone. The results suggest that lymphocytes express CYP21, but also possess a 21-hydroxylase distinct from CYP21 (Zhou et al., 1997).

Xenobiotic Metabolizing Cytochrome P450s Found in the Blood

Steroidogenic CYPS are not the only cytochromes that have been found in the blood. CYP1B1 was found to be the major cytochrome P450 in the blood by a study in which human blood monocytes and macrophage subsets 27E10 and RM3/1 derived from healthy human donors were incubated *in vitro* with various toxicants for 24 hours. Monocytes and the pro-inflammatory macrophage subset 27E10 expressed CYP1B1, CYP2E1, and CYP2B6/7. The anti-inflammatory macrophage subtype RM3/1 expressed predominantly CYP1B1 and to some extent CYP2B6/7 (Baron et al., 1998). Another study identified the presence of low levels of CYP1A1, CYP2D6, CYP2E1, CYP3A4, and CYP2F1 in peripheral lymphocytes isolated from ten healthy donors using qRT-PCR (Krovat et al., 2000). Concentrations of CYP2D6 and CYP2E1 in human blood lymphocytes have been shown to reflect the *in vivo* activity of their corresponding liver counterparts (Carcillo et al., 1996). Basal activity levels of mEH in fresh lymphocytes have also been shown to correlate with levels in the liver and lung (Omiecinski et al., 1993).

As previously stated, exposure to conazole fungicides alters the expression of CYP1A1, CYP1A2, CYP2B1/2, CYP2B6, and CYP3A4 enzymes in the liver. It is possible that peripheral blood lymphocytes may have correlating expression of these enzymes following conazole exposure, and this will be assessed using surrogate tissue analysis.

Hypotheses

This study focused on four hypotheses. The first hypothesis is that exposure to myclobutanil and triadimefon results in an altered gene expression profile in the blood, producing biomarkers of exposure in male Sprague Dawley rats. The second hypothesis is that exposure to myclobutanil and triadimefon causes changes in serum hormone levels and that these changes correlate with gene expression changes in the blood of male Sprague Dawley rats. The third hypothesis is that gene expression changes in blood are concordant with gene expression changes in liver and testes of male Sprague Dawley rats. The fourth hypothesis is that cytochrome P450 enzymes and other xenobiotic enzymes are expressed in blood leukocytes and their expression is altered following exposure to myclobutanil and triadimefon and is correlated with gene expression changes in the liver and testis in male Sprague Dawley rats.

In order to test these hypotheses, RNA was extracted from blood and gene expression changes were analyzed through the use of microarrays. Particular genes of interest are cytochrome P450 enzymes, those involved in steroid hormone biosynthesis and xenobiotic metabolism. Serum hormone levels for testosterone were measured to identify any disturbance in hormone production.

Microarray technology is a new tool that is becoming more commonly used in toxicology. Microarrays are valuable tools because of their capability to identify relative gene expression changes for a multitude of genes for a chemical exposure in a tissue at the same time point.

For this study, glass oligonucleotide microarray slides that include over four thousand genes were used to measure gene expression in rat blood following conazole exposure. The resultant gene expression profiles in blood and correlation with gene expression profiles in liver and testes will help determine the utility of surrogate tissue analysis and determine possible biomarkers of effect.

MATERIALS AND METHODS

Animals

Adult male Sprague Dawley rats were obtained from Charles River Laboratory (Wilmington, MA) on postnatal day (PND) 72. The U.S. EPA NHEERL Institutional Animal Care and Use Committee approved all of the procedures performed. The rats were acclimated for six days before dosing. The rats were randomly assigned to treatment groups to ensure equivalent weight means across the dose groups prior to dosing. All rats were individually housed in the animal facility with a 12:12-hour light: dark cycle under controlled temperature (72°F) and humidity (45%) with unrestricted access to LabDiet 5001 Rodent Diet (PMI LabDiet, Richmond, IN) and water. Each experimental group consisted of eight males treated with one of the two test compounds; in addition, eight males were treated with the vehicle solvent. A total of 40 rats were used in this study.

Chemicals and Treatment

Myclobutanil was purchased from LKT laboratories Inc, (St. Paul, MN) and triadimefon was the gift of Bayer Crop Science (Kansas City, KS). Both chemicals were technical grade, at purities above 95%. Triadimefon and myclobutanil were dissolved in a 15% Alkamuls EL-620/distilled water solution. Alkamuls EL-120 was a gift of Rhodia Inc. (West Point, GA). Dosing was staggered, so that 20 rats (four animals from each dose group and four control animals) were dosed from PND 78 to PND 91, and the other twenty rats were dosed from PND 79 to PND 92. All treatments were administered by oral gavage during the early morning of each of the 14 consecutive days. The myclobutanil treatment groups received 10 or 150 mg/kg/day. The triadimefon treatment groups received 5 or 115 mg/kg/day.

Necropsy

Following the final dosing, the animals were transferred to a holding room with similar environmental conditions to their original rooms in the animal facility four hours before terminal harvests. The rats were euthanized via decapitation.

Testes and liver were weighed. Several pieces of liver and testis (~50 mg) were snap-frozen in liquid nitrogen for RNA isolation. The tissues were stored in a cell freezer at -196°C. Two and a half milliliters of blood was collected from the neck of the severed trunk into a Paxgene blood collection tube (PreAnalytiX, Franklin Lakes, NJ) and the remainder into a serum separator tube.

Serum Hormone Levels

Serum samples were assayed in duplicate using the Coat-a-count Total Testosterone Kit (Diagnostic Products Corp. Los Angeles, CA). Radioimmunoassay results were measured using the Wallac model 1272 automatic gamma counter (Perkin Elmer, Boston, MA). Statistical analysis was performed using analysis of variance, measures with $p < 0.05$ were considered significant from controls (Figure 12).

DNA Microarray Design

Microarrays were printed on UltraGAP Corning glass slides using the rat genome oligonucleotide set v (Operon, Alameda, CA) by the DNA Microarray Facility at Duke University Medical Center (Durham, NC) via the US EPA-Duke University Materials Cooperative Research and Development Agreement. The arrays contain 4992 total spots. The

total spots include 4289 Qiagen (Operon) oligos, 97 EPA custom gene spots, 597 empty spots and 9 negative spots.

RNA Isolation and Probe Labeling

The Paxgene Blood RNA tube (Preanalytix, Franklin Lakes, NJ) contains an additive that stabilizes cellular RNA and prepares the sample for RNA purification. The Tubes contain 6.9 ml of additive. It yields a ratio of 2.76 ml of additive per milliliter of blood when the evacuated tube is filled correctly to its 2.5 ml draw volume. The Paxgene Blood RNA tubes required a two-hour incubation at room temperature to completely lyse the cells. After the two-hour incubation, total RNA was isolated from whole blood according to the Paxgene Blood RNA Kit manufacturer's protocol. Samples were then subjected to quality control tests (Figure 6). The samples were first inspected through polymerase chain reaction (PCR) for DNA contamination. If necessary, the samples were DNAsed using Ambion's DNA-free kit (Ambion Inc., Austin, TX). The samples were analyzed on the spectrophotometer to determine A260:A280 ratio and concentration. Samples with an A260:A280 ratio of greater than 1.6 were then further analyzed using the Agilent 2100 Bioanalyzer to compare the 28S to 18S ribosomal RNA ratio to determine the quality of the RNA samples (Figure 7).

To ensure the purity of the blood RNA samples, the RNeasy mini kit (Qiagen, Valencia, CA) was used. The RNeasy mini kit removes any impurities that can interfere with amplification, such as hemoglobin degradation byproducts (RNeasy mini handbook, Qiagen, Valencia, CA) (see Appendix 1 for further discussion of RNA preparation).

Because of the relatively small amount of RNA isolated from the blood samples, RNA amplification was necessary to produce the required amount of RNA for the microarrays. MessageAmp™ aRNA Kit (Ambion, Austin, TX) was used to amplify the RNA. This kit

employs a procedure that consists of reverse transcription with an oligo (dT) primer that bears a T7 promoter and in vitro transcription of the resulting DNA with T7 RNA polymerase generates hundreds to thousands of antisense RNA (aRNA) copies of each mRNA in the samples. The samples were subjected to two rounds of amplification, with the second round incorporating 5-(3-aminoallyl)-UTP to enable dye labeling after the completion of RNA amplification. Aminoallyl-modified aRNA targets were chemically labeled using Amersham's Cy Dye cyanine5 (Cy5) (Amersham Biosciences Corp, Piscataway, NJ) for the experimental aRNA channel and cyanine3 (Cy3) (Amersham Biosciences Corp) for the reference aRNA. Reference RNA, kindly supplied by Dr. Douglas Tully (US EPA), was a mixture of rat liver and testis samples from 84 rats, which were collected on PND 24 and 37.

Hybridization, Scanning and Quantitation

25 microarrays were hybridized for this study. The five highest quality RNA samples were selected from each dose group based on a 260:280 ratio of 1.6 or greater and a Bioanalyzer 28s:18s ribosomal RNA ratio of 1.4 or greater. Five samples were chosen from each dose group because some groups only had five samples with good quality RNA.

To identify biomarkers of effect following conazole exposure, blood samples from the five treatment groups were analyzed on DNA microarrays. Hybridizations were set up in five blocks. The first block had two high dose triadimefon samples and three high dose myclobutanil samples. The second block had three high dose triadimefon samples and two high dose myclobutanil samples. The third and fourth blocks had two samples from each of the following treatment groups, control, low dose triadimefon, and low dose myclobutanil. The fifth block had one sample each from control, low dose triadimefon, low dose myclobutanil, and three repeat slides from high dose triadimefon. This generated five replicates per treatment group and

twenty-five total slides. Cy5 labeled treatment aRNA targets and Cy3 labeled reference aRNA targets were combined and hybridized to microarrays eighteen hours overnight at 42° C. After hybridization was completed, microarrays were washed, dried and scanned using ScanArray 4000 (Perkin-Elmer Life Sciences, Boston MA) (Figure 13). Fluorescence intensities of the Cy5 and Cy3 channels were quantitated using GenePix Pro (Molecular Devices Corporation, Union City, CA). GenePix Pro presented the data in an excel file format, which was then analyzed using SAS software.

Data Analysis

The mean intensity values from all pixels for each probe were used in the analysis. Mean intensity values were transformed to the log (base 2) scale. The use of a log scale results in more normally distributed data than the linear scale and reduces the relationship of the variance with the intensity level (variance tends to increase with intensity). The spacing of log (ratio) intensity values is also symmetric about zero; so that, for example, a ratio of two is equivalent in scale to a ratio of one-half (Figure 14).

The data was normalized by slide using an intensity dependent local regression procedure (SAS Proc Loess) (SAS, 1999). The model used was $\log_2(\text{Cy5/Cy3}) = \alpha + \beta \times \log_2((\text{Cy3} \times \text{Cy3})^{1/2}) + \varepsilon$, where α is the intercept, β the slope, and ε is the regression value defined as the error. A smoothing parameter of 0.2 was applied. Residuals from the model were used as the normalized values, which centered the data around zero across all neighborhoods of intensity.

Saturation of the spots on the arrays was examined. A spot was considered to be saturated in Cy5 or Cy3 if more than twenty-five percent of the pixels were saturated. Spots were considered to be present when the mean intensity was greater than the background intensity plus two standard deviations. Genes were considered to be expressed when the relevant spots were

present in the Cy5 channel in at least four of the five slides in a treatment group, or in at least seventy percent of all available slides. The total number of spots per gene was sometimes smaller than 25, as spots labeled 'Bad' (Flag=-100) were deleted from the analysis. Genes that were consistently present in the Cy3 channel but not Cy5 were considered to be uninteresting for this study. There were 214 genes present in the Cy5 channel, which were included in the rest of the analysis (Figure 15).

Since only a small percentage of the genes were consistently expressed on these slides, the normalization for the expressed genes was examined separately to eliminate noise from the graphs.

A second normalization was then performed on the 214 present genes. Quantile normalization takes the order of intensities within each array, and assigns all spots with the same ordered value the same intensity. In this case, the spots with the lowest intensity on each array were assigned the mean of the 25 lowest intensity spots. For the second lowest intensity, the mean of the 25 second lowest intensities were assigned; and so on (Figure 16).

Analysis of variance was performed on each of the 214 genes for each of four outcome values: loess normalized intensity with and without background subtraction and quantile normalized intensity with and without background subtraction. First, a two-way analysis of variance was calculated, which adjusted for any block effect before looking for treatment differences. Where there was a measurable block effect ($p < 0.1$), tests and estimates were calculated from the two-way ANOVA. Where there was not a block effect, a one-way ANOVA was performed, and tests and estimates were calculated from the one-way analysis. There were 51 genes with a significant treatment effect from this analysis. Treatment means from a two-way analysis were adjusted for block differences. Those from a one-way analysis assume no block differences.

Quantitative real time RT-PCR

Eight genes were selected for quantitative real time polymerase chain reaction (qRT-PCR)(Table 14) based on concordance of blood microarray data and liver and testis microarray data (Table 12 and 14). The quantification of the selected genes was performed by qRT-PCR. One microgram of RNA was reverse transcribed with random hexamer primers using ImProm-II Reverse Transcriptase (Promega Madison, WI) in accordance with the manufacturer's instructions. cDNA from the reaction was then diluted to 10 ng/μl. Five microliters of each cDNA was then used in the PCR reaction. Each cDNA was combined with TaqMan Universal PCR Master Mix (Applied Biosystems, Bedford, MA) and one of the TaqMan gene expression primers (Applied Biosystems, Bedford, MA) and then amplified in accordance with the manufacturer's instructions. PCR cycling conditions were an initial denaturation for ten minutes at 95°C followed by forty cycles of fifteen seconds at 95°C, and one minute at 60°C. Quantitative real time PCR was performed in a BioRad iCycler (Biorad, Hercules, CA) with the use of the appropriate filter set. All samples were tested in duplicate and were on the same plate for each assay. The same RNA samples used for the microarrays were used in the qRT-PCR assays. The threshold crossing level for the duplicate sets were averaged and compared using the student's t-test between appropriate treatment and control groups. Differences were considered significant when $p \leq 0.05$. Fold change between treatment and control was determined by transforming the data from exponential to linear terms by using the means of each treatment and control group in the equation $2^{(\text{treatment mean} - \text{control mean})}$. The inverse of this value is representative of the fold change of the gene in the treatment group compared to control (Livak and Schmittgen, 2001).

RESULTS

Body Weights

Analysis of variance was used to determine effect of treatment on body weight. Pair wise t-tests were carried out to determine differences between each of treatment groups and the control group on weights that had significant overall treatment effects ($p < 0.05$). There was no significant difference in body weights following treatment with triadimefon and myclobutanil (Figure 8).

Organ Weights

Analysis of covariance was used to detect effect of treatment on organ weights after an adjustment for body weight. Pair wise t-tests were carried out to test for differences between each of the treatment groups and the control group on weights that had significant overall treatment effects ($p < 0.05$).

Exposure to myclobutanil increased liver weights of the high dose (150 mg/kg) group relative to control by an average 16.54% of body weight. Triadimefon treatment increased liver weights of the high dose (115 mg/kg) group relative to control by an average of 27.90% of body weight (Figure 9).

Left and right testis weights showed no significant difference in weights following exposure to triadimefon and myclobutanil (Figures 10 and 11).

Serum Hormones

Testosterone serum levels were measured in the low and high doses for Myclobutanil and triadimefon. The overall p-value for treatment effect was not different, but the pair wise comparison between treatment groups yielded a significant increase ($p = .0329$) in the low myclobutanil treatment group (Figure 12). In the previous conazole dosing study, there was an

increase in testosterone in the high myclobutanil dose group when compared to control (Tully et al., 2004).

Microarray Analysis

Statistical analysis revealed 214 genes were present for the 25 blood microarrays. Out of the 214 present genes, 48 genes exhibited significant change in gene expression between control and low and high dose myclobutanil and triadimefon (see Table 11).

For the 48 significant genes identified in the blood gene expression data, the low dose myclobutanil group had 17 differentially expressed genes and the high dose myclobutanil group had 30 differentially expressed genes. Ten differentially expressed genes were common between the two doses of myclobutanil (Figure 17 and Table 16). Low dose triadimefon had 11 differentially expressed genes and high dose triadimefon had 27 differentially expressed genes. Six differentially expressed genes were common between both doses of triadimefon (Figure 17 and Table 17). When gene expression was compared for myclobutanil and triadimefon, there were no differentially expressed genes in all four dose groups, which means that there were no conazole biomarkers (Figure 17 and Table 18).

When the blood microarray data was compared with microarray data for rat liver and testis (Tully et al., 2004), nine of the 48 significant genes were found to be in common (Table 12).

qRT-PCR

Analysis of the qRT-PCR data revealed three genes with significant differences when compared to control. Chemokine CX3C, H2A histone family, member Z and thioredoxin-like 2 were all significantly up regulated when compared to control.

Chemokine CX3C was up regulated in the high myclobutanil dose group compared to the control group with a fold change of 3.34. It was also found to be up regulated in the high myclobutanil dose group in the blood microarray data with a fold change of 5.39, and in the liver microarray data with a fold change of 1.49 (Table 15).

H2A histone family, member Z was up regulated in the high triadimefon dose group compared to the control group with a fold change of 1.59. It was also found to be up regulated in the high triadimefon dose group according to the blood microarray data with a fold change of 1.74. It was down regulated in the high triadimefon in the testis microarray data with a fold change of 0.761 (Table 15).

Thioredoxin-like 2 was up regulated in the low triadimefon dose group with a fold change of 2.00. This compares to a change of 2.51 in the blood microarray data (Table 15).

Discussion

Serum Hormones and Steroidogenic Enzyme Expression

It was hypothesized that exposure to myclobutanil and triadimefon would cause changes in serum hormone levels that would correlate with gene expression changes in blood cells in male Sprague dawley rats.

The overall p-value for treatment effect on serum testosterone levels was not different, but the pair wise comparison between treatment groups did yield a significant difference for the low myclobutanil dose group when compared to the control. The low dose myclobutanil group had the highest levels of testosterone out of all five dose groups. The mean for the low myclobutanil dose group was 3.541 nanograms per milliliter compared to 1.658 nanograms per milliliter for the control group.

This difference in testosterone levels for the low myclobutanil is unexpected as the previous conazole study found an increase in the high myclobutanil dose group. The difference in testosterone levels may best be explained as a U-shaped dose-response relationship where a low dose causes stimulation, while a high dose causes inhibition. Low dose stimulation of sub-inhibitory doses is referred to as hormesis, based on the Greek word “to excite”. Dose-response relationships that display an inverted U- or U-shaped curve depend on the endpoint measured, and have typically been viewed as examples of hormesis. Hormesis is thought to represent overcompensation to disruption in homeostasis. U-shaped dose-responses have been seen in numerous pharmacological investigations as well as for endpoints significant to public health, like cholesterol and longevity and alcohol consumption and cardiovascular disease incidence (Calabrese and Baldwin, 2001).

In this case, the testosterone hormone data forms an inverted U-shaped dose-response curve. To determine if the hormone data truly fits an inverted U-shaped dose-response, the T-RIA

would need to be repeated and it may be necessary to repeat the dosing and collect more serum samples to see if these samples also fit the trend.

Even though over 20 steroidogenic genes were present on the microarray, none appeared to be expressed in the blood. As previously discussed, steroidogenic enzymes have been detected in blood, like CYP19, CYP17, CYP11A1, CYP11B1, and CYP21, but in most instances the samples yielding these genes were human. Furthermore, the expression of these genes in the blood is minimal and has been detected using very sensitive assays like nested PCR. Even if these genes were expressed in rat blood it may be that the microarrays are not a sensitive enough method for detection. Because many of these steroidogenic genes appear in the liver and testis microarray data (Tully et al., 2004), it is unlikely for most of these genes that bad probe design is a factor. It is most likely that if these genes are indeed present in the blood then a more sensitive assay (e.g. qRT-PCR) would be necessary to detect them.

Microarrays

It was hypothesized that exposure to myclobutanil and triadimefon would result in an altered gene expression profile in the blood producing biomarkers of exposure in male Sprague dawley rats.

There were a total of 214 present genes and 48 significant genes across all four doses of myclobutanil and triadimefon. Liver microarray data yielded 1137 present genes and 376 significant genes and testis microarray data yielded 2249 present genes and 357 significant genes. When the blood microarray data is compared to the target tissue data it is obvious that the gene expression in blood is very sparse. As preparation and interpretation of microarray is complicated and subject to numerous sources of variability, it cannot be assumed that this is an accurate depiction of blood gene expression.

The microarrays used require at least 10 μ g of RNA and in this study 10 μ g was the maximum amount available. It may be necessary to increase this amount to ensure there is an adequate amount of sample to bind to the probes.

Preparation of the microarrays involves applying the RNA and a cover slip. In this process it is possible to introduce air bubbles or to not have even coverage of all probes, especially those located near the edge of the slide. If an air bubble is present it will prevent binding of the sample to the probes covered by the air bubbles.

Variation can also be introduced by the individual preparing the slides and by preparing the slides on different days. In this instance, the microarray data showed more variation within a day than between different days.

Another source of variation may have been introduced into the RNA samples themselves. The blood RNA isolation process did not yield enough RNA for the microarrays, so amplification was necessary. A study of the impact of amplification of RNA showed that significant number of genes that were detected in unamplified testis RNA were not detected in the amplified testis RNA. This suggests that amplification may be limiting and that it may be necessary to compare amplified RNA only to other amplified RNA (Ren et al., 2003). It is likely that when blood RNA was amplified, gene transcripts with a high copy number were more readily copied than transcripts that had fewer copies. These means that the amplified blood would not be an accurate representation of all transcripts that were originally present in the blood RNA. Testis and liver RNA was abundant and did not require amplification. When the blood microarray data is compared to the target tissues microarray data, amplified RNA is being compared to unamplified RNA. It would be ideal to compare unamplified RNA to unamplified RNA.

The low dose myclobutanil group had 17 differentially expressed genes, the high dose myclobutanil dose group had 30 differentially expressed genes and there were ten differentially expressed genes common to the low and high myclobutanil dose groups, which represent possible biomarkers of myclobutanil exposure (Table 16). It would be expected that the higher dose would affect the expression of more genes than the lower dose. When the ten genes that were common to both doses of myclobutanil were examined to compare their fold change values in the blood microarray data, all of the genes had correlating fold change values and these values only differed by at most a few tenths of a point (Tables 11 and 12). While ten genes are a small percentage of the 214 genes that were present on the blood microarrays, this data supports the idea that exposure to myclobutanil causes change in gene expression and this change may be unique to this particular conazole.

The low triadimefon dose group had 11 differentially expressed genes, the high triadimefon dose group had 27 differentially expressed genes, and six differentially expressed genes were common to both dose groups, which represent possible biomarkers of triadimefon exposure (Table 17). When the six differentially expressed genes common to both dose groups were examined to compare their fold change values in the blood microarray data, four of the six had correlating fold change values, which only differed by at most a few tenths of a point. The other two genes, macrophage inflammatory protein 1 alpha receptor and protein kinase, AMP-activated, gamma, do not share the same magnitude of fold change (Tables 11 and 12). Six genes are a very small percentage of the 214 genes present on the blood microarrays, but this data does support the idea that triadimefon exposure does cause changes in gene expression and the changes may be distinctive to triadimefon.

It was hypothesized that gene expression changes in blood would be correlated with gene expression changes in the liver and testis in male Sprague dawley rats. Out of the 48 genes that

were significantly changed in blood between exposed and control animals, nine were also significantly changed according to liver and testis microarray data (Table 12).

Eight of these were chosen for qRT-PCR (Table 14). The ninth gene was not selected to be assayed because a primer was not available. These genes represent possible biomarkers that could support the utility of STA.

While it is possible that these genes may be biomarkers supporting the utility of STA, five of these genes have changes in the blood that are not concordant with the change seen in the liver and testis (see Table 12). In these instances if the change indicates up regulation in the blood then the change in the liver and/or testis indicates down regulation and vice versa. It would be necessary to repeat the microarrays, with amplified and unamplified blood RNA if possible, to see if these genes again show significant change and if the change in the three tissues is contradictory and whether the amplification affects the outcome.

The 48 significantly changed genes fall into nine functional categories. Eighteen genes encode enzymes (Table 2). Four of the genes encoding enzymes, thioredoxin-like 2, vacuolar ATPase subunit M9.2, ornithine aminotransferase, and alcohol dehydrogenase, (class I) alpha polypeptide, were selected for RT-PCR.

Thioredoxin-like 2 was up regulated in blood in the high triadimefon dose group (Table 11) and has been identified in lymphocytes, testis, lung and many other tissues. Thioredoxin-like 2 was formerly named PKC-interacting cousin of thioredoxin (PICOT). Transient expression of thioredoxin-like 2 inhibited the activation of JNK and two transcription factors, AP-1 and NF- κ B, induced by PKC θ or by combination of T cell-activating stimuli, which suggests that thioredoxin-like 2 plays an important role in the regulation of T cell activation and the function of PKC θ (Witte et al., 2000). Thioredoxin-like 2 mRNA is ubiquitously expressed, with testis and lung having the highest levels of expression. The protein is associated with microtubular

structures such as lung epithelial cilia and the manchette of and axoneme of spermatids. Thioredoxin-like 2 binds microtubules and might be a novel regulator of microtubule physiology. The localization of thioredoxin-like 2 in the axoneme in sperm flagella and lung cilia indicates that it is a component of the axonemal machinery taking part in regulation of ciliary and flagellar movement (Sadek et al, 2003).

Vacuolar ATPase subunit M9.2 was down regulated in blood in the low dose triadimefon dose group and up regulated in liver in the high dose triadimefon dose group (Tully et al., 2004) (Table 12). The vacuolar H⁺-ATPase (V-ATPase) is one of the most fundamental enzymes in nature. It functions in almost every eukaryotic cell and energizes a wide variety of organelles and membranes. V-ATPases function exclusively as ATP-dependent proton pumps. The proton motive force generated by V-ATPases in organelles and membranes of eukaryotic cells is utilized as a driving force for numerous secondary transport processes. The V-ATPases play a major role as energizers of animal plasma membranes, especially apical plasma membranes of epithelial cells. The list of animals with plasma membranes that are energized by V-ATPases now includes members of most, if not all, animal phyla. This includes the classical Na⁺ absorption by frog skin, male fertility through acidification of the sperm acrosome and the male reproductive tract, bone resorption by mammalian osteoclasts, and regulation of eye pressure. V-ATPase was first detected in organelles connected with the vacuolar system. It is the main, if not the only, primary energy source for numerous transport systems in these organelles. The driving force for the accumulation of neurotransmitters into synaptic vesicles is proton motive force generated by V-ATPase. The acidification of lysosomes, which are required for the proper function of most of their enzymes, is provided by V-ATPase. The enzyme is also vital for the proper function of endosomes and the Golgi apparatus (Nelson et al, 1999).

Ornithine aminotransferase was down regulated in blood in the low myclobutanil dose group, high myclobutanil dose group and high triadimefon dose group, and was down regulated in liver in the high triadimefon dose group (Table 12) (Tully et al., 2004). Ornithine aminotransferase encodes the mitochondrial enzyme ornithine aminotransferase, which is a key enzyme in the pathway that converts arginine and ornithine into the major excitatory and inhibitory neurotransmitters glutamate and GABA (Ariadne Genomics). Ornithine aminotransferase enzyme levels are sexually dimorphic with females having higher amounts of the enzyme in their kidneys and liver. Estrogen administration can increase the amount of ornithine aminotransferase in kidney and liver in both sexes (Herzfeld et al 1968).

Alcohol dehydrogenase (class I) alpha polypeptide was down regulated in blood in the low dose triadimefon group and up regulated in testis in the high dose myclobutanil group (Table 12) (Tully et al, 2004). Class I alcohol dehydrogenase, alpha subunit is a member of the alcohol dehydrogenase family. Members of this enzyme family metabolize a wide variety of substrates, including ethanol, retinol, other aliphatic alcohols, hydroxysteroids, and lipid peroxidation products. Class I alcohol dehydrogenase, consisting of several homo- and heterodimers of alpha, beta, and gamma subunits, exhibits high activity for ethanol oxidation and plays a major role in ethanol catabolism. Three genes encoding alpha, beta and gamma subunits are tandemly organized in a genomic segment as a gene cluster (Ariadne Genomics).

It was hypothesized that cytochrome P450 enzymes and other xenobiotic metabolizing enzymes are expressed in blood leukocytes and that their expression would be altered following conazole exposure and would correlate with cytochrome P450 gene expression in the liver and testis in male Sprague dawley rats.

Conazole fungicides are xenobiotics and therefore it would be expected that cytochromes P450s and other xenobiotic metabolizing enzymes would have altered expression following

exposure to myclobutanil and triadimefon. However, while there were 18 significantly changed genes, which encoded enzymes, none of the previously discussed cytochromes identified in blood were present in the blood microarray data (Table 13). Only one of the 18 genes encodes a cytochrome P450, and that gene is CYP2A2 (Table 2). Only four other cytochromes were included in the 214 present genes. These included CYP49, cytochrome P450-like protein, CYP2C39, and CYP2B19. CYP2C39 and CYP2B19 were present but not significantly changed (p -value >0.05) in the testis microarray data. CYP2A2 was present but not significantly changed in the liver microarray data (Tully et al., 2004).

CYP1A1, CYP1A2, CYP2B1/2, CYP2B6 and CYP3A4 have altered expression in the liver as a result of conazole exposure (EPA, 2003). Two of these genes were included on the microarray, CYP1A1 and CYP1A2, yet neither was on the present gene list or significant genes list from the blood microarray data. CYP1A2 was, however, present in both the liver and testis microarray data, but was not differentially expressed (Tully et al., 2004).

Another important cytochrome not present in the blood microarray data was CYP51. A CYP51 probe was present on the microarrays. However, it was not expressed in blood and was found to be absent in the liver and testis microarray data from the previous conazole dosing study (Tully et al., 2004). It is possible that the CYP51 probe on the microarrays was poor quality or that the microarray was not sensitive enough to detect it.

The 18 genes encoding enzymes includes four xenobiotic metabolizing enzymes, rat odorant metabolizing protein (RY2D1), alcohol dehydrogenase (class 1), alpha polypeptide, *Rattus norvegicus* arylamine N-acetyltransferase-2 (AT-2) and resiniferatoxin-binding, phosphotriesterase-related protein (Table 2). These four genes encode enzymes that metabolize a variety of compounds, but none are involved in conazole metabolism. While alcohol

dehydrogenase was significantly changed in the testis as previously discussed, the other three genes were not differentially expressed in liver or testis (Tully et al., 2004).

Six of the 48 significantly changed genes from the blood microarray data encode proteins involved in nucleic acid binding or act as transcription factors (Table 4). Histone 2A, Pituitary-tumor transforming 1, Paired-like homeodomain transcription factor 3, H2A histone family, member Z, MAD homolog 2, and ribosomal protein S11 are genes included in this category. Two of these genes, H2A histone family and MAD homolog 2, were selected for qRT-PCR.

H2A histone family, member Z was up regulated in blood in the low and high dose myclobutanil groups and the high dose triadimefon group and down regulated in testis in high dose triadimefon (Tully et al., 2004). The H2A.Z variant family is highly conserved. H2A.Z amino acid sequence is more conserved than the amino acid sequence of major H2A, suggesting that H2A.Z plays an important role in chromosome function. It has been proposed that one important function of H2A.Z is to recruit a specific nuclear factor(s) and to modulate nucleosome - nucleosome interactions and the subsequent formation of high-order chromatin structures. H2A.Z has been found to be important in development as mouse embryos lacking H2A.Z die early in development prior to implantation (Rangasamy et al., 2003).

MAD homolog 2 was up regulated in blood in the high dose myclobutanil group and the low and high dose triadimefon groups, up regulated in testis in high dose myclobutanil group and down regulated in liver in high dose triadimefon group. MAD homolog 2 (SMAD2) is a transcriptional modulator activated by TGF-beta and activin type 1 receptor kinase. SMAD2 is a receptor-regulated SMAD (R-SMAD). SMAD2 may act as a tumor suppressor in colorectal carcinoma. SMAD2 is expressed at high levels in skeletal muscle, heart and placenta (Takenoshita et al., 1998).

Out of the 48 significantly changed genes, six encode for binding and transport proteins (Table 5). Two of these genes, retinol-binding protein 2, cellular and group-specific component (vitamin D-binding protein) were selected for qRT-PCR

Retinol-binding protein 2, cellular (crbp2) was down regulated in blood in low and high myclobutanil dose groups and in the high triadimefon dose groups and also down regulated in testis in the high triadimefon and myclobutanil dose groups (Tully et al., 2004). Crbp2 is an abundant 134-residue protein present in the small intestinal epithelium. Crbp2 is thought to participate in the uptake and/or intracellular metabolism of vitamin A. This gene is highly conserved in rats, mice, and humans. Crbp2 belongs to a protein family that contains liver fatty acid-binding protein (Demmer et al, 1987).

Group specific component (vitamin D-binding protein) was down regulated in blood in the high triadimefon dose group and was up regulated in liver in the high triadimefon and myclobutanil dose groups (Tully et al, 2004). Vitamin D-binding protein (DBP) is a monomeric, multifunctional glycoprotein that was first identified as the group-specific component of serum or Gc-globulin. It is essential to the transport of vitamin D sterols in the blood and to the removal of plasma actin monomers released to the blood subsequent to tissue damage. DBP also contributes to complement C5a-mediated chemotaxis, macrophage activation, and fatty acid transport. DBP is predominantly expressed in the liver. During embryonic development, expression of the rat DBP genes is induced in the yolk sac and maintained in the fetal liver. DBP expression remains high in the liver throughout adult life (Song et al., 1998).

As previously mentioned, CYP3A4 is altered following conazole exposure. CYP3A4 is a vitamin D 25-hydroxylase and studies have shown that ketoconazole inhibits this enzyme (Gupta et al., 2004). If this enzyme is inhibited then it could lead to a decrease in the amount of activated vitamin D causing a reduced need for vitamin D binding protein. CYP3A4 was not a

probe on the microarray, so it is unknown what effect triadimefon and myclobutanil had on its gene expression, but vitamin D binding protein was down regulated in the blood in the high triadimefon dose group. The reduction in gene expression seems to support this idea, however the liver data showed up-regulation of this gene. This difference may be related to vitamin D binding protein being predominantly expressed in the liver. Furthermore, qRT-PCR did not confirm the differential expression of this gene in the blood. It would be necessary to determine if this gene is differentially expressed in the blood by repeating the microarrays and examining more genes involved in vitamin D biosynthesis and catabolism to investigate the significance and validity of this reasoning.

Out of the 48 significant genes, three encode for immune-related proteins (Table 6). *Rattus norvegicus* chemokine CX3C, myxovirus (influenza) resistance, and *Rattus norvegicus* Bcl-interacting coiled-coil protein beclin are the genes included in this category. Chemokine CX3C was selected for qRT-PCR.

Chemokine CX3C was up regulated in blood in the high myclobutanil dose group and up regulated in liver in the high myclobutanil and triadimefon dose groups (Tully et al, 2004). Chemokine CX3C, also known as fractalkine, exists as a secreted glycoprotein and in a membrane anchored form. The soluble form is a potent chemoattractant for T-cells and monocytes. Fractalkine is expressed in resting or activated peripheral blood mononuclear cells, T-cells, B-cells, Natural Killer (NK) cells and in endothelial cells. Fractalkine is capable of controlling the key regulatory mechanisms of cell trafficking at sites of inflammation. Vascular endothelial cells produce Fractalkine in response to IFN-gamma (Imaizumi et al, 2004). Soluble Fractalkine enhances NK-cell cytolytic activity and may play an important role in the binding of NK-cells to endothelial cells and in NK-cell mediated endothelium damage (Yoneda et al., 2003). The expression of Fractalkine in rat aortic endothelial cells is induced by IL1-beta, TNF-

alpha, and bacterial lipopolysaccharides and involves activation of transcription factor NF-kappa-B (Garcia et al, 2000).

The remainder of the significant genes fell into five categories. These genes were not concordant with the testis and liver microarray data from the previous conazole dosing study (Tully et al, 2004) and were not selected for qRT-PCR. Six of the 48 significant genes from the blood microarray data encode G protein coupled receptors and G proteins (Table 3), two genes encode for peptide hormones (Table 7), two genes encode ion channels (Table 8), two genes encode proteins that suppress or promote tumorigenesis (Table 9), and four genes were lumped into a various category because their functions did not fit into the other categories (Table 10).

While the 48 significantly changed genes represent many different biological functions, there were genes that are common in blood gene expression profiles that were absent in the blood microarray data. In one study the ten most common genes in normal whole blood were identified as aminolevulinic acid synthase, peripherin 1, tumor protein, translationally controlled, cold shock domain protein A, peroxidoxin 2, neuroligin 2, ketohexokinase poly (a) binding protein, cytoplasmic 1, non-histone chromosomal architectural protein and receptor associated protein of the synapse, 4 globin (Ganter et al., 2004). Though aminolevulinic acid synthase, peripherin 1, neuroligin 2, ketohexokinase, and non-histone chromosomal architectural protein are present on the microarray template, none appeared to be expressed (Tully et al., 2004).

While only 48 genes were significantly changed from the blood microarray data, only 4273 genes were examined. Statistically, if a whole genome had been examined on the array, eight times more genes may have been significantly changed in the blood of the treatment groups. This in turn would probably mean that there would have been a higher number of concordant changes found in blood, liver and testis.

qRT-PCR

Three of the eight genes selected for qRT-PCR yielded differential expression when compared to controls (Table 15). Four genes of the eight genes selected for qRT-PCR were identified as conazole biomarkers. These biomarkers are genes that are expressed in blood, liver and testis that may support the utility of STA. Only one of these, H2A histone family, member Z, had a fold change in expression that correlated with the blood microarray data. According to qRT-PCR, it had a fold change increase of 1.59. In the blood microarray data it had a fold change increase of 1.74, but it had a fold change decrease in testis of 0.761.

The difference in outcomes between the qRT-PCR and microarray data might be due to amplification. The qRT-PCR assays utilized unamplified blood RNA where as the microarrays were hybridized with RNA that had been subjected to two rounds of amplification. It may be necessary to use amplified RNA for qRT-PCR if amplified RNA has been used for the microarrays. It would be ideal to be able to use unamplified RNA for both processes.

Summary

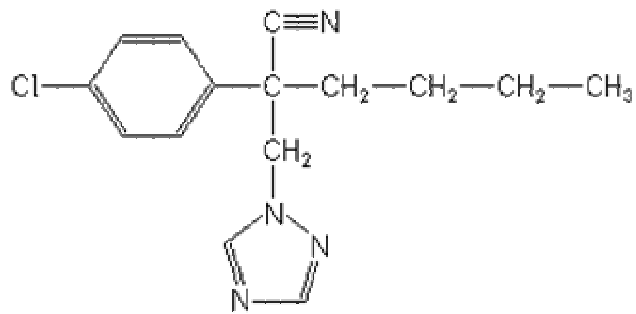
Exposure of male rats to the conazole fungicides, myclobutanil and triadimefon, resulted in the presence of 214 genes on microarrays containing 4273 gene probes and the differential expression of 48 of these genes. Only one of these 48 significantly changed genes was a cytochrome P450 enzyme and it was not significantly changed in liver or testis microarray data. Nine of these differentially expressed genes appeared to be concordant with liver and testis microarray data and represent possible biomarkers that support the utility of STA. qRT-PCR results indicate that only one of these nine genes was significantly changed when compared to controls and while the fold change correlated with the blood microarray data it did not correlate

with the testis. There was an increase in testosterone levels in the low myclobutanil dose group when compared to control, but this change did not correlate with blood gene expression.

Further research will be required to validate the utility of surrogate tissue analysis. Because of the limitations introduced by amplification, it is necessary to identify a method to collect higher quantities of blood RNA to eliminate the need for amplification. It is likely that the genes present on the microarray would have been more abundant without RNA amplification and there would have been higher concordance with the testis and liver microarray data, which represents unamplified RNA.

Figure 1: Structures of 1, 2, 4-N substituted azole ring conazoles myclobutanil and triadimefon.

Myclobutanil:



Triadimefon:

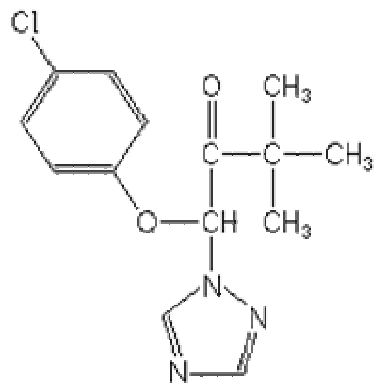


Figure 2: Ergosterol biosynthesis. Used with permission from Dr. Thomas Polakowski.
(Polakowski et al., 1998).

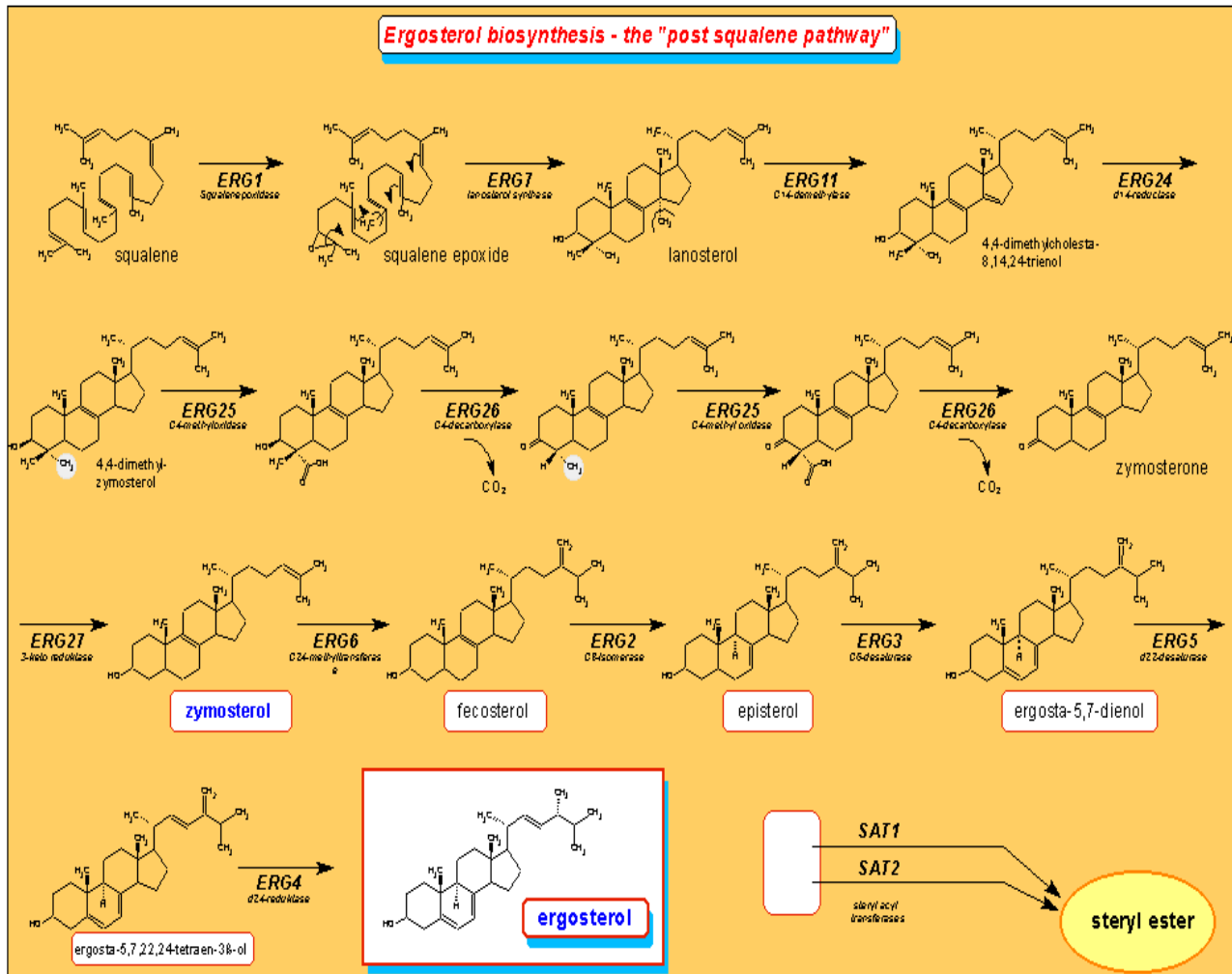


Figure 3: Ergosterol biosynthetic pathway from squalene to ergosterol. Adapted from White et al., 1998.

Name	Enzyme	Intermediate	Inhibitor
		Squalene	
ERG1	Squalene Epoxidase	↓	
		2,3-Oxidosqualene	
ERG7	Lanosterol Synthase	↓	
		Lanosterol	
ERG11	Lanosterol (C-14) Demethylase	↓	Azoles
ERG24	C-14 Sterol Reductase	↓	
ERG25 ERGX ERGY	C-4 Sterol Demethylase Enzymes	↓ ↓	
		Zymosterol	
ERG6	C-24 Sterol Methyltransferase	↓	
		Fecosterol	
ERG2	C-8 Sterol Isomerase	↓	
		Episterol	
ERG3	C-5 Sterol Desaturase	↓	
ERG5	C-22 Sterol Desaturase	↓	Azoles (?)
ERG4	C-24 Sterol Reductase	↓	
		Ergosterol	

Figure 4: Biosynthesis of phytosterols, ergosterol and mammalian sex steroid hormones.

The arrows indicate one or more enzymatic steps. Adapted from Zarn et al, 2003.

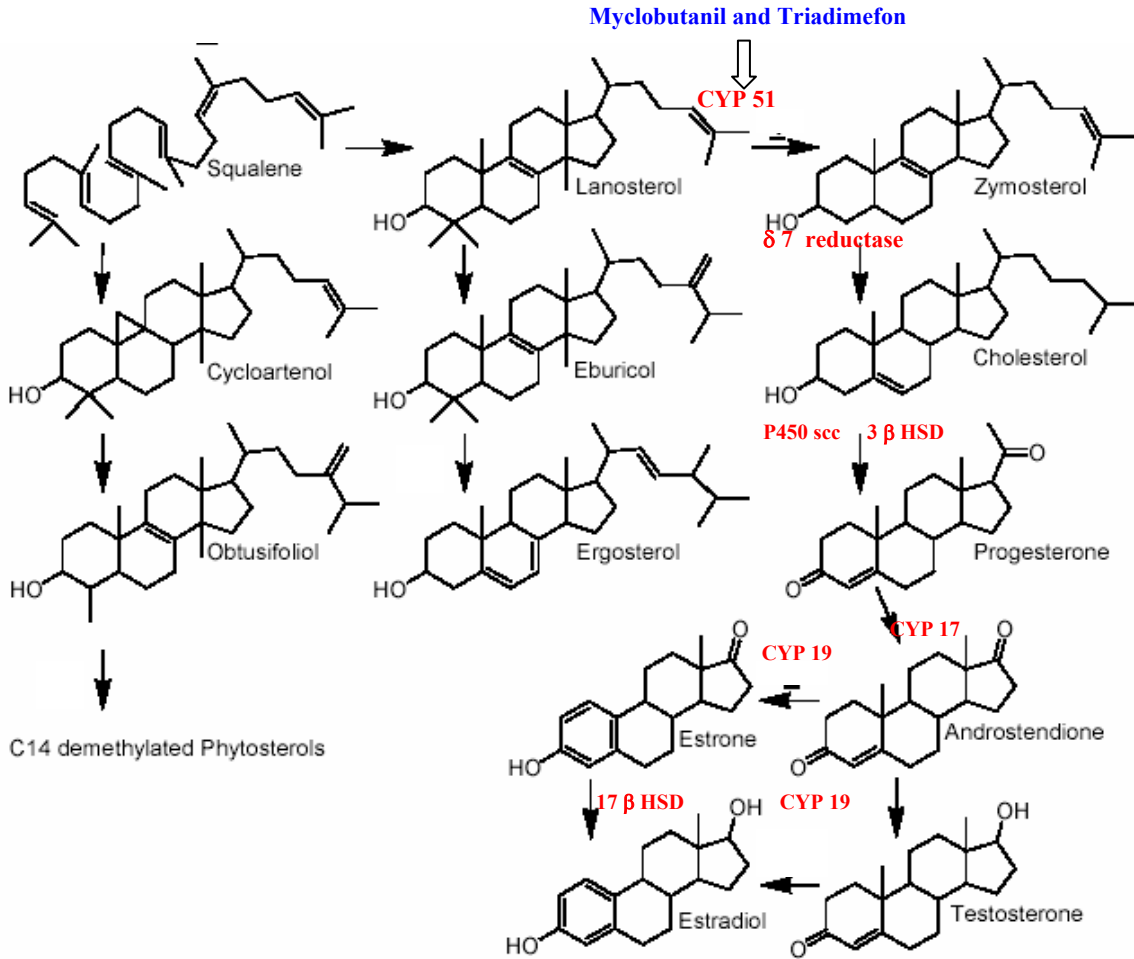


Figure 5: Biosynthesis of MAS. C14 demethylation of lanosterol in animals produces the follicle fluid meiosis-activating sterol (FF-MAS), which is further metabolized to the testis meiosis-activating sterol (T-MAS). If lanosterol is reduced by the sterol δ 24-reductase to 24, 25-dihydrolanosterol prior to demethylation, the resulting metabolites are MAS-412 and MAS-414. Adapted from Zarn et al, 2003.

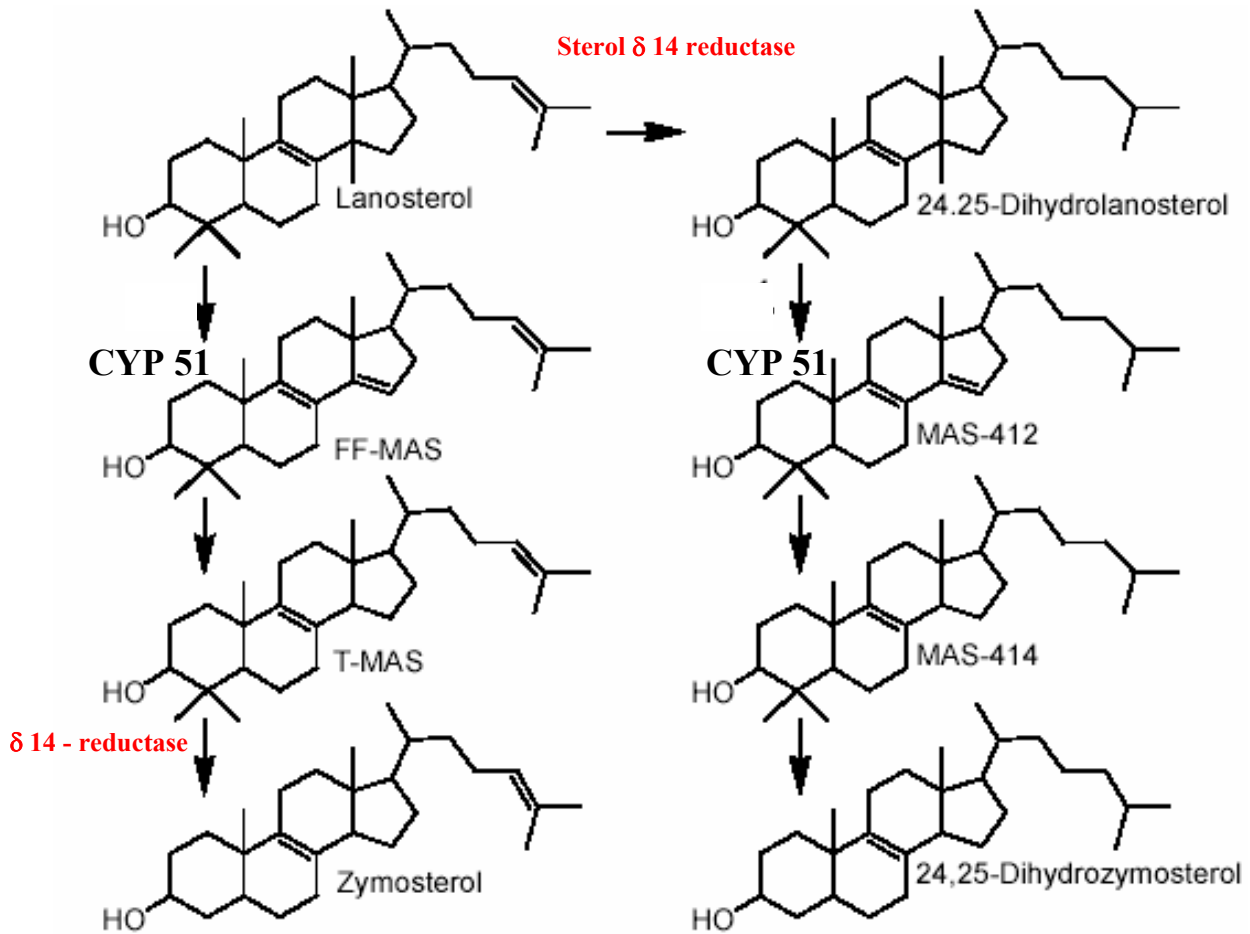


Figure 6: Process of sample preparation for microarrays and subsequent analysis.

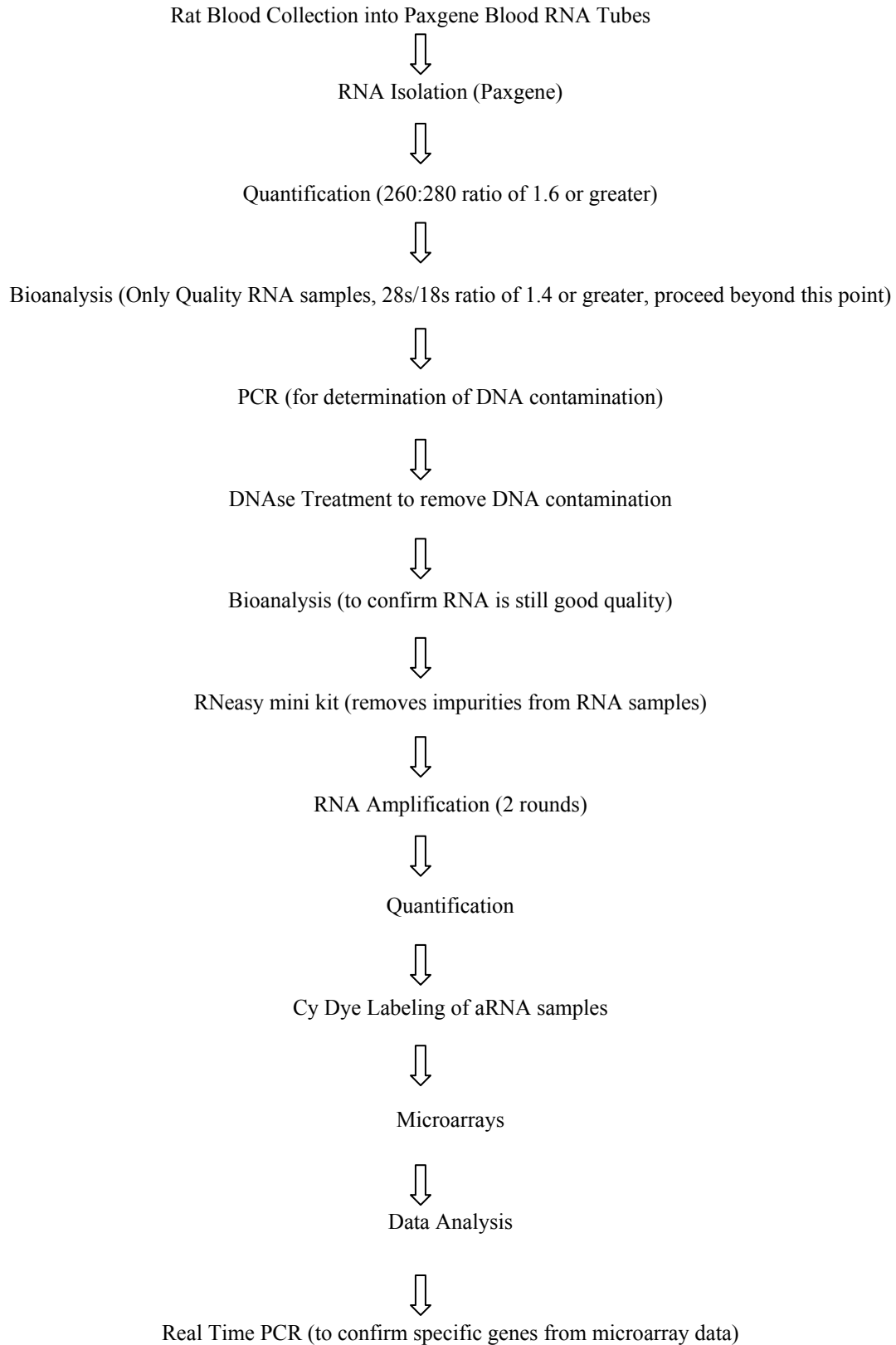


Figure 7: Bioanalyzer results showing the gel and graph for analyzed samples. Sample RNM37 is an example of a good RNA sample with an rRNA ratio (28S/18S) of 1.76. Sample RNM02 is an example of a bad RNA sample with an rRNA ratio (28S/18S) of .49, which was not used for microarray analysis.

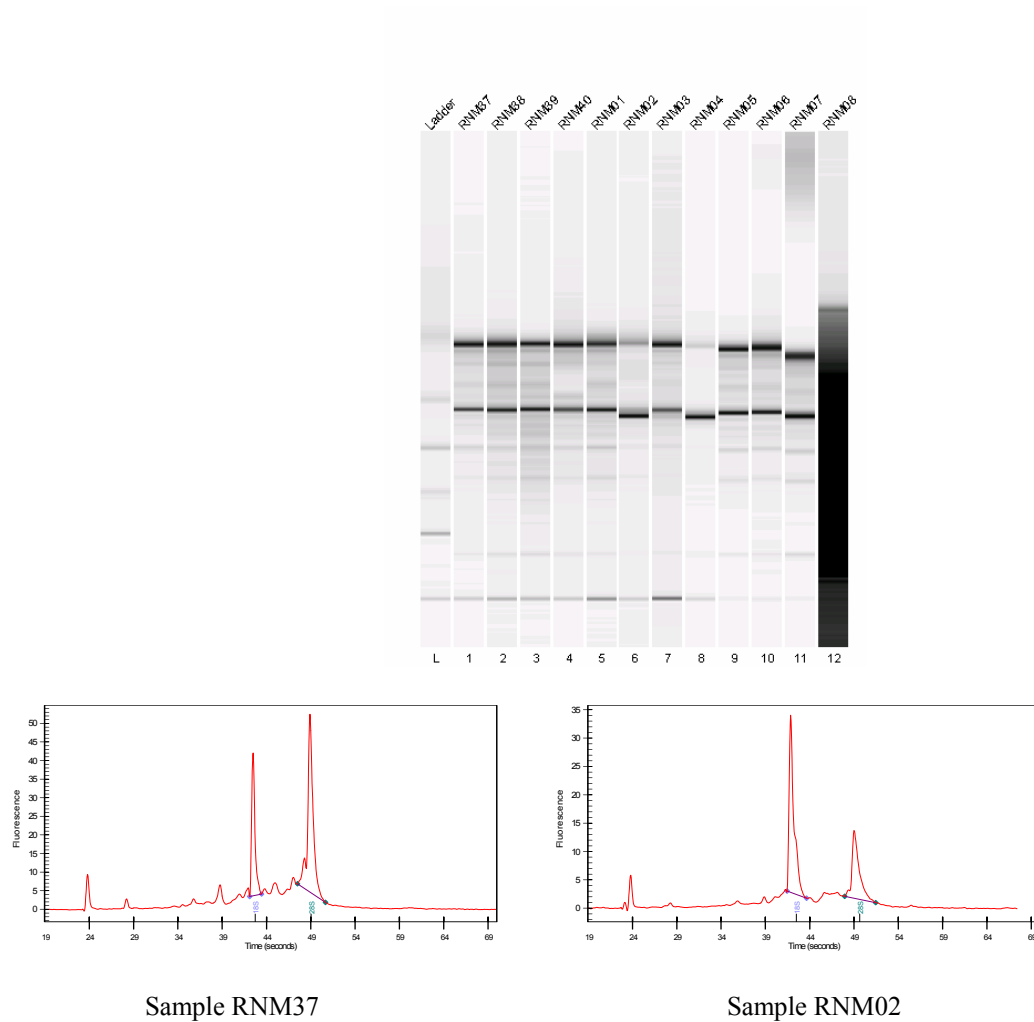


Figure 8: Analysis of Variance of triadimefon and myclobutanil treated male rat body weights. No significant difference was seen between the dose groups.

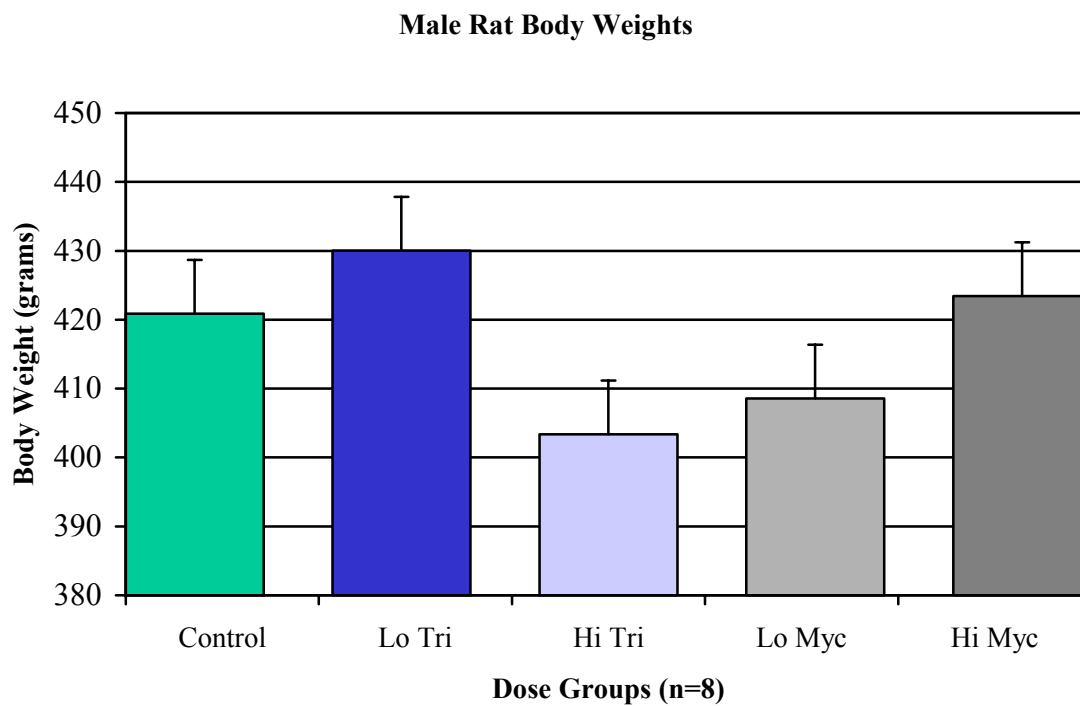


Figure 9: Analysis of covariance of triadimefon and myclobutanil-treated liver weights in male Sprague-Dawley rats. (*) p-value<0.05. A significant difference from control was seen for high triadimefon and high myclobutanil.

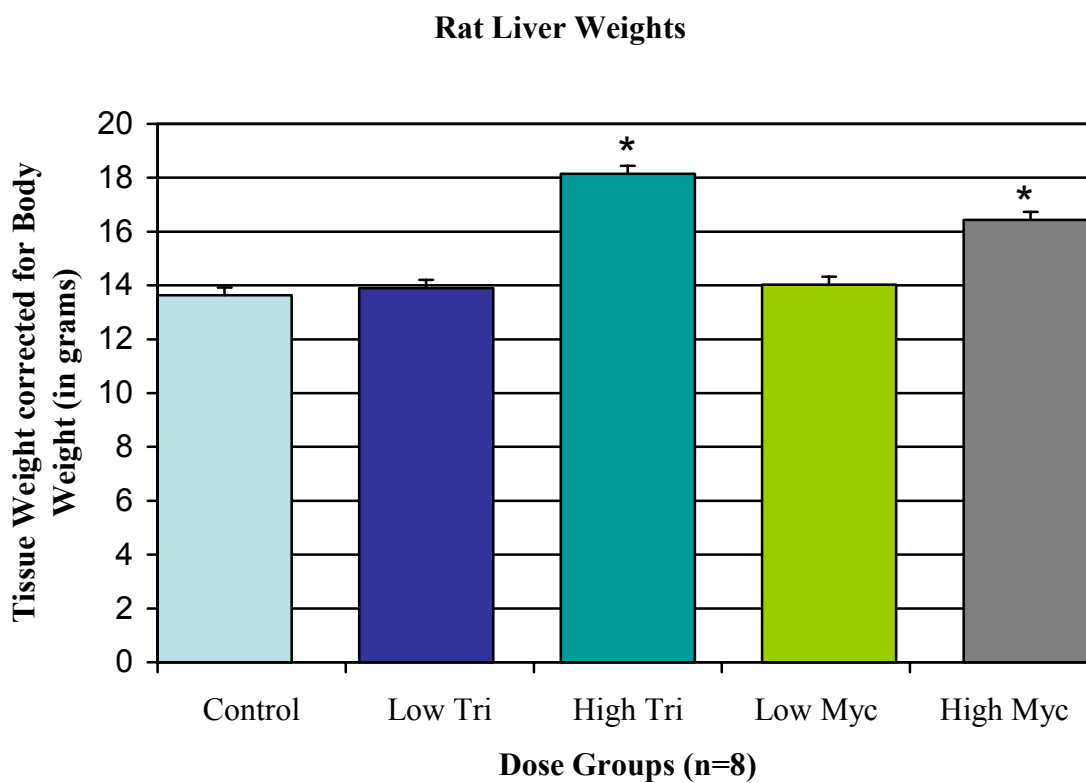


Figure 10: Analysis of covariance of triadimefon and myclobutanil-treated left testes weights in male Sprague-Dawley rats. No significant differences existed between the five dose groups.

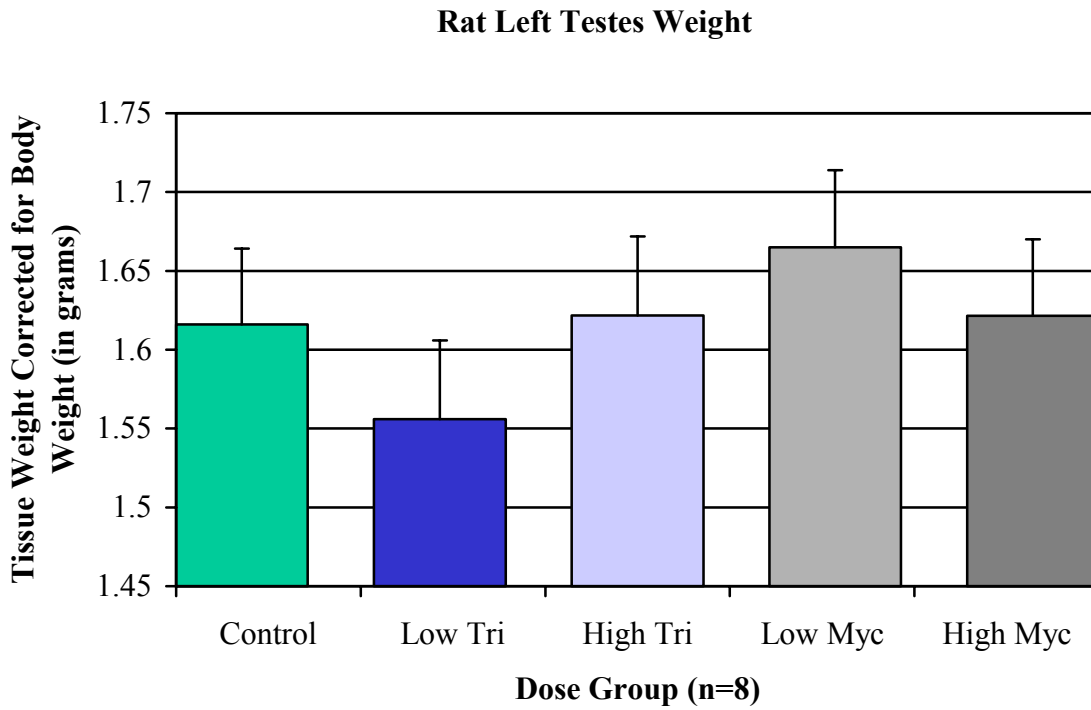


Figure 11: Analysis of covariance of triadimefon and myclobutanil-treated right testes weights in male Sprague-Dawley rats. No significant differences existed between the five dose groups.

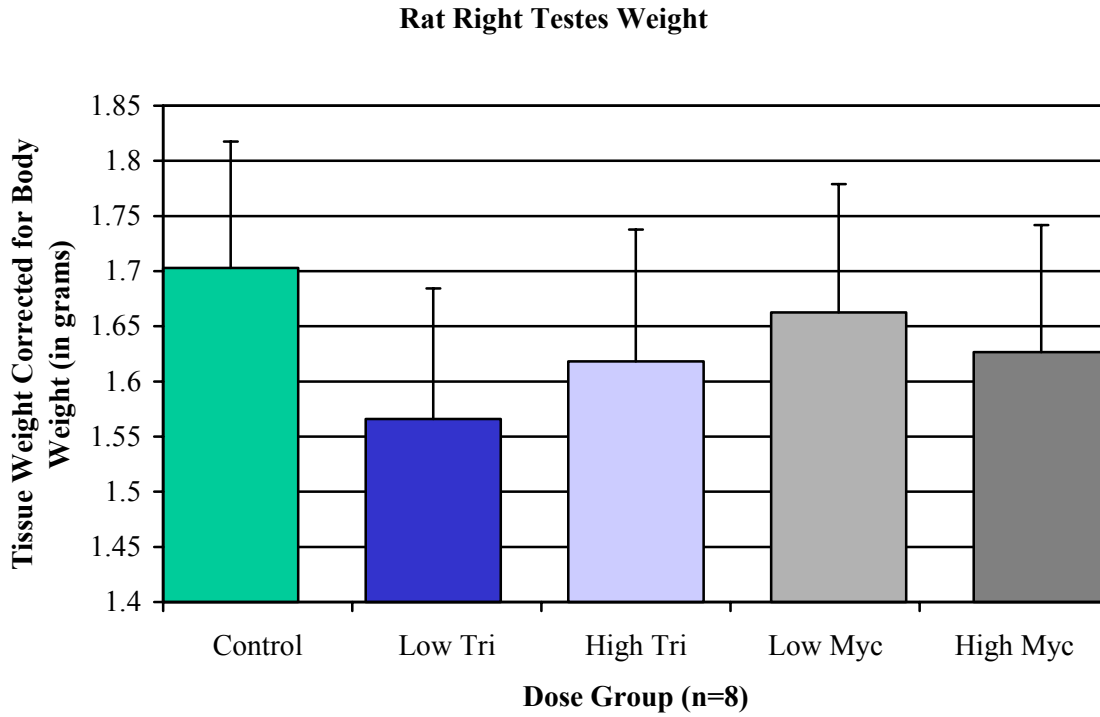


Figure 12: Testosterone Radio Immunoassay results. Mean and standard error estimates from ANOVA. The overall p-value for the linear scale one-way ANOVA is 0.083. While the overall p-value for treatment effect is not different, the pair wise comparison between treatment groups yielded a difference between the low myclobutanil treatment group and control with a p-value= .0329.

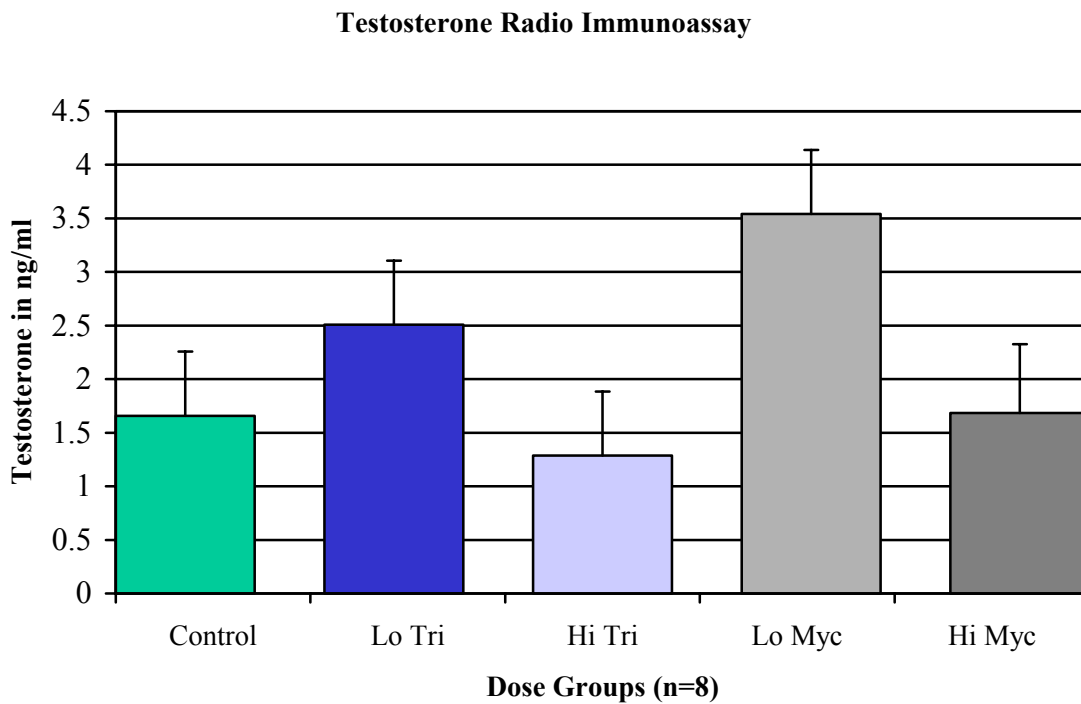


Figure 13: Example of Blood RNA Microarray slide. Blood RNA was labeled with Cy5 (red) and reference RNA was labeled with Cy3 (green). After labeling, hybridization and washing, the slide was scanned using ScanArray Express, which resulted in the composite image below.

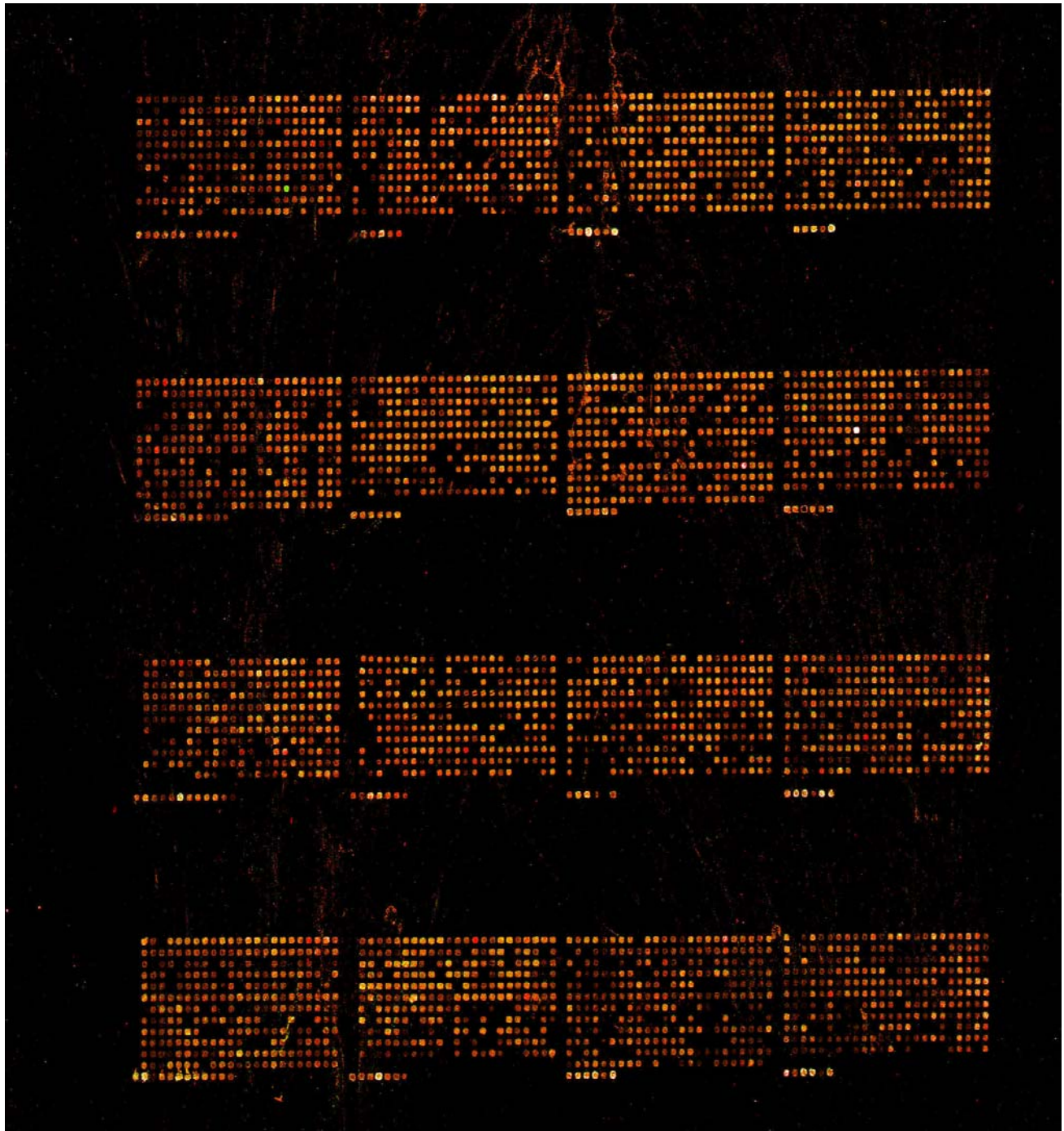
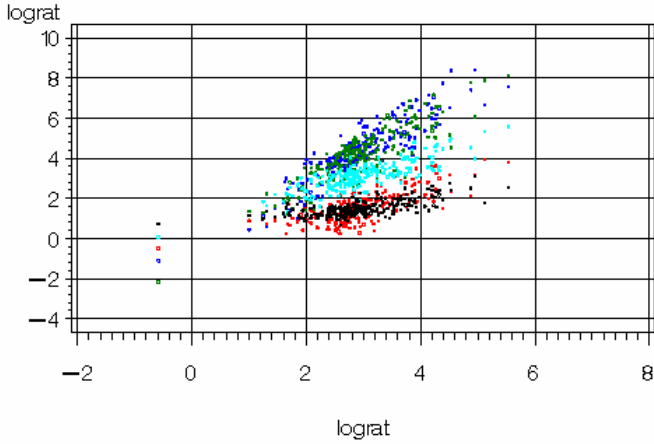


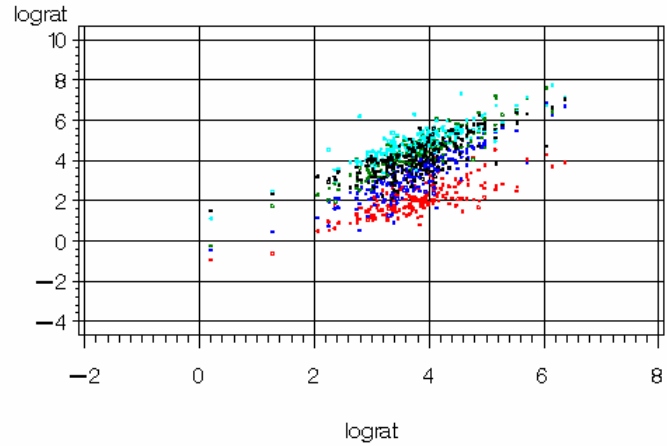
Figure 14: Data distribution prior to normalization for expression of 214 genes in blood following myclobutanil and triadimefon treatment.

Murrell, 214 Genes, PreNorm, Inc Bak
trt= HMyc



slide2 ○ ○ ○ 031904 —slide22 ○ ○ ○ 031904 —slide23
 ○ ○ ○ 031904 —slide24 ○ ○ ○ 032504 —slide15
 ○ ○ ○ 032504 —slide16

Murrell, 214 Genes, PreNorm, Inc Bak
trt= HTri



slide2 ○ ○ ○ 031904 —slide20 ○ ○ ○ 031904 —slide21
 ○ ○ ○ 043004 —slide45 ○ ○ ○ 043004 —slide46
 ○ ○ ○ 043004 —slide47

Figure 15: Loess normalization data distribution for expression of 214 genes in blood following myclobutanil and triadimefon treatment.

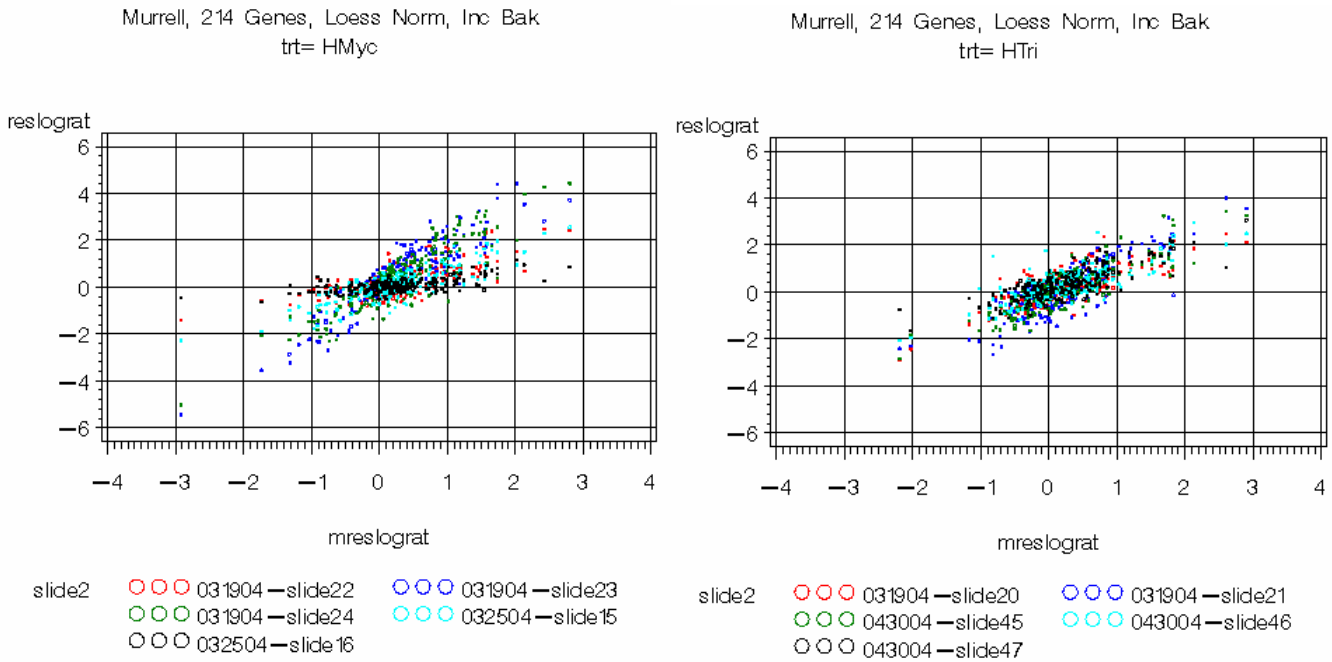


Figure 16: Quantile normalization data distribution for expression of 214 genes in blood following myclobutanil and triadimefon treatment.

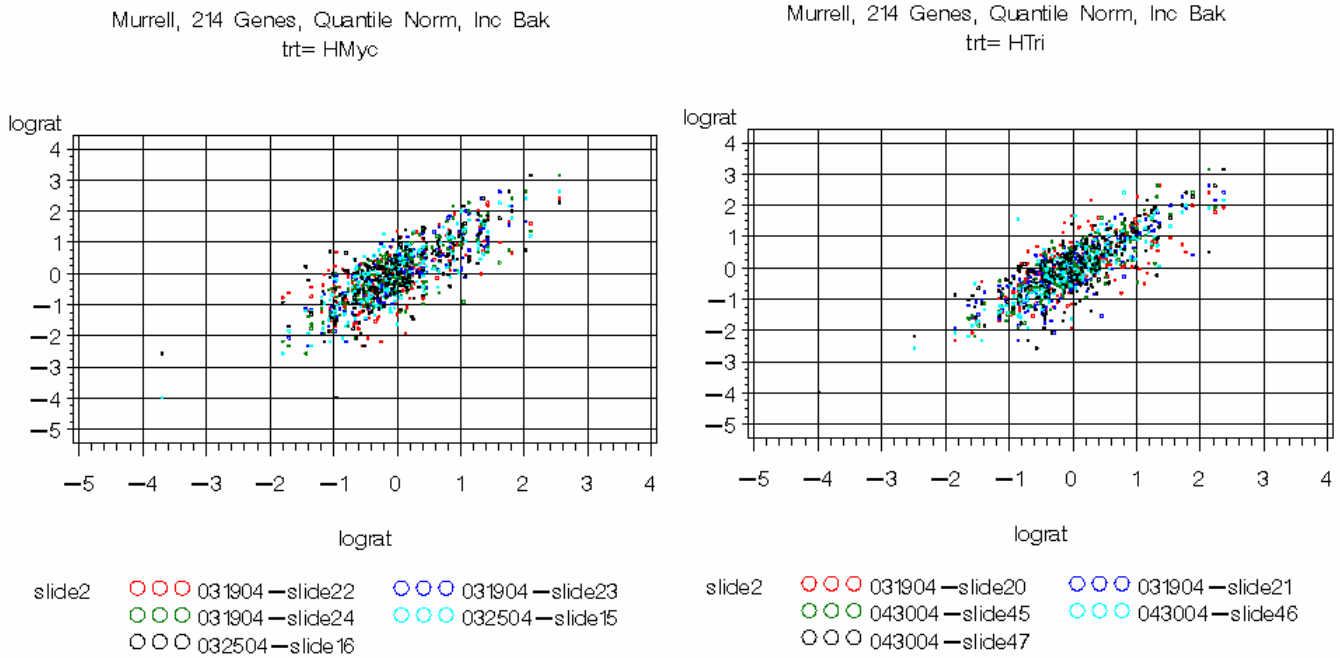


Figure 17: Possible blood biomarkers for myclobutanil, triadimefon, and for both conazoles.

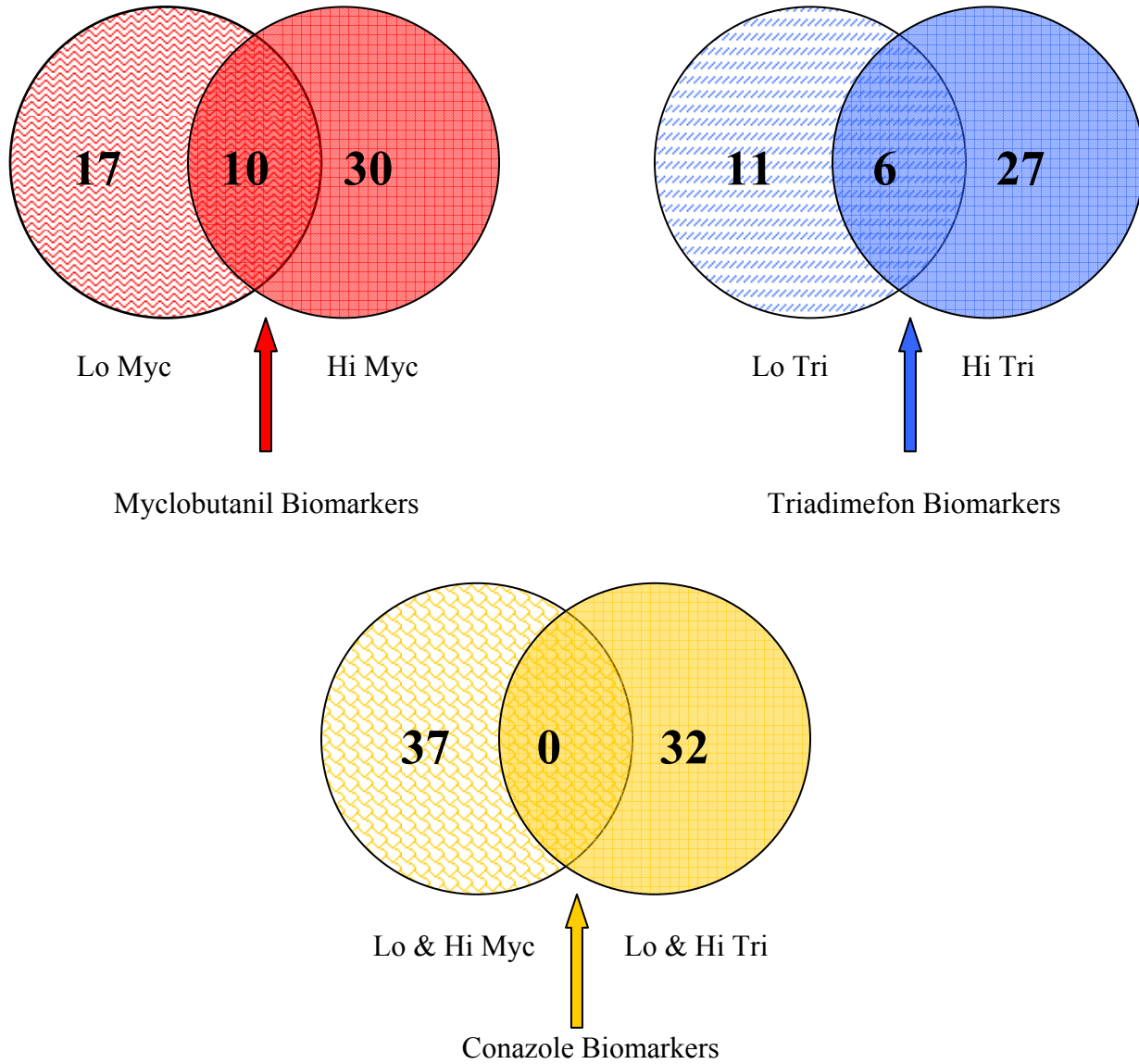


Table 1: Multiple conazoles-scientific names, trade names, and uses.

	CAS Registration #	Scientific Name	Trade Names	Uses
Azaconazole	60207-31-0	Dichlorophenyl)-1,3-dioxolan-2-yl) methyl) – 1H-1, 2, 4- triazole	Rodewod, R 28644, Madurox, Vanguard	Curative & preventive wood protection
Bromuconazole	116255-48-2	Bromo-2- (2,4-dichlorophenyl) tetrahydro-2-furanyl) methyl)-1H-1, 2, 4- triazole	LS 860263, Chipco ® Bromuconazole Brand Fungicide	Agricultural fungicide
Clotrimazole	23593-75-1	1 - [(2 - chlorophenyl) diphenylmethyl] imidazole	Gynelotrimin, Lotrimin, Mycelex Canesten,	Pharmaceutical-For treatment of tinea versicolor, ringworm, thrush, and vaginitis
Chlortrimazole	42074-68-0	Diphenyl (2- chlorophenyl) chloro- methane		Agricultural and Pharmaceutical- For treatment of tinea, candida, dermatophytes, thrush, and candida vaginitis
Cyproconazole	94361-06-5	Chlorophenyl)-alpha- (1-cyclopropylethyl) - 1H-1, 2, 4-triazole-1- ethanol	SAN 619F, Alto, Sentinel	Agricultural-food crops; Wood preservative
Difenoconazole	119446-68-3	1-((2-(2-chloro-4 - (4-chlorophenoxy) phenyl)-4-methyl -1,3-dioxolan-2-yl) methyl)- triazole	Dividend, Technical CGA-169374, Dividend 0.31 FS Fungicide, Dividend 0.15 FS Fungicide	Agricultural- food crops
Dininconazole	83657-18-5	(R- (E))-1-(2,4-dichlorophenyl-4, 4-dimethyl-2- (1H-1, 2, 4- triazol-1-yl) pent -1-en-3-ol	Spotless (XE-779L) W Fungicide, S-3308 L	Agricultural- food crops
Econazole	27220-47-9	1-[2-[(4-Chlorophenyl) methoxy]-2-(2,4-dichlorophenyl) ethyl]- 1H-imidazole	Spectazole	Pharmaceutical-For treatment of tinea corporis, tinea pedis, tinea cruris, tinea versicolor
Epoconazole	106325-08-0	RS, 3SR)-3-(2-chlorophenyl)-2-(4-fluorophenyl)-2-{(1H-1, 2, 4-triazol-1-yl) methyl} oxirane		Agricultural
Etaconazole	60207-93-4	Dichlorophenyl)-4-ethyl-1, 3-dioxolan-2-yl) methyl-1H-1, 2, 4- triazole	CGA-64251, Benit, Sonax, Vanguard	Agricultural; Wood preservative
Fenbuconazole	114369-43-6	Cyano-2-phenyl-2- (beta-p- chlorophenethyl) ethyl- 1H-1, 2, 4-triazole	RH-7592, RH-7592-2F, RH-7592 Technical Fungicide, RH-7592 2F Experimental Fungicide	Agricultural

	CAS Registration #	Scientific Name	Trade Names	Uses
Fluconazole		2,4-difluoro-a, a ¹ -bis (1H-1,2,4-triazol-1- ylmethyl) benzyl alcohol	Diflucan	Pharmaceutical- For treatment of infections due to Cryptococcus neoformans, Candida albicans, In mouse studies it has been shown to be effective against Aspergillus flavus, Aspergillus fumigatus, Blastomyces dermatitidis, Coccidioides immitis, and Histoplasma capsulatum
Flusilazole	85509-19-9	Bis (4-fluorophenyl) methyl ((1H-1, 2, 4- triazol-1-yl) methyl) silane	DPX-H6573, INH- 6473, Nustar, Punch, Olymp	Agricultural
Flutriafol	76674-21-0	Fluorophenyl)-alpha- (4-fluorophenyl)-1H-1, 2, 4-triazole-1-ethanol	PP 450, Impact	Agricultural
Hexaconazole	79983-71-4	RS)-2-(2,4- Dichlorophenyl) -1- (1H-1, 2, 4-triazole-1- yl) hexan-2-ol	PP 523, Anvil	Agricultural
Imazalil*	35554-44-0	Dichlorophenyl)-2-(2- propenyloxy) ethyl)- 1H-imidazole	Deccozil, Flo-Pro IMZ, Nuzone, Freshgard (Fungicide), Fungaflor, Bromazil	Agricultural
Itraconazole	84625-61-6	(+)- 1 - sec - butyl - 4 - [p - [4 - [p - [[(2R*, 4S*) - 2 - (2, 4 - dichlorophenyl) - 2 - (1H - 1, 2, 4 - triazol - 1 - yl methyl) - 1, 3 - dioxolan - 4 - yl] methoxy] phenyl] - 1 - piperazinyl] phenyl] - Δ^2 - 1, 2, 4 - triazolin - 5 - 1	Sporanox Sporanos; Sporonox Oriconazole Itrizole Triasporn Sporal	Pharmaceutical- For treatment of Malessezia/Yeast Dermatitis, Blastomycosis, Cryptococcosis, Histoplasmosis, Aspergillosis, Candidiasis, and Coccidiomycosis
Ketoconazole	65277-42-1	(±)-cis-1-Acetyl-4- [p- [[2-(2,4- dichlorophenyl)-2- (imidazol-1-ylmethyl)- 1,3-dioxolan-4-yl] methoxy] phenyl] piperazine,	Nizoral	Pharmaceutical-For treatment of candidiasis, chronic mucocutaneous candidiasis, candiduria, histoplasmosis, chromomycosis, oral thrush, blastomycosis, coccidioidomycosis, paracoccidioidomycosis, and recalcitrant cutaneous dermatophyte infections not responding to other therapy.
Metconazole	125116-23-6	Cyclopentanol, 5-[(4- chlorophenyl) methyl]- 2,2-dimethyl-1- (1H-1, 2, 4-triazol-1-ylmethyl)		Agricultural

	CAS Registration #	Scientific Name	Trade Names	Uses
Myclobutanil*	88671-89-0	Butyl-alpha- (4-chlorophenyl)-1H-1, 2, 4-triazole-1-propanenitrile	Sythane, RH 3866, Rally	Agricultural
Penconazole	66246-88-6	Triazole, 1-(2-(2,4-dichlorophenyl)pentyl)-	CGA-71818, Award Fungicide, Topas Plus Fungicide, Topas 10W Fungicide, Topas, Award	Agricultural
Prochloraz	67747-09-5	Propyl-n-2- (2, 4, 6-trichlorophenoxy) ethyl-1H-imidazole-1-carboxamide		Agricultural
Propiconazole	60207-90-1	Dichlorophenyl)-4-propyl -1, 3-dioxolan-2-yl) methyl)-1H-1, 2,4-triazole	Tilt, Desmel, Banner, CGA-64250	Agricultural
Tebuconazole	107534-96-3	Triazole-1-ethanol, alpha- (2-(4-chlorophenyl) ethyl)-alpha - (1,1-dimethylethyl)-, (+-),	Folicular Technical Lynx 1.2 Turf Fungicide, Folicular 1.2 EC Foliar Fungicide	Agricultural
Triadimefon*	43121-43-3	Chlorophenoxy)-3,3-dimethyl-1-(1H-1,2,4-triazol-1-yl)-2-butanone	Bayleton, Amiral, BAY MEB 6447, MEB 6447	Agricultural
Triadimenol*	55219-65-3	Chlorophenoxy)-alpha-(1,1-dimethylethyl)-1H-1,2,4-triazole-1-ethanol	Bay KWG 0519, Bayfidan, Summit, TriBaytan	Agricultural
Triticonazole	131983-72-7	Chlorophenyl) methylene]-2,2-dimethyl-1- (1H-1,2,4-triazol-1-ylmethyl) cyclopentanol		Agricultural
Uniconazole	83657-17-4	Chlorophenyl)-4,4-dimethyl-2- (1,2,4-triazol-1-yl)-pent-1-ene-3-ol	XE-1019D Technical, Ortho Prunit Tree Growth Regulator, S-3307	Agricultural; Plant Growth Regulator
Voriconazole		(2R, 3S)-2-(2,4-difluorophenyl)-3-(5-fluoropyrimidin-4-yl)-1-(1,2,4-triazol-1-yl)butan-2-ol)	Vfend	Pharmaceutical- For treatment of fungal infections caused by <i>Candida</i> spp., <i>Aspergillus</i> spp., <i>Cryptococcus neoformans</i> , <i>Blastomyces dermatitidis</i> , <i>Coccidioides immitis</i> , <i>Histoplasma capsulatum</i> , <i>Fusarium</i> spp., and <i>Penicillium marneffe</i>

- Indicates chemical detected in food samples tested by Food and Drug Administration Pesticide
- Program Residue Monitoring 1999. Red lettering indicates chemical used in this study.

Table 2: Rat blood differentially expressed genes identified in Microarray data that encode enzymes.

Gene	GB Accession #	Entrez Gene ID#	Description	Gene Product Function
1) Rat odorant metabolizing protein (RY2D1)	M76733	259233	A homologue of rat glutathione peroxidase, an enzyme involved in cellular detoxification pathways. It has been proposed that olfactory-specific detoxification enzymes may terminate diverse odorant signals, enabling new signals to be received. The primary termination signal in olfactory transduction is most likely initiated at the receptor site itself by removal of the odorant from the receptor at the cilia surface. The predicted RY2D1 protein is unlikely to be secreted from the Bowman's glands and, therefore, would not contribute to such a process. The expression of presumptive detoxification enzymes in the subepithelial Bowman's glands suggests that they could encounter odorants that are present in the mucus layer but have not accessed ciliary receptor sites. Consequently, these enzymes may contribute to the clearance of such odorants from the neuroepithelium, thereby preventing the initiation of new olfactory signals from residual odorant molecules. Alternatively, these enzymes may act as a primary defense against potentially harmful odorants by metabolizing them into less harmful compounds. (Dear et al., 1991).	Oxidoreductase Peroxidase
2) Thioredoxin-like 2 (Txnl2)	NM_032614	58815	Txl-2 mRNA is ubiquitously expressed, with testis and lung having the highest levels of expression. Light and electron microscopy have shown that the protein is associated with microtubular structures such as lung epithelial cilia and the manchette of and axoneme of spermatids. Txl-2 binds microtubules and might be a novel regulator of microtubule physiology. The prominent expression of Txl-2 in microtubular structure in lung and testis may make a candidate gene for diseases such as primary ciliary dyskinesia (PCD), an autosomal recessive disorder characterized by a failure of proper ciliary and flagellar movement. Txl-2's axonemal localization in sperm flagella and lung cilia indicates that it is a component of the axonemal machinery taking part in regulation of ciliary and flagellar movement and that it is a potential susceptibility gene involved in the PCD phenotype. (Sadek et al, 2003).	Oxidoreductase
3) Vacuolar proton-ATPase subunit M9.2 (aliases Atp6k, Atp6vOe)	AB037248	94170	The vacuolar H ⁺ -ATPase (V-ATPase) is one of the most fundamental enzymes in nature. It functions in almost every eukaryotic cell and energizes a wide variety of organelles and membranes. V-ATPases function exclusively as ATP-dependent proton pumps. The pmf generated by V-ATPases in organelles and membranes of eukaryotic cells is utilized as a driving force for numerous secondary transport processes. The V-ATPases play a major role as energizers of animal plasma membranes, especially apical plasma membranes of epithelial cells. This role was first recognized in plasma membranes of lepidopteran midgut and vertebrate kidney. The list of animals with plasma membranes that are energized by V-ATPases now includes members of most, if not all, animal phyla. This includes the classical Na ⁺ absorption by frog skin, male fertility through acidification of the sperm acrosome and the male reproductive tract, bone resorption by mammalian osteoclasts, and regulation of eye pressure. V-ATPase may function in Na ⁺ uptake by trout gills and energizes water secretion by contractile vacuoles in Dictyostelium. V-ATPase was first detected in organelles connected with the vacuolar system. It is the main if not the only primary energy source for numerous transport systems in these organelles. The driving force for the accumulation of neurotransmitters into synaptic vesicles is pmf generated by V-ATPase. The acidification of lysosomes, which are required for the proper function of most of their enzymes, is provided by V-ATPase. The enzyme is also vital for the proper function of endosomes and the Golgi apparatus. (Nelson et al, 1999)	Hydrotase, Nucleotide Phosphatase
4) C-terminal binding protein 2 (CTBP2)	AF222712	81717	This gene produces two transcripts encoding two distinct proteins. One protein is a transcriptional repressor, while the other isoform is a major component of specialized synapses known as synaptic ribbons. Both proteins contain a NAD ⁺ binding domain similar to NAD ⁺ -dependent 2-hydroxyacid dehydrogenases. A portion of the 3' untranslated region was used to map this gene to chromosome 21q21.3; however, it was noted that similar loci elsewhere in the genome are likely. Blast analysis shows that this gene is present on chromosome 10. (Ariadne Genomics) CtBP2 is known to be present in adult human heart, pancreas, intestine, colon and spleen. (Katsanis et al., 1998)	Oxidoreductase Dehydrogenase

Table 2 continued: Rat blood Differentially expressed genes identified in Microarray data that encode enzymes.

Gene	GB Accession #	Entrez Gene ID#	Description	Gene Product Description
5) Choroideremia (Chm)	NM_017067	24942	Choroideremia is an X-chromosome-linked disease that leads to the degeneration of the choriocapillaris, the retinal pigment epithelium and the photoreceptor layer in the eye. The gene product defective in choroideremia, CHM, is identical to Rab escort protein 1 (REP1). CHM/REP1 is an essential component of the catalytic geranylgeranyltransferase II complex (GGTrII) that delivers newly synthesized small GTPases belonging to the RAB gene family to the catalytic complex for post-translational modification. CHM/REP family members are evolutionarily related to members of the guanine nucleotide dissociation inhibitor (GDI) family, proteins involved in the recycling of Rab proteins required for vesicular membrane trafficking through the exocytic and endocytic pathways, forming the GDI/CHM superfamily. (Alory et al., 2001).	Transferase, Acyltransferase
6) Septin-like protein (aliases Slpa, Msf)	NM_031837	83788	Septins are a family of phylogenetically conserved proteins, which share a common GTPase motif and can form homodimeric heteromers <i>in vitro</i> . They were first discovered in yeast and subsequently detected in most eukaryotic organisms including other fungi, fruit fly, rat, mouse and man, but not in plants. Septins are involved in defining the cleavage plane during cell division, and play a direct role in cytokinesis from yeast to mammals. Recent reports on the presence of septins in postmitotic cells suggest that a more general role of this protein family has to be considered. The detection of septins in the exocytosis complex of presynaptic vesicles and in postsynaptic membranes gave rise to the assumption that septins rather act as active scaffolds for other proteins at sites of membrane remodeling. Because of the presence of a conserved GTP-binding domain, members of the septin family may be participants of a signaling net network involving, for example, Nim 1-related kinases in yeast. Clinical implications have been shown for the septin genes <i>MSF</i> (MLL septin-like fusion) and <i>hCDCrel-1</i> as fusion partner genes of <i>MLL</i> in therapy-related acute myeloid leukemia. The corresponding fusion proteins are likely to affect cytokinesis and may play a role in the progression of the disease. (Jackisch et al., 2000).	Small GTPase, Hydrolase
7) Carbonic anhydrase 3 (Ca3)	NM_019292	54232	Carbonic anhydrase III (CAIII) is a member of a multigene family (at least six separate genes are known) that encode carbonic anhydrase isozymes. These carbonic anhydrases are a class of metalloenzymes that catalyze the reversible hydration of carbon dioxide and are differentially expressed in a number of cell types. The expression of the CA3 gene is strictly tissue specific and present at high levels in skeletal muscle and much lower levels in cardiac and smooth muscle. A proportion of carriers of Duchenne muscle dystrophy have a higher CA3 level than normal. The gene spans 10.3 kb and contains seven exons and six introns. (Ariadne Genomics)	Lyase, Dehydratase
8) Serine/threonine kinase 10 (Lymphocyte Oriented Kinase)	NM_019206	29398	Designated <i>lok</i> (lymphocyte-oriented kinase), it encodes a 966-amino acid protein kinase whose catalytic domain at the N terminus shows homology to that of the STE20 family members involved in mitogen-activated protein (MAP) kinase cascades. The non-catalytic domain of LOK does not have any similarity to that of other known members of the family. There is a proline-rich motif with Src homology region 3 binding potential, followed by a long coiled-coil structure at the C terminus. LOK is expressed as a 130-kDa protein, which was detected predominantly in lymphoid organs such as spleen, thymus, and bone marrow, in contrast to other mammalian members of the STE20 family. LOK phosphorylated itself as well as substrates such as myelin basic protein and histone IIA on serine and threonine residues but not on tyrosine residues, establishing LOK as a novel serine/threonine kinase. When coexpressed in COS7 cells with the known MAP kinase isoforms (ERK, JNK, and p38), LOK activated none of them in contrast to PAK- and GCK-related kinases. These results suggest that LOK could be involved in a novel signaling pathway in lymphocytes, which is distinct from the known MAP kinase cascades. (Kuramochi et al., 1997)	Kinase

Table 2 continued: Rat blood differentially expressed genes identified in Microarray data that encode enzymes.

Gene	GB Accession #	Entrez Gene ID#	Description	Function
9) Protein kinase, amp-activated, gamma 1 non-catalytic subunit (Prkag1)	NM_013010	25520	Mammalian AMP-activated protein kinase (AMPK) is activated by stresses, which deplete ATP, leading to a rise in the AMP: ATP ratio within the cell. AMP activates AMPK allosterically and ATP antagonizes this effect. In addition, AMPK is activated by phosphorylation catalysed by an upstream kinase, the AMP-activated protein kinase kinase (AMPKK), which is itself activated by AMP. AMP has also been shown to activate AMPK by making it a better substrate for AMPKK and a worse substrate for protein phosphatases. These effects make AMPK acutely sensitive to changes in the AMP: ATP ratio and have led to the suggestion that AMPK may act as a cellular fuel gauge. Once activated, AMPK switches off a number of ATP-consuming pathways, including fatty acid and cholesterol synthesis, thereby conserving the immediate energy expenditure of the cell. Another consequence of AMPK activation that is beginning to emerge is an increase in the supply of fuel, or ATP, available to the cell. AMPK increases the rate of fatty acid oxidation by inactivating acetyl-CoA carboxylase and causing a decrease in malonyl-CoA. Recently, evidence has accumulated indicating that AMPK may also increase the rate of glucose oxidation in muscle by increasing the rate of glucose transport. Taken together, these findings suggest that the AMPK cascade plays an important role in restoring the energy balance of the cell in response to a decrease in ATP during periods of cellular stress. (Cheung et al., 2000)	Kinase
10) Cytochrome P450 IIA2 (alias CYP2A21)	NM_012693	24895	Cytochrome P450IIA2 hydroxylates testosterone at eight positions on the molecule, with one of the most abundant metabolites being 15 alpha-hydroxytestosterone. (Hanioka et al., 1990)	Oxidoreductase Oxygenase
11) Ornithine aminotransferase (alias Oat)	NM_022521	64313	OAT encodes the mitochondrial enzyme ornithine aminotransferase, which is a key enzyme in the pathway that converts arginine and ornithine into the major excitatory and inhibitory neurotransmitters glutamate and GABA. Mutations that result in a deficiency of this enzyme cause the autosomal recessive eye disease Gyrate Atrophy. (Ariadne Genomics). Ornithine aminotransferase was found to be very low in fetal tissues and undifferentiated transplanted neoplasms and higher in slow growing hepatomas and in liver, kidney, and intestine. The relatively high level in adult kidney developed with a sex difference, which led to the discovery that estrogen increased the postnatal accumulation of ornithine aminotransferase. (Heinzfeld et al., 1968).	Transaminase Transferase
12) Alcohol dehydrogenase I (alias Adh, Adh1)	M15327	24172	This gene encodes class I alcohol dehydrogenase, alpha subunit, which is a member of the alcohol dehydrogenase family. Members of this enzyme family metabolize a wide variety of substrates, including ethanol, retinol, other aliphatic alcohols, hydroxysteroids, and lipid peroxidation products. Class I alcohol dehydrogenase, consisting of several homo- and heterodimers of alpha, beta, and gamma subunits, exhibits high activity for ethanol oxidation and plays a major role in ethanol catabolism (Ariadne Genomics).	Oxidoreductase, Dehydrogenase
13) Serine protease gene	L38482			Protease
14) Arachidonic acid epoxygenase	NM_031839	83790	Arachidonic acid epoxygenase catalyzes the NADPH-dependent conversion of arachidonic acid to a mixture of epoxyeicosatrienoic acids in arachidonic acid metabolism (Imaoka et al.). Epoxyeicosatrienoic acids (EETs), which are synthesized from arachidonic acid by cytochrome P450 epoxygenases, function primarily as autocrine and paracrine effectors in the cardiovascular system and kidney (Spector et al., 2004).	Oxidoreductase, Oxygenase

Table 2 continued: Rat blood differentially expressed genes identified in Microarray data that encode enzymes.

Gene	GB Accession #	Entrez Gene ID#	Description	Function
15) Pyruvate dehydrogenase E1a alpha like (alias Pdha1)	U44125	117098	The prostate gland of humans and other animals has the unique function of accumulating and secreting extraordinarily high levels of citrate. The prostate secretory epithelial cells synthesize citrate which, due to a limiting mitochondrial (m-) aconitase, accumulates rather than being oxidized. Thus citrate is essentially an end product of metabolism in prostate. For continued net citrate production, a continual source of oxaloacetate (OAA) and acetyl CoA is required. Glucose via pyruvate oxidation provides the source of Acetyl CoA. In prostate cells, citrate production is regulated by testosterone and/or by prolactin. Both hormones selectively regulate the level and activity of pyruvate dehydrogenase E1 alpha (E1a) in animal prostate cells; thereby regulating the availability of acetyl CoA for citrate synthesis (Costello et al., 2000).	Oxidoreductase, Dehydrogenase
17) N-acetyltransferase-2 (alias Nat2)	U01348	116632	The N-acetyltransferases catalyze acetylation of aromatic amines and hydrazines, which include carcinogenic compounds and therapeutic drugs. Many of the drugs are commonly used and include isoniazid, dapsone, procainamide, and sulfamethazine. Carcinogens metabolized by N-acetyltransferase include 2-naphthylamine, 2-aminofluorene, 4-aminobiphenyl, and benzidine. Thus, N-acetylation can modulate drug activities and detoxify carcinogens. (Gross et al., 1999).	Acetyltransferase, Transferase
18) Phosphotriesterase-related (Pter) (alias Rpr1, Rpr-1)	NM_022224	63852	Resiniferatoxin-binding, phosphotriesterase-related protein binds resiniferatoxin, which desensitizes nociceptive neurons and may play a role in resiniferatoxin toxicity. It has similarity to bacterial phosphotriesterases, which catalyze the hydrolysis of phosphotriester-containing organophosphate pesticides. (Davies et al., 1997).	Phosphotriesterase

Table 3: Rat blood differentially expressed genes identified in Microarray data that encode G protein coupled receptors and G proteins.

Gene	GB Accession #	Entrez Gene ID#	Description	Gene Product Function
1) Macrophage inflammatory protein-1 alpha receptor (Ccr1)	NM_020542	57301	The macrophage inflammatory protein-1 alpha (MIP-1alpha) belongs to the chemokine subfamily containing a cysteine-cysteine motif ("CC chemokines"). MIP-1alpha is chemoattractive to monocytes, neutrophils, eosinophils, dendritic cells, NK, and T cells. MIP-1alpha exerts a potent antitumoral effect because of its ability to recruit immune cells at the tumor site. Indeed, tumor cells engineered to express MIP-1alpha possess a reduced tumorigenicity <i>in vivo</i> , an effect attributed to the recruitment of macrophages and neutrophils at the tumor site. MIP-1alpha also elicited a long-term immune response, which resulted in the protection of the animals against challenge with the parental tumor cells (Nakashima et al., 1996).	Receptor; G-protein coupled receptor
2) Nociceptin receptor ORL1 gene	AF178674	29256	Opioid receptor-like protein ORL1, is a member of the G protein-coupled, seven-transmembrane receptor super-family. ORL1 possesses a very high sequence-homology to all three types of opioid receptors at both the nucleotide level and the amino acid level (60%). It is demonstrated that ORL1 is the receptor for nociceptin (noc) (also named orphanin FQ), a heptadeca-peptide that significantly resembles the opioid peptide dynorphin A (dyn A). Noc receptor ORL1, upon the binding of noc, activates inhibitory G proteins to inhibit adenylyl cyclase and in turn to inhibit the production of second messenger cyclic AMP (cAMP). ORL1 mediates a variety of physiological and pharmacological actions, including the modulation of nociceptin and locomotion, the modification of long-term potentiation and spatial learning, and the regulation of auditory system. (Xie et Al., 2000).	Receptor; G-protein coupled receptor
3) Melanocortin 5 receptor (Mc5r)	NM_013182	25726	The melanocortin 5 receptor (MC5-R) mediates increase in cAMP accumulation with a characteristic pharmacology. Very low expression levels have been detected in brain, while high levels are found in adrenals, stomach, lung and spleen. In situ hybridization studies have also shown the MC5 receptor to be expressed in the three layers of the adrenal cortex, predominantly in the aldosterone-producing zona glomerulosa cells (Griffon et al, 1994). Melanocortins (αMSH and ACTH-related peptides) influence the physiological functions of certain peripheral organs, including exocrine and endocrine glands. MC5-R messenger RNA was found in exocrine glands, including lacrimal, Harderian, preputial, and prostate glands and pancreas, as well as in adrenal gland, esophagus, and thymus, as demonstrated by ribonuclease protection assays. In exocrine glands, MC5-R messenger RNA expression was restricted to secretory epithelia. MC5 receptor is commonly and selectively expressed in exocrine glands and other peripheral organs. A functional coherence is suggested between central and peripheral actions of melanocortins and melanocortin receptors in physiological functions, including thermoregulation, immunomodulation, and sexual behavior. (van der Kraan et Al., 1998).	Receptor; G-protein coupled receptor
4) Putative pheromone receptor (Go-VN3) mRNA	AF016180	286983	Mammals have retained two functionally and anatomically independent collections of olfactory neurons located in the main olfactory epithelium and in the vomeronasal organ (VNO). Pheromones activate the VNO in order to elicit fixed action behaviors and neuroendocrine changes involved in animal reproduction and aggression. Differential screening of cDNA libraries constructed from individual rat VNO neurons has led to the isolation of a novel family of z100 genes encoding seven transmembrane receptors with sequence similarity with Ca21-sensing and metabotropic glutamate receptors. These genes are likely to encode a novel family of pheromone receptors. Patterns of receptor gene expression suggest that the VNO is organized into discrete and sexually dimorphic functional units that may permit segregation of pheromone signals leading to specific arrays of behaviors and neuroendocrine responses (Herrada et al., 1997).	Receptor; G-protein coupled receptor

Table 3 continued: Rat blood differentially expressed genes identified in Microarray data that encode G protein coupled receptors and G proteins.

Gene	GB Accession #	Entrez Gene ID#	Description	Gene Product Function
5) Guanine nucleotide binding protein, alpha transducing 3 (gnat3)	X65747	286924	A novel G protein alpha-subunit (alpha-gustducin) has been identified and cloned from taste tissue. Alpha-Gustducin messenger RNA is expressed in taste buds of all taste papillae (circumvallate, foliate and fungiform); It is not expressed in non-sensory portions of the tongue, nor is it expressed in the other tissues examined. Alpha-Gustducin most closely resembles the transducins (the rod and cone photoreceptor G proteins), suggesting that gustducin's role in taste transduction is analogous to that of transducin in light transduction. (McLaughlin et Al., 1992).	Select regulatory molecule; Large G-protein; G-protein
6) Chimerin (chimaerin) 1 (Chn1)	NM_032083	84030	Chimerin is a GTPase-activating protein specific for Rac and Cdc42 and is a p35-binding protein. Chimerin has a regulatory function in actin repolymerization. Regulation of neurocytoskeleton dynamics by Cdk5 is mediated at least in part by chimerin (Qi et al., 2004).	Select regulatory molecule; G-protein modulator

Table 4: Rat blood differentially expressed genes identified in Microarray data that encode proteins involved in nucleic acid binding and that act as transcription factors.

Gene	GB Accession #	Entrez Gene ID#	Description	Gene Product Function
1) Histone 2a	NM_021840	64646	Histones are basic nuclear proteins that are responsible for the nucleosome structure of the chromosomal fiber in eukaryotes. Nucleosomes consist of approximately 146 bp of DNA wrapped around a histone octamer composed of pairs of each of the four core histones (H2A, H2B, H3, and H4). The chromatin fiber is further compacted through the interaction of a linker histone, H1, with the DNA between the nucleosomes to form higher order chromatin structures. This gene encodes a replication-independent member of the histone H2A family that is distinct from other members of the family. Studies in mice have shown that this particular histone is required for embryonic development and indicate that lack of functional histone H2A leads to embryonic lethality. (Ariadne Genomics).	Histone; Nucleic acid binding
2) Pituitary tumor-transforming 1 (Pttg1) (alias Pttg)	NM_022391	64193	The encoded protein is a homolog of yeast securin proteins, which prevent separins from promoting sister chromatid separation. It is an anaphase-promoting complex (APC) substrate that associates with a separin until activation of the APC. The gene product has transforming activity in vitro and tumorigenic activity in vivo, and the gene is highly expressed in various tumors. The gene product contains 2 PXXP motifs, which are required for its transforming and tumorigenic activities, as well as for its stimulation of basic fibroblast growth factor expression. It also contains a destruction box (D box) that is required for its degradation by the APC. The acidic C-terminal region of the encoded protein can act as a transactivation domain. The gene product is mainly a cytosolic protein, although it partially localizes in the nucleus. (Ariadne Genomics)	Transcription factor; Nucleic acid binding
3) Paired-like homeodomain transcription factor 3 (Pitx3)	NM_019247	29609	This gene encodes a member of the RIEG/PITX homeobox family, which is in the bicoid class of homeodomain proteins. Members of this family act as transcription factors. Mutations of this gene have been associated with anterior segment mesenchymal dysgenesis (ASMD) and congenital cataracts. This protein is involved in lens formation during eye development. (Ariadne Genomics).	Homeobox transcription factor; Transcription factor
4) H2A histone family, member Z (H2afz)	NM_022674	58940	Histones are basic nuclear proteins that are responsible for the nucleosome structure of the chromosomal fiber in eukaryotes. Nucleosomes consist of approximately 146 bp of DNA wrapped around a histone octamer composed of pairs of each of the four core histones (H2A, H2B, H3, and H4). The chromatin fiber is further compacted through the interaction of a linker histone, H1, with the DNA between the nucleosomes to form higher order chromatin structures. This gene encodes a replication-independent member of the histone H2A family that is distinct from other members of the family. Studies in mice have shown that this particular histone is required for embryonic development and indicate that lack of functional histone H2A leads to embryonic lethality. (Ariadne Genomics).	Histone; Nucleic acid binding
5) MAD homolog 2 (drosophila) (Madh2) (alias Smad2)	NM_019191	29357	Transcriptional modulator activated by TGF-beta and activin type 1 receptor kinase. SMAD2 is a receptor-regulated SMAD (R-SMAD). May act as a tumor suppressor in colorectal carcinoma. Expressed at high levels in skeletal muscle, heart and placenta. (Takenoshita et al., 1998).	Transcription factor
6) Ribosomal protein S11 (Rps11)	NM_031110	81774	Ribosomes, the organelles that catalyze protein synthesis, consist of a small 40S subunit and a large 60S subunit. Together these subunits are composed of 4 RNA species and approximately 80 structurally distinct proteins. This gene encodes a ribosomal protein that is a component of the 40S subunit. The protein belongs to the S17P family of ribosomal proteins. It is located in the cytoplasm. The gene product of the E. coli ortholog (ribosomal protein S17) is thought to be involved in the recognition of termination codons. This gene is co-transcribed with a small nucleolar RNA gene, which is located in its third intron. As is typical for genes encoding ribosomal proteins, there are multiple processed pseudogenes of this gene dispersed through the genome. (Ariadne Genomics).	Nucleic acid binding; Ribosomal protein

Table 5: Rat blood differentially expressed genes encoding binding and transport proteins.

Gene	GB Accession #	Entrez Gene ID#	Description	Gene Product Function
Tropomyosin 1 (alpha) (Tpm1)	M34136	24851	Tropomyosins are ubiquitous proteins of 35 to 45 kD associated with the actin filaments of myofibrils and stress fibers. In vertebrates, 4 known tropomyosin genes code for diverse isoforms that are expressed in a tissue-specific manner and regulated by an alternative splicing mechanism. The vertebrate alpha-tropomyosin gene consists of 15 exons; 5 exons are found in all transcripts, while 10 exons are alternatively used in different alpha-tropomyosin RNAs. The striated muscle isoform is expressed in both cardiac and skeletal muscle tissues (Lees-Miller et al., 1991).	Cytoskeletal protein; Actin family cytoskeletal protein; Non-motor actin binding protein
Syntenin (aliases Sdcbp, mda-9, TACIP1 8)	NM_031986	83841	Syntenin is a PDZ protein that binds the cytoplasmic C-terminal FYA motif of the syndecans. Syntenin is widely expressed. In cell fractionation experiments, syntenin partitions between the cytosol and microsomes. Immunofluorescence microscopy localizes endogenous and epitope-tagged syntenin to cell adhesion sites, microfilaments, and the nucleus. These results suggest a role for syntenin in the composition of adherens junctions and the regulation of plasma membrane dynamics, and imply a potential role for syntenin in nuclear processes. (Zimmermann et Al., 2001).	Other transfer/carrier protein; Transfer/carrier protein;
Retinol-binding protein 2, cellular (Rbp2)	NM_012640	24710	RBP2 is an abundant protein present in the small intestinal epithelium. It is thought to participate in the uptake and/or intracellular metabolism of vitamin A. Vitamin A is a fat-soluble vitamin necessary for growth, reproduction, differentiation of epithelial tissues, and vision. RBP2 may also modulate the supply of retinoic acid to the nuclei of endometrial cells during the menstrual cycle. (Demmer et al, 1987).	Transfer/carrier protein
Group-specific component (Gc)	NM_012564	24384	Vitamin D-binding protein (DBP) is a monomeric, multifunctional glycoprotein first identified as the group-specific component of serum or Gc-globulin. It is essential to the transport of vitamin D sterols in the blood and to the removal of plasma actin monomers released to the blood subsequent to tissue damage. DBP also contributes to complement C5a-mediated chemotaxis, macrophage activation, and fatty acid transport. The <i>DBP</i> gene is a member of the multigene family that includes albumin, alpha-fetoprotein, and alpha-albumin. The members of this gene family are tightly linked on chromosome 4 in human and chromosome 14 in rat (r) and encode proteins with conservation of both primary and secondary structures. All four genes in this family are predominantly expressed in the liver. During embryonic development, expression of the rat albumin, alpha-fetoprotein, and <i>DBP</i> genes is induced in the yolk sac and maintained in the fetal liver, whereas alpha-albumin expression begins in the liver during the subsequent perinatal period. Alpha-Fetoprotein is selectively silenced at the end of the fetal period, whereas alpha-albumin, albumin, and DBP expression remains high in the liver throughout adult life (Song et Al., 1998).	Transfer/carrier protein; Cytoskeletal protein; Actin family cytoskeletal protein; Non-motor actin binding protein
Matrin 3 (Matr3)	NM_01949	29150	The protein encoded by this gene is localized in the nuclear matrix. It may play a role in transcription or may interact with other nuclear matrix proteins to form the internal fibrogranular network. (Ariadne Genomics).	Transporter

Table 6: Rat blood differentially expressed genes identified in microarray data that encode immune related proteins.

Gene	GB Accession #	Entrez Gene ID#	Description	Gene Product Function
Chemokine (C-X3-C motif) ligand 1 (3c3c11) (aliases Cx3c, Scyd1)	AF30358	89808	Abbr. FKN or FK. Fractalkine exists as a 95 kDa secreted glycoprotein and in a membrane anchored form. The soluble form is a potent chemoattractant for T-cells and monocytes but not for neutrophils. Fractalkine thus is capable of controlling the key regulatory mechanisms of cell trafficking at sites of inflammation. Antigen-presenting cells in psoriasis express high levels of Fractalkine and may contribute to the accumulation of T-cells at sites of psoriasis lesions (Raychaudhuri et al, 2001) Vascular endothelial cells produce Fractalkine in response to IFN-gamma (Imaizumi et al, 2004). Soluble Fractalkine enhances NK-cell cytolytic activity and may play an important role in the binding of NK-cells to endothelial cells and in NK-cell mediated endothelium damage (Yoneda et al., 2003). The expression of Fractalkine in rat aortic endothelial cells is induced by IL1-beta, TNF-alpha, and bacterial lipopolysaccharides and involves activation of transcription factor NF-kappa-B (Garcia et al, 2000). Fractalkine is expressed in resting or activated peripheral blood mononuclear cells, T-cells, B-cells, or NK-cells. Interactions between Fractalkine and its receptor mediate the rapid capture, integrin-independent firm adhesion, and activation of circulating leukocytes under flow (Fong et al., 1998). Fractalkine induces firm adhesion between monocytes and endothelial cells by interactions with membrane-bound forms of Fractalkine and its receptor on monocytes and also through activation of integrin avidity for their ligands (Goda et al., 2000).	Chemokine; Signaling molecule
Myxovirus (influenza) resistance, homolog of marine Mx (also interferon-inducible protein IFI78)	NM_017028	24575	Mouse homolog is an interferon inducible gene that confers influenza resistance to mice (also formerly known as interferon-inducible protein IFI78) (Pavlovic et al., 1990).	Interferon inducible protein
Beclin 1 (coiled-coil, myosin-like Bcl2 interacting protein (Becn1)	AY033824	114558	The cellular antiapoptotic gene <i>bcl-2</i> represents a novel class of antiviral host defense molecules, which function both by restricting viral replication and by preventing virus-induced cell death. Bcl-2 blocks apoptosis in vitro induced by several different RNA viruses, including Sindbis virus, influenza virus, reovirus, Semliki Forest virus, LaCrosse virus, and Japanese B encephalitis virus. It has been shown that Bcl-2 over expression in virally infected neurons in vivo also protects mice against fatal encephalitis caused by the prototypic alpha virus, Sindbis virus. The protective effects of Bcl-2 against fatal Sindbis virus encephalitis were associated with a reduction both in neuronal apoptotic death and in central nervous system (CNS) viral replication. A similar antiviral effect of Bcl-2 over expression has been observed during Sindbis virus infection in cultured AT3 cells as well as during influenza virus infection of MDCK cells, Japanese B encephalitis virus infection of N18 cells, and Semliki Forest virus infection of AT3 cells. Although the role of endogenous Bcl-2 in antiviral defense has yet to be evaluated, these studies support the hypothesis that Bcl-2 may be important in protecting cells against viral infections (Liang et Al., 1998).	Antiviral defense molecule

Table 7: Rat blood differentially expressed genes identified in microarray data that encode for peptide hormones.

Gene	GB Accession #	Entrez Gene ID#	Description	Gene Product Function
Decidual trophoblast prolactin-related protein (Dtprp) (aliases Dprp, d/tPRP)	NM_022846	24315	Decidual tissue represents a specialized uterine compartment arising in association with implantation of the rodent embryo. During its development, decidual cells completely surround the post implantation embryo and are situated in direct contact with trophoblast cells at the maternal-embryo interface. It has long been speculated that the decidua plays a critical role in the establishment of pregnancy, but knowledge concerning the exact mechanism(s) by which it does so is limited. Postulated functions of decidual cells include 1) providing a nutritive role in maintenance of the embryo before development of the fetal circulatory system, 2) limiting invasion of trophoblast cells into the uterus, 3) preventing immunological rejection of the fetal allograft, and 4) producing hormones that act in paracrine or endocrine modes to influence the functions of embryonic, extra embryonic, or maternal tissues. The latter function is probably fundamental to each of the responsibilities of decidual cells. Decidual prolactin related protein (dPRP) was first identified in rat decidual tissue based on its homology with members of the placental PRL family. The dPRP protein and complementary DNA (cDNA) have been isolated and characterized. dPRP is a 29-kDa glycoprotein with approximately 70% amino acid sequence homology to a member of the placental PRL family, PRL-like protein C (PLP-C). In addition, evidence exists for the presence of a rat decidual protein related to PRL possessing actions on the ovary and uterus. (Rasmussen et al., 1996).	Peptide hormone; Signaling molecule
Galanin (Gal) (alias Galn)	J03624	29141	Contracts smooth muscle of the gastrointestinal and genitourinary tract, regulates growth hormone release, modulates insulin release, and may be involved in the control of adrenal secretion. (Ariadne Genomics).	Peptide hormone; Signaling molecule
Variable coding sequence A2 (Vcsa2)	X77817	289526	The first described VCSA gene (Rn. VCSA1) was found to encode a prohormone-like protein named SMR1 (-VA1), expressed mainly in the submandibular glands (SMG) of male rats (Ariadne Genomics).	

Table 8: Rat blood differentially expressed genes identified in microarray data that encode ion channels.

Gene	GB Accession #	Entrez Gene ID#	Description	Gene Product Function
Potassium voltage-gated channel, subfamily H (eag-related), member 1 (Kcnh1)	NM_031742	65198	Voltage-gated potassium (Kv) channels represent the most complex class of voltage-gated ion channels from both functional and structural standpoints. Their diverse functions include regulating neurotransmitter release, heart rate, insulin secretion, neuronal excitability, epithelial electrolyte transport, smooth muscle contraction, and cell volume. This gene encodes a member of the potassium channel, voltage-gated, subfamily H. This member is a pore-forming (alpha) subunit of a voltage-gated non-inactivating delayed rectifier potassium channel. It is activated at the onset of myoblast differentiation. The gene is highly expressed in brain and in myoblasts. Over expression of the gene may confer a growth advantage to cancer cells and favor tumor cell proliferation. Alternative splicing of this gene results in two transcript variants encoding distinct isoforms. (Ariadne Genomics).	Voltage-gated potassium channel

Table 9: Rat blood differentially expressed genes identified in microarray data that encode proteins that suppress or promote tumorigenesis.

Gene	GB Accession #	Entrez Gene ID#	Description	Gene Product Function
Suppression of tumorigenicity 13 (colon carcinoma) Hsp70-interacting protein (alias St13)	NM_031122	81800	The protein encoded by this gene is an adaptor protein that mediates the association of the heat shock proteins HSP70 and HSP90. This protein has been shown to be involved in the assembly process of glucocorticoid receptor, which requires the assistance of multiple molecular chaperones. The expression of this gene is reported to be down regulated in colorectal carcinoma tissue suggesting that is a candidate tumor suppressor gene. (Ariadne Genomics).	Adaptor Protein
Myeloid/lymphoid or mixed – lineage leukemia (Trithorax (drosophila) homolog); translocated to, 3 (alias Mllt3, Af9, Af-9)	AJ006295	114510	Expression of this transcript is down regulated after puberty in females and can be subsequently up regulated in adults by ovariectomy. Hormone replacement studies have provided direct evidence that rAF-9 mRNA expression is suppressed by estrogen. The cellular AF-9 gene is alternatively expressed in a manner that reflects the presence of translocated, functionally active (oncogenic) AF-9 sequences in leukemias. The use of a novel antisera raised against a rAF-9 peptide demonstrated tissue- and sex-specific expression of a nuclear 41 kDa anterior pituitary protein and has localized this protein to a major population of growth hormone synthesizing cells. By localizing the expression and defining the physiological regulation of rAF-9, studies have provided novel insights into the AF-9 gene that will facilitate an understanding of both oncogenic and endocrine roles. Abnormalities associated with band q23 of human chromosome 11 are involved in over 20% of acute leukemias. A gene termed ALL-1 (MLL or HRX) located at the 11q23 breakpoint region (1) is involved in multiple different translocations that fuse the amino-terminal of ALL-1 to a variety of different partner proteins. A common translocation in acute myeloid leukemia is (p22; q23) in which the AF-9 gene (ALL-1 fused gene from chromosome 9) encodes the oncogenic partner protein. The biological activity of AF-9 has not been completely defined, although studies have demonstrated transcriptional regulatory activity within a carboxyl-terminal domain, which is suggested to be oncogenic in the context of the ALL-1 fusion. (Morgan et al., 2000).	
Wingless-type MMTV integration site family member 2B	AF204873	116466	May be involved in ovarian tumorigenesis (Ariadne Genomics).	

Table 10: Rat blood differentially expressed genes identified in microarray data that encode proteins with various functions.

Gene	GB Accession #	Entrez Gene ID#	Description	Gene Product Function
Peroxisomal biogenesis factor 14 (Pex14)	AB017544	64460	Peroxisomal membrane anchor protein is also known as PEX14. PEX14 interacts with the receptors of both matrix protein import pathways as well as with PEX13 and PEX17 (Girzlinsky et al., 1999). In addition, mammalian cell lines lacking PEX14 display a defect in receptor docking (Shimizu et al., 1999). Taken together, these data suggest that PEX14 is the initial docking site for the receptors at the peroxisome membrane, and that it forms a docking complex with PEX13 and PEX17 (Agne et al., 2003).	Membrane anchor protein
GTP cyclohydrolase I feedback regulatory protein (alias Gchfr)	U85512	171128	GTP cyclohydrolase I feedback regulatory protein (GFRP) mediates feedback inhibition of GTP cyclohydrolase I activity by tetrahydrobiopterin and also mediates the stimulatory effect of phenylalanine on the enzyme activity. (6R)-L-erythro-5, 6, 7, 8-Tetrahydrobiopterin (BH4) 1 is an essential cofactor for aromatic amino-acid hydroxylases and nitric-oxide synthases. The intracellular level of BH4 is sub saturating for these enzyme reactions and thus is thought to be an important regulator of the activities of these enzymes. BH4 is synthesized from GTP by a pathway composed of four enzyme reactions. Most important for regulation of BH4 biosynthesis is GTP cyclohydrolase I, which catalyzes the first and rate-limiting step of the conversion of GTP to dihydroneopterin triphosphate. GTP cyclohydrolase I is present in many organisms, ranging from bacteria to animal. Rat GTP cyclohydrolase I is composed of multiple identical subunits and shows positive cooperativity against GTP. We have recently reported the identification of a new regulatory protein (GFRP) which mediates the feedback inhibition of GTP cyclohydrolase I by the end product of this pathway, BH4. GFRP and BH4 inhibit the enzyme activity of GTP cyclohydrolase I by decreasing its maximum velocity while having little effect on the affinity of GTP, indicating noncompetitive inhibition. GFRP exerts its inhibitory effect on GTP cyclohydrolase I by forming a complex with GTP cyclohydrolase I in the presence of BH4 and GTP. Formation of the complex between the two proteins is reversible, depending on the presence of BH4 and GTP. Furthermore, the inhibition of GTP cyclohydrolase I by GFRP and BH4 is specifically reversed by L-phenylalanine. Phenylalanine is the substrate of phenylalanine hydroxylase, which requires BH4 as a cofactor. (Yoneyama et Al., 1997).	Regulatory Protein
Fibronectin 1 (Fn1) (alias FIBNEC)	NM_019143	25661	This gene encodes fibronectin, a glycoprotein present in a soluble dimeric form in plasma, and in a dimeric or multimeric form at the cell surface and in extracellular matrix. Fibronectin is involved in cell adhesion and migration processes including embryogenesis, wound healing, blood coagulation, host defense, and metastasis. The gene has three regions subject to alternative splicing, with the potential to produce 20 different transcript variants. However, the full-length sequence of only two variants is known. (Ariadne Genomics)	Extracellular matrix linker protein; Extracellular matrix
Saccharomyces cerevisiae Nip7p homolog (alias pEachy)	AF158186	192180		

Table 11: Genes from microarray data that show significant ($p \leq 0.05$) gene expression change in blood. Fold change values of <1 are down regulated, where as fold change values of >1 are up regulated. Normq is quantile normalization. Normq-b is quantile normalization minus background. Reslograt is loess normalization. Reslograt is loess normalization minus background.

Gene	Genebank accession #	P-Value	Fold change
1) Rat odorant-metabolizing protein (RY2D1)	M76733	<i>Hi Myc</i> Normq= .002 Normq-b= .049	<i>Hi Myc</i> Normq= .519 Normq-b= .417
2) Saccharomyces cerevisiae Nip7p homolog (alias pEachy)	AF158186	<i>Hi Myc</i> Loess= .002 -b= .003 <i>Hi Tri</i> Normq= .010 Normq-b= .002 Reslograt= .002 Reslograt-b= .003 <i>Lo Myc</i> Normq-b= .032	<i>Hi Myc</i> Normq= .218 Normq-b= .116 Reslograt= .218 Reslograt-b= .155 <i>Hi Tri</i> Normq= .443 Normq-b= .258 Reslograt= .359 Reslograt-b= .266 <i>Lo Myc</i> Normq-b= .534
3) Tropomyosin 1 (alpha) (Tpm1)	M34136	<i>Hi Myc</i> Normq= .002 Normq-b= .002 Reslograt= .039 Reslograt-b= .039 <i>Hi Tri</i> Normq= .036 Reslograt= .015 <i>Lo Myc</i> Normq= .041	<i>Hi Myc</i> Normq= .442 Normq-b= .425 Reslograt= .381 Reslograt-b= .502 <i>Hi Tri</i> Normq= .597 Reslograt= .443 <i>Lo Myc</i> Normq= .606
4) Thioredoxin-like 2 (Txnl2)	NM_032614	<i>Hi Tri</i> Reslograt-b= .038	<i>Hi Tri</i> Reslograt-b= 2.514
5) Guanine nucleotide binding protein, alpha transducing 3	X65747	<i>Hi Tri</i> Reslograt= .006 Reslograt-b= .030 <i>Lo Myc</i> Reslograt= .017	<i>Hi Tri</i> Reslograt= 2.592 Reslograt-b= 2.335 <i>Lo Myc</i> Reslograt= 1.763
6) Macrophage Inflammatory protein-1 alpha receptor (Ccr1)	NM_020542	<i>Hi Myc</i> Normq= .003 Normq-b= .008 Reslograt= .008 Reslograt-b= .008 <i>Hi Tri</i> Normq= .031 Normq-b= .023 Reslograt-b= .015 <i>Lo Tri</i> Reslograt= .020 Reslograt-b= .011	<i>Hi Myc</i> Normq= .167 Normq-b= .159 Reslograt= .344 Reslograt-b= .330 <i>Hi Tri</i> Normq= .421 Normq-b= .344 Reslograt-b= .499 <i>Lo Tri</i> Reslograt= 1.569 Reslograt-b= 1.679
7) Rattus norvegicus nociceptin ORL1	AF178674	<i>Hi Myc</i> Normq= .046 Normq-b= .021	<i>Hi Myc</i> Normq= 2.311 Normq-b= 2.818
8) Peroxisomal biogenesis factor 14 (Pex14)	AB017544	<i>Hi Myc</i> Normq= .020	<i>Hi Myc</i> Normq= 2.806

Table 11 continued: Genes from microarray data that show significant ($p \leq 0.05$) gene expression change in blood. Fold change values of <1 are down regulated, where as fold change values of >1 are up regulated. Normq is quantile normalization. Normq-b is quantile normalization minus background. Reslograt is lowess normalization. Reslograt is loess normalization minus background.

Gene	Genebank accession #	P-Value	Fold change
9) C-terminal binding protein 2 (Ctbp2)	AF222712	<i>Hi Myc</i> Normq= .036 Normq-b= .049 Reslograt-b= .039 <i>Lo Myc</i> Normq= .019 Normq-b= .023 Reslograt= .046	<i>Hi Myc</i> Normq= 1.760 Normq-b= 2.032 Reslograt-b= 2.203 <i>Lo Myc</i> Normq= 1.904 Normq-b= 2.299 Reslograt= 1.745
10) Histone 2a	NM_021840	<i>Hi Myc</i> Normq-b= .029 <i>Hi Tri</i> Reslograt= .001 Reslograt-b= .001	<i>Hi Myc</i> Normq-b= .502 <i>Hi Tri</i> Reslograt= .269 Reslograt-b= .260
11) Choroideremia (Chm)	NM_017067	<i>Hi Myc</i> Normq= .013 Normq-b= .007	<i>Hi Myc</i> Normq= .288 Normq-b= .196
12) Septin-like protein (aliases Slpa, Msf)	NM_031837	<i>Lo Myc</i> Normq= .007 Normq-b= .018	<i>Lo Myc</i> Normq= .311 Normq-b= .313
13) Melanocortin 5 receptor (Mc5r)	NM_013182	<i>Hi Myc</i> Reslograt= .028 <i>Hi Tri</i> Reslograt= .009	<i>Hi Myc</i> Reslograt= .323 <i>Hi Tri</i> Reslograt= .380
14) Wingless-type MMTV integration site family member 2B	AF204873	<i>Hi Myc</i> Normq-b= .043 <i>Hi Tri</i> Reslograt= .022 <i>Lo Tri</i> Normq-b= .038 Reslograt-b= .015	<i>Hi Myc</i> Normq-b= 2.102 <i>Hi Tri</i> Reslograt= .463 <i>Lo Tri</i> Normq-b= 2.140 Reslograt-b= 2.546
15) Carbonic Anhydrase 3 (Ca3)	NM_019292	<i>Hi Myc</i> Normq= .007 Normq-b= .006 Reslograt-b= .025	<i>Hi Myc</i> Normq= 5.644 Normq-b= 8.620 Reslograt-b= 6.618
16) Serine/Threonine kinase 10	NM_019206	<i>Hi Myc</i> Normq= .017 Reslograt= .007 Reslograt-b= .029	<i>Hi Myc</i> Normq= 1.338 Reslograt= 1.715 Reslograt-b= 1.570
17) Syntenin (aliases Sdcbp, mda-9, TACIP18)	NM_031986	<i>Hi Myc</i> Normq= .019 Normq-b= .028 Reslograt= .008 Reslograt-b= .008 <i>Hi Tri</i> Normq= .005 Normq-b= .013 Reslograt= .009 Reslograt-b= .017	<i>Hi Myc</i> Normq= 2.578 Normq-b= 2.971 Reslograt= 4.264 Reslograt-b= 5.432 <i>Hi Tri</i> Normq= 2.278 Normq-b= 2.406 Reslograt= 2.711 Reslograt-b= 2.852
18) Decidual trophoblast prolactin-related protein (Dtprp) (aliases Dprp, d/tPRP)	NM_022846	<i>Hi Myc</i> Reslograt= .016 Reslograt-b= .009	<i>Hi Myc</i> Reslograt= 2.225 Reslograt-b= 2.293

Table 11 continued: Genes from microarray data that show significant ($p \leq 0.05$) gene expression change in blood. Fold change values of <1 are down regulated, where as fold change values of >1 are up regulated. Normq is quantile normalization. Normq-b is quantile normalization minus background. Reslograt is loess normalization. Reslograt is loess normalization minus background.

Gene	Genebank accession #	P-Value	Fold change
19) Protein kinase, AMP-activated, gamma 1 non-catalytic subunit (Prkg1)	NM_013010	<i>Hi Tri</i> Normq-b= .014 <i>Lo Tri</i> Normq= .047 Reslograt-b= .025	<i>Hi Tri</i> Normq-b= .272 <i>Lo Tri</i> Normq= 1.586 Reslograt-b= 2.227
20) Rattus norvegicus GTP cyclohydrolase I feedback regulatory protein (alias Gchfr)	U85512	<i>Hi Myc</i> Normq= .025 Reslograt= .027	<i>Hi Myc</i> Normq= 1.812 Reslograt= 1.960
21) Pituitary tumor-transforming 1 (Pttg1) (alias Pttg)	NM_022391	<i>Hi Myc</i> Normq= .007 Normq-b= .008 <i>Hi Tri</i> Normq= .003 Normq-b= .002 Reslograt-b= .023	<i>Hi Myc</i> Normq= .565 Normq-b= .508 <i>Hi Tri</i> Normq= .510 Normq-b= .430 Reslograt-b= .436
22) Cytochrome P450 IIA2 (alias CYP2A21)	NM_012693	<i>Hi Tri</i> Normq= .041 Reslograt-b= .006	<i>Hi Tri</i> Normq= .661 Reslograt-b= .281
23) Myxovirus (influenza) resistance, homolog of murine Mx	NM_017028	<i>Hi Tri</i> Normq= .010 Normq-b= .005 Reslograt-b= .006	<i>Hi Tri</i> Normq= .556 Normq-b= .443 Reslograt-b= .482
24) Putative pheromone receptor (Go-VN3)	AF016180	<i>Hi Myc</i> Normq= .031 Normq-b= .025 Reslograt= .009 Reslograt-b= .004 <i>Lo Myc</i> Reslograt= .023 Reslograt-b= .009	<i>Hi Myc</i> Normq= .468 Normq-b= .386 Reslograt= .476 Reslograt-b= .342 <i>Lo Myc</i> Reslograt= .530 Reslograt-b= .383
25) Paired-like homeodomain transcription factor 3 (Pitx3)	NM_019247	<i>Hi Tri</i> Normq= .045 Reslograt= .003 Reslograt-b= .003	<i>Hi Tri</i> Normq= .656 Reslograt= .423 Reslograt-b= .364
26) Fibronectin 1 (Fn1) (alias FIBNEC)	NM_019143	<i>Hi Myc</i> Normq= .004 Normq-b= .044 <i>Hi Tri</i> Normq= .010 <i>Lo Tri</i> Normq= .016 Reslograt= .018	<i>Hi Myc</i> Normq= 2.118 Normq-b= 2.082 <i>Hi Tri</i> Normq= 1.902 <i>Lo Tri</i> Normq= 1.821 Reslograt= 1.864
27) Suppression of tumorigenicity 13 (colon carcinoma) Hsp-70-interacting protein (alias St13)	NM_031122	<i>Hi Tri</i> Normq= .044 Normq-b= .050 Reslograt= .002 Reslograt-b= .005	<i>Hi Tri</i> Normq= .560 Normq-b= .506 Reslograt= .341 Reslograt-b= .240
28) Myeloid/lymphoid or mixed-lineage leukemia (trithorax (drosophila) homolog); translocated to, 3 (aliases Mllt3, Af9, Af-9)	AJ006295	<i>Hi Myc</i> Normq= .007 Normq-b= .013	<i>Hi Myc</i> Normq= 1.720 Normq-b= 1.767

Table 11 continued: Genes from microarray data that show significant ($p \leq 0.05$) gene expression change in blood. Fold change values of <1 are down regulated, where as fold change values of >1 are up regulated. Normq is quantile normalization. Normq-b is quantile normalization minus background. Reslograt is loess normalization. Reslograt is loess normalization minus background.

Gene	Genebank accession #	P-Value	Fold change
29) Ribosomal protein S11 (Rps11)	NM_031110	<i>Hi Tri</i> Normq= .007 Reslograt= .009 Reslograt-b= .027	<i>Hi Tri</i> Normq= 2.138 Reslograt= 2.738 Reslograt-b= 2.602
30) Variable Coding sequence A2 (Vcsa2) (alias VCS- α 2)	X77817	<i>Hi Myc</i> Reslograt= .024 Reslograt-b= .038 <i>Lo Myc</i> Reslograt= .022 <i>Lo Tri</i> Normq-b= .022 Reslograt= .002 Reslograt-b= .004	<i>Hi Myc</i> Reslograt= 1.497 Reslograt-b= 1.681 <i>Lo Myc</i> Reslograt= 1.509 <i>Lo Tri</i> Normq-b= 1.846. Reslograt= 1.828 Reslograt-b= 2.117
31) Beclin1 (coiled-coil, myosin-like Bcl2-interactig protein) (Becn1)	AY033824	<i>Hi Myc</i> Normq-b= .029 <i>Hi Tri</i> Normq-b= .039	<i>Hi Myc</i> Normq-b= .560 <i>Hi Tri</i> Normq-b= .582
32) Arachidonic acid epoxygenase	NM_031839	<i>Hi Tri</i> Normq= .031 Normq-b= .001 Reslograt= .001 Reslograt-b= .001 <i>Lo Myc</i> Normq-b= .019	<i>Hi Tri</i> Normq= .609 Normq-b= .288 Reslograt= .353 Reslograt-b= .262 <i>Lo Myc</i> Normq-b= .562
33) Galanin (Gal) (alias Galn)	J03624	<i>Hi Myc</i> Normq-b= .045 Reslograt-b= .036 <i>Lo Myc</i> Normq= .003 Normq-b= .002 Reslograt-b= .016 <i>Lo Tri</i> Normq= .011 Normq-b= .007 Reslograt-b= .005	<i>Hi Myc</i> Normq-b= .570 Reslograt-b= .617 <i>Lo Myc</i> Normq= .466 Normq-b= .393 Reslograt-b= .567 <i>Lo Tri</i> Normq= .536 Normq-b= .457 Reslograt-b= .504
34) Potassium voltage-gated channel, subfamily H (eag-related), member 1 (Kcnh1)	NM_031742	<i>Lo Myc</i> Normq-b= .031	<i>Lo Myc</i> Normq-b= .568
35) Pyruvate dehydrogenase E1a alpha subunit (alias Pdha1)	U44125	<i>Lo Myc</i> Reslograt= .045 <i>Lo Tri</i> Reslograt= .049	<i>Lo Myc</i> Reslograt= 1.642 <i>Lo Tri</i> Reslograt= 1.624
36) Chimerin 1 (Chn1)	NM_032083	<i>Hi Tri</i> Normq-b= .041 Reslograt= .008 Reslograt-b= .007	<i>Hi Tri</i> Normq-b= .379 Reslograt= .283 Reslograt-b= .214
37) Matrin 3 (Matr3)	NM_019149	<i>Hi Myc</i> Normq= .003 Normq-b= .005	<i>Hi Myc</i> Normq= 4.657 Normq-b= 5.598

Table 11 continued: Genes from microarray data that show significant ($p \leq 0.05$) gene expression change in blood. Fold change values of <1 are down regulated, where as fold change values of >1 are up regulated. Normq is quantile normalization. Normq-b is quantile normalization minus background. Reslograt is loess normalization. Reslograt is loess normalization minus background.

Gene	Genebank accession #	P-Value	Fold change
38) N-acetyltransferase-2 (alias Nat2)	U01348	<i>Hi Myc</i> Normq= .001 Normq-b= .005 Reslograt= .028 Reslograt-b= .044 <i>Lo Myc</i> Reslograt= .046	<i>Hi Myc</i> Normq= 2.533 Normq-b= 2.541 Reslograt= 2.158 Reslograt-b= 2.258 <i>Lo Myc</i> Reslograt= 1.994
39) Phosphotriesterase-related protein (Pter) (alias Rpr1, Rpr-1)	NM_022224	<i>Hi Tri</i> Normq= .035 <i>Lo Myc</i> Reslograt= .029 Reslograt-b= .017	<i>Hi Tri</i> Normq= 1.964 <i>Lo Myc</i> Reslograt= 1.627 Reslograt-b= 1.807

Table 12: Genes from microarray data that show significant ($p \leq 0.05$) gene expression change in blood and in liver and testis target tissues. Fold change values of <1 are down regulated, where as fold change values of >1 are up regulated. Normq is quantile normalization. Normq-b is quantile normalization minus background. Loess-b is loess minus background.

Gene	Genebank accession #	Tissues exhibiting gene expression changes	P-Value	Fold change
1) Vacuolar proton-ATPase subunit M9.2 (aliases Atp6k, Atp6vOe)	AB037248	Blood and liver	Blood <i>Lo Tri</i> Normq= .022 Normq-b= .028 Liver <i>High Tri</i> Loess= .0406	Blood <i>Lo Tri</i> Normq= .601 Normq-b= .610 Liver <i>High Tri</i> Loess= 1.553
2) Chemokine (C-X3-C motif) ligand 1 (3x3c11) (aliases Cx3c, Scyd1)	AF030358	Blood and liver	Blood <i>Hi Myc</i> Loess= .003 Loess-b= .014 Liver <i>Hi Myc</i> Loess= .039 Loess+range= .014 <i>Hi Tri</i> Loess= .0075 Loess+range= .0027	Blood <i>Hi Myc</i> Loess= 5.386 Loess-b= 5.590 Liver <i>Hi Myc</i> Loess= 1.485 Loess+range= 1.520 <i>Hi Tri</i> Loess= 1.717 Loess+range= 1.725
3) Ornithine aminotransferase (alias Oat)	NM_022521	Blood and liver	Blood <i>Hi Myc</i> Loess-b= .020 <i>Hi Tri</i> Loess= .019 Loess-b= .004 <i>Lo Myc</i> Loess-b= .012 Liver <i>Hi Tri</i> Loess= .049 Loess+range= .042	Blood <i>Hi Myc</i> Loess-b= .348 <i>Hi Tri</i> Loess= .313 Loess-b= .260 <i>Lo Myc</i> Loess-b= .312 Liver <i>Hi Tri</i> Loess= .626 Loess+range= .630
4) Alcohol dehydrogenase I (aliases Adh, Adh1)	M15327	Blood and testis	Blood <i>Lo Tri</i> Loess-b= .021 Testis <i>Hi Myc</i> Loess= .013 Loess+range= .022	Blood <i>Lo Tri</i> Loess-b= .538 Testis <i>Hi Myc</i> Loess= 1.744 Loess+range= 1.611

Table 12 continued: Genes from microarray data that show significant (p<0.05) gene expression change in blood and in liver and testis target tissues. Fold change values of <1 are down regulated, where as fold change values of >1 are up regulated. Normq is quantile normalization. Normq-b is quantile normalization minus background. Loess-b is Loess minus background.

Gene	Genebank accession #	Tissues exhibiting gene expression changes	P-Value	Fold change
5) Retinol-binding protein 2, cellular (rbp2)	NM_012640	Blood and testis	Blood <i>Hi Myc</i> Normq= .003 <i>Hi Tri</i> Normq= .007 <i>Lo Myc</i> Normq= .043 Testis <i>Hi Myc</i> Loess= .013 Loess+range= .004 <i>Hi Tri</i> Loess+range= .047	Blood <i>Hi Myc</i> Normq= .486 <i>Hi Tri</i> Normq= .521 <i>Lo Myc</i> Normq= .626 Testis <i>Hi Myc</i> Loess= .803 Loess+range= .784 <i>Hi Tri</i> Loess+range= .857
6) Group-specific component (Gc)	NM_012564	Blood and liver	Blood <i>Hi Tri</i> Loess-b= .043 Liver <i>Hi Myc</i> Loess= .029 Loess+range= .026 <i>Hi Tri</i> Loess= .040 Loess+range= .032	Blood <i>Hi Tri</i> Loess-b= .567 Liver <i>Hi Myc</i> Loess= 1.569 Loess+range= 1.556 <i>Hi Tri</i> Loess= 1.519 Loess+range= 1.526
7) H2a histone family, member Z (H2afz)	NM_022674	Blood and testis	Blood <i>Hi Myc</i> Normq= .013 Normq-b= .029 <i>Hi Tri</i> Loess= .035 <i>Lo Myc</i> Loess= .001 Loess-b= .023 Testis <i>Hi Tri</i> Loess= .020 Loess+range= .027	Blood <i>Hi Myc</i> Normq= 1.683 Normq-b= 1.725 <i>Hi Tri</i> Loess= 1.450 <i>Lo Myc</i> Loess= 1.619 Loess-b= 1.499 Testis <i>Hi Tri</i> Loess= .761 Loess+range= .750

Table 12 continued: Genes from microarray data that show significant ($p \leq 0.05$) gene expression change in blood and in liver and testis target tissues. Fold change values of <1 are down regulated, where as fold change values of >1 are up regulated. Normq is quantile normalization. Normq-b is quantile normalization minus background. Loess-b is normalization minus background.

Gene	Genebank accession #	Tissues exhibiting gene expression changes	P-Value	Fold change
8) MAD homolog 2 (Madh2) (alias Smad2)	NM_019191	Blood, testis and liver	Blood <i>Hi Myc</i> Loess= .038 <i>Hi Tri</i> Loess= .048 <i>Lo Tri</i> Loess= .040 Loess-b= .045 Testis <i>Hi Myc</i> Loess= .040 Loess+range= .041 Liver <i>Hi Tri</i> Loess= .050 Loess+range= .028	Blood <i>Hi Myc</i> Loess= 2.329 <i>Hi Tri</i> Loess= 2.222 <i>Lo Tri</i> Loess= 2.308 Loess-b= 2.384 Testis <i>Hi Myc</i> Loess= 1.281 Loess+range= 1.173 Liver <i>Hi Tri</i> Loess= .714 Loess+range= .699
9) Serine protease gene	L38482	Blood and liver	Blood <i>Hi Tri</i> Loess= .003 <i>Lo Myc</i> Loess= .003 Loess-b= .028 <i>Lo Tri</i> Loess= .027 Liver <i>Hi Myc</i> Loess= .026	Blood <i>Hi Tri</i> Loess= 1.989 <i>Lo Myc</i> Loess= 1.991 Loess-b= 1.620 <i>Lo Tri</i> Loess= 1.617 Liver <i>Hi Myc</i> Loess= 1.591

Table 13: Cytochrome P450 expression in blood, liver and testis according to microarray data following conazole exposure.

Gene	GB Accession #	Present on 4K Microarray	Present in Blood Microarray Data	Present in Testis Microarray Data	Present in Liver Microarray Data
CYP19	NM_017085	yes	no	yes	no
CYP17	NM_012753	yes	no	yes	yes
CYP11A1	NM_017286	yes	no	yes	no
CYP11B1	NM_012537	yes	no	yes	no
CYP21	NM_057101	yes	no	yes	yes
CYP51	NM_012941	yes	no	no	no
CYP4B1	NM_016999	yes	no	no	no
CYP2E1	NM_031543	yes	no	yes	no
CYP2F1	NM_019303	yes	no	no	yes
CYP1B1	NM_012940	yes	no	yes	no
CYP1A1	X00469	yes	no	no	no
CYP2A2	NM_012693	yes	yes	no	yes
CYP49	X53477	yes	yes	no	no
CYP2B19	NM_017156	yes	yes	yes	no
CYP2C39	NM_017158	yes	yes	yes	no
CYP P450-like protein	AF311886	yes	yes	no	no

Table 14: Genes selected for qRT-PCR. Selection was based on gene change common in blood and liver, blood and testis, or blood, liver and testis. \uparrow represents up-regulation. \downarrow represents down-regulation. β -actin was also assayed to serve as a control.

Gene	Gene Expression Change based on Microarray Data	Dose Groups with gene expression change in blood
Alcohol Dehydrogenase1	\downarrow	Lo Tri
Chemokine (C-X3-C motif) ligand 1	\uparrow	Hi Myc
Vacuolar Proton ATPase Subunit M9.2	\downarrow	Lo Tri
Retinol-Binding Protein 2, Cellular	\downarrow	Lo Myc, Hi Myc, & Hi Tri
H2A histone family, member Z	\uparrow	Hi Myc, Hi Tri, & Lo Myc
MAD homolog 2	\uparrow	Hi Myc, Hi Tri, & Lo Tri
Ornithine aminotransferase	\downarrow	Hi Myc, Hi Tri, & Lo Myc
Thioredoxin-Like 2	\uparrow	Hi Tri

Table 15: qRT-PCR results. Three of the eight genes selected for qRT-PCR yielded significant differences when compared to control and these changes correlated with the Blood microarray results. NC= no change.

Gene	Dose Group	Blood qRT-PCR		Blood Microarray Data		Liver & Testis Microarray data			
						Liver		Testis	
		p-value	fold change	p-value	fold change	p-value	fold change	p-value	fold change
Alcohol Dehydrogenase 1	Hi Myc & Lo Tri	NC	NC	.021	↓.538 (Lo Tri)	NC	NC	.013	↑ 1.744 (Hi Myc)
Vacuolar Proton ATPase subunit M9.2	Lo & Hi Tri	NC	NC	.022	↓.601 (Lo Tri)	.0406	↑ 1.553 (Hi Tri)	NC	NC
Chemokine (C-X3-C motif) ligand 1	Hi Myc	0.05	↑ 3.34	0.003	↑ 5.386	0.039	↑ 1.485	NC	NC
Group Specific Component	Hi Myc & Hi Tri	NC	NC	.043	↓.567 (Hi Tri)	.029, .040 (Hi Myc & Hi Tri)	↑ 1.569, 1.519 (Hi Myc & Hi Tri)	NC	NC
Retinol Binding Protein 2	Hi Myc, Hi Tri & Lo Myc	NC	NC	.003, .007, .043, (Hi Myc, Hi Tri & Lo Myc)	↓.486, .521, .626 (Hi Myc, Hi Tri & Lo Myc)	NC	NC	.013, .047 (Hi Myc & Hi Tri)	↓.803, .857 (Hi Myc & Hi Tri)
H2A histone family, member Z	Hi Tri	0.03	↑ 1.59 (Hi Tri)	0.035	↑ 1.450	NC	NC	0.02	↓.761
MAD homolog 2	Hi Myc, Lo Tri & Hi Tri	NC	NC	.038, .048, .040 (Hi Myc, Lo Tri & Hi Tri)	↑ 2.329, 2.222, 2.308 (Hi Myc, Lo Tri & Hi Tri)	.050 (Hi Tri)	↓.714 (Hi Tri)	.040 (Hi Myc)	↑ 1.281 (Hi Myc)
Ornithine Aminotransferase	Lo Myc, Hi Myc & Hi Tri	NC	NC	.020, .019, .012 (Lo Myc, Hi Myc & Hi Tri)	↓.348, .313, .312 (Lo Myc, Hi Myc & Hi Tri)	.049	↓.626 (Hi Tri)	NC	NC
Thioredoxin-like 2	Lo & Hi Tri	0.03	↑ 2.00 (Lo Tri)	0.04	↑ 2.51 (Hi Tri)	NC	NC	NC	NC

Table 16: Ten possible myclobutanil blood biomarkers of conazole exposure identified in microarray data. * Represents genes selected for qRT-PCR and genes that may be useful in STA.

Gene	GB Accession#	Entrez Gene ID#
Saccharomyces cerevisiae Nip7p homolog (alias pEachy)	AF158186	192180
Tropomyosin 1 alpha	M34136	24851
C-terminal binding protein 2	AF222712	81717
Rattus norvegicus putative pheromone receptor (GO-VN3)	AF016180	286983
Ornithine aminotransferase*	NM_022521	64313
Retinol-binding protein 2, cellular*	NM_012640	24710
H2A histone family, member Z*	NM_022674	58940
Variable coding sequence A2	X77817	289526
Galanin	J03624	29141
N-acetyltransferase-2	U01348	116632

Table 17: Six possible triadimefon blood biomarkers of conazole exposure identified in microarray data. * Represents genes selected for qRT-PCR and genes that may be useful in STA.

Gene	GB Accession#	Entrez Gene ID#
Macrophage inflammatory protein-1 alpha receptor	NM_020542	57301
Wingless type MMTV integration site family member 2B	AF204873	116466
Protein kinase, AMP-activated, gamma	NM_013010	25520
Fibronectin 1	NM_019143	25661
MAD homolog 2 (drosophila)*	NM_019191	29357
Rattus norvegicus serine protease	L38482	

Table 18: Twenty-one possible conazole blood biomarkers of exposure identified in microarray data. * Represents genes selected for qRT-PCR and genes that may be useful in STA.

Gene	GB Accession #	Entrez Gene ID#
Saccharomyces cerevisiae Nip7p homolog (alias pEachy)	AF158186	192180
Tropomyosin 1 alpha	M34136	24851
Guanine nucleotide binding protein alpha transducing 3	X65747	286924
Ornithine aminotransferase*	NM_022521	64313
Retinol-binding protein 2, cellular*	NM_012640	24710
H2A histone family, member Z*		
Variable coding sequence A2	X77817	289526
Serine protease	L38482	
Arachidonic acid epoxygenase	NM_031839	83790
Galanin	J03624	29141
Pyruvate dehydrogenase E1a alpha subunit	U44125	117098
Phosphotriesterase-related protein	NM_022224	63852
Macrophage inflammatory protein-1 alpha receptor	NM020542	57301
Histone 2a	NM_021840	64646
Melanocortin 5 receptor	NM_013182	25726
Wingless type MMTV integration site family member 2B	AF204873	116466
Syntenin	NM_031986	83841
Pituitary tumor-transforming 1	NM_022391	64193
Fibronectin 1	AF15818	192180
MAD homolog 2 (drosophila)	NM_019191	29357
Beclin 1 coiled-coil, myosin-like Bcl2 interacting protein	AY033824	114558

REFERENCES

- 1) Agne, B., N. M. Meindl, K. Niederhoff, H. Einwachter, P. Rehling, A. Sickmann, H. E. Meyer, W. Girzalsky and W. H. Kunau. Pex8p: an intraperoxisomal organizer of the peroxisomal import machinery. *Molecular Cell*. 11.3 (2003): 635-646.
- 2) Alory, C. and W. E. Balch. Organization of the Rab-GDI/CHM Superfamily: The Functional Basis for Choroideremia Disease. *Traffic*. 2.8 (2001): 532-543.
- 3) Amundson, Sally A., K. T. Do, S. Shahab, M. Bittner, P. Meltzer, J. Trent, and A. J. Fornace Jr. Identification of Potential mRNA Biomarkers in Peripheral Blood Lymphocytes for Human Exposure to Ionizing Radiation. *Radiation Research*. 154 (2000): 342-346.
- 4) Ansehn, S. and L. Nilsson. Direct Membrane-Damaging Effect of Ketoconazole and Tioconazole on *Candida albicans* Demonstrated by Bioluminescent Assay of ATP. *Antimicrobial Agents and Chemotherapy*. 26.1 (1984): 22-25.
- 5) Aoyama, Y., M. Noshiro, O. Gotoh, S. Imaoka, Y. Funae, N. Kurosawa, T. Horiuchi, Y. Yoshida. Sterol 14 demethylase P450 (P45014DM*) is one of the most ancient and conserved P450 species. *Journal of Biochemistry*. 119.5 (1996): 926-933.
- 6) Ariadne Genomics. Pathway Assist pathway analysis software. 2004.
- 7) Barrett-Bee, K., J. Lees, P. Pinder, J. Campbell, and L. Newbould. Biochemical studies with a model antifungal agent, ICI 195, 739. *Annals of the New York Academy of Science*. 544 (1988): 231-244.
- 8) Baron, J. M., G. Zwadlo-Klarwasser, F. Jugert, W. Hamann, A. Rubben, H. Mukhtar, and H F. Merk. Cytochrome P450 1B1: A Major P450 Isoenzyme in Human Blood Monocytes and Macrophage Subsets. *Biochemical Pharmacology*. 56 (1998): 1105-1110.
- 9) Berstein, L. M., A. A. Larionov, T. E. Poroshina, T. S. Zimarina, and E. E. Leenman. Aromatase (CYP19) expression in tumor-infiltrating lymphocytes and blood mononuclears. *Journal of Cancer Research and Clinical Oncology*. 128.3 (Mar 2002): 173-6.
- 10) Byskov, A. G., C. Y. Anderson, L. Nordholm, H. Thogersen, X. Guoliang, O. Wassman, J. V. A. E. Guddal, and T. Roed. Chemical structure of sterols that activate oocyte meiosis. *Nature*. 374 (1995): 559-562.

- 11) Carcillo, J.A., R. A. Parise, A. Adedoyin, R. Frye, R. A. Branch, and M. Romkes. CYP2D6 mRNA expression in circulating peripheral blood mononuclear cells correlates with *in vivo* debrisoquine hydroxylase activity in extensive metabolizers. *Research Communications in Molecular Pathology and Pharmacology*. 91 (1996): 149-159.
- 12) Cheung, P. C. F., I. P. Salt, S. P. Davies, D. G. Hardie, and D. Carling. Characterization of AMP-activated protein kinase γ -subunit isoforms and their role in AMP binding. *Journal of Biochemistry*. 346 (2000): 659-669.
- 13) Costello, L. C., Y. Liu, J. Zou, and R. B. Franklin. The pyruvate dehydrogenase E1 alpha gene is testosterone and prolactin regulated in prostate epithelial cells. *Endocrine Research*. 26.1 (2000): 23-39.
- 14) Davies, J. A., V. L. Buchman, O. Krylova, and N. N. Ninkina. Molecular cloning and expression pattern of rpr-1, a resiniferatoxin-binding, phosphotriesterase-related protein, expressed in rat kidney tubules. *FEBS Letters*. 410.2-3 (1997): 378-82.
- 15) Dear, T.N., K. Campbell and T.H. Rabbitts. Molecular Cloning of Putative Odorant-Binding and Odorant-Metabolizing Proteins. *Biochemistry*. 30 (1991): 10376-10382.
- 16) Debeljak, N., M. Fink, and D. Rozman. Many facets of mammalian lanosterol 14 α -demethylase from the evolutionarily conserved cytochrome P450 family CYP51. *Archives of Biochemistry and Biophysics*. 409 (2003): 159-171.
- 17) Demmer, L. A., E. H. Birkenmeier, D. A. Sweetser, M. S. Levin, S. Zollman, R. S. Sparkes, T. Mohandas, A. J. Lusic and J. L. Gordon. The cellular retinol binding protein II gene: sequence analysis of the rat gene, chromosomal localization in mice and humans, and documentation of its close linkage to the cellular retinol binding protein gene. *Journal of Biological Chemistry*. 262 (1987): 2458-2467.
- 18) EPA. *Identifying and Validating Biologic Indicators of Susceptibility and Sensitivity among Children to Assess Potential Risk of Adverse Health Outcomes Associated with Environmental Exposures*. 2001.
- 19) EPA. *Human Health Research Implementation Plan*.. 2003.
- 20) FAO/WHO (Food and Agriculture Organization/ World Health Organization). Triadimefon. In: Pesticide Residues in Food-1981 evaluations. *FAO Plant Production and Protection Paper 42 (1982)*. Rome: FAO, 512-547.

- 21) FAO/WHO (Food and Agriculture Organization/ World Health Organization). Triadimefon. In: Pesticide Residues in Food-1985 evaluations. Part II- Toxicology. *FAO Plant Production and Protection Paper 72/2. (1986). Rome: FAO, 199-202.*
- 22) FAO/WHO (Food and Agriculture Organization/ World Health Organization). Myclobutanil. In: Pesticide Residues in Food-1992 Evaluations. Part II-Toxicology. *WHO/PCS/93.34. Geneva: WHO (1993a): 267-289.*
- 23) Fong, A. M., L. A. Robinson, D. A. Steeber, T. F. Tedder, O. Yoshie, T. Imai and D. D. Patel. Fractalkine and CX3CR1 mediate a novel mechanism of leukocyte capture, firm adhesion, and activation under physiologic flow. *Journal of Experimental Medicine.* 188.8 (1998): 1413-1419.
- 24) Fromtling, R. A. Overview of medically important antifungal azole derivatives. *Clinical Microbiology Reviews.* 1.2 (1988): 187-217.
- 25) Herrada, G., and C. Dulac. A novel family of putative pheromone receptors in mammals with a topographically organized and sexually dimorphic distribution. *Cell.* 90 (1997): 763.
- 26) Ganter, B., S. Tugendreich, C. I. Pearson, E. Ayanoglu, S. Baumhueter, K. A. Bostian, L. Brady, L. J. Browne, J. T. Calvin, G. Day, N. Breckenridge, S. Dunlea, B. P. Eynon, L. M. Furness, J. Ferng, M. R. Fielden, S. Y. Fujimoto, L. Gong, C. Hu, R. Idury, M. S.B. Judo, K. L. Kolaja, M. D. Lee, C. McSorley, J. M. Minor, R. V. Nair, G. Natsoulis, P. Nguyen, S. M. Nicholson, H. Pham, A. H. Roter, D. Sun, S. Tan, S. Thode, A. M. Tolley, A. Vladimirova, J. Yang, Z. Zhou, and K. Jarnagin. Development of a Large- Scale Chemogenomics Database to Improve Drug Candidate Selection and to Understand Mechanisms of Chemical Toxicity and Action. *In Press.* 2004.
- 27) Garcia G. E., Y. Xia, S. Chen, Y. Wang, R. D. Ye, J. K. Harrison, K. B. Bacon, H. G. Zerwes, L. Feng. NF-kappa B-dependent fractalkine induction in rat aortic endothelial cells stimulated by IL-1beta, TNF-alpha, and LPS. *Journal of Leukocyte Biology.* 67.4 (2000): 577-584.
- 28) Georgopapadakou, N. H. and T. J. Walsh. Antifungal Agents: Chemotherapeutic Targets and Immunologic Strategies. *Antimicrobial Agents and Chemotherapy.* 40.2 (Feb 1996): 279-291.

- 29) Ghannoum, M.A. and L. B. Rice. Antifungal Agents: Mode of Action, Mechanisms of resistance, and Correlation of These Mechanisms with Bacterial Resistance. *Clinical Microbiology Reviews*. 12.4 (Oct 1999): 501-517.
- 30) Goda S., T. Imai, O. Yoshie, O. Yoneda, H. Inoue, Y. Nagano, T. Okazaki, H. Imai, E. T. Bloom, N. Domae, and H. Umehara. CX3C-chemokine, fractalkine-enhanced adhesion of THP-1 cells to endothelial cells through integrin-dependent and -independent mechanisms. *Journal of Immunology*. 164.8 (2000): 4313-4320.
- 31) Golub, T. R., D. K. Slonim, P. Tamayo, C. Huard, M. Gaasenbeek, J. P. Mesirov, H. Coller, M. L. Loh, J. R. Downing, M. A. Caligiuri, C. D. Bloomfield, and E. S. Lander. Molecular classification of cancer: class discovery and class prediction by gene expression monitoring. *Science*. 286 (1999): 531- 537.
- 32) Griffon, N., V. Mignon, P. Facchinetti, J. Diaz, J. C. Schwartz, and P. Sokoloff. Molecular cloning and characterization of the rat fifth melanocortin receptor. *Biochemical and Biophysical Research Communications*. 200 (1994): 1007-1014.
- 33) Girzalsky, W., P. Rehling, K. Stein, J. Kipper, L. Blank, W. H. Kunau, R. Erdmann. Involvement of Pex13p in Pex14p localization and peroxisomal targeting signal 2-dependent protein import into peroxisomes. *Journal of Cellular Biology*. 144.6 (1999): 1151-1162.
- 34) Gross, M., T. Kruisselbrink, K. Anderson, N. Lang, P. McGovern, R. Delongchamp, and F. Kadlubar. Distribution and accordance of N-acetyltransferase genotype and phenotype in an American population. *Cancer Epidemiology, Biomarkers and Prevention*. 8 (1999): 683-692.
- 35) Gupta, R. P., B. W. Hollis, S. B. Patel, K. S. Patrick and N. H. Bell. CYP3A4 is a human microsomal vitamin D 25-hydroxylase. *Journal of Bone Mineral Research*. 19.4 (2004): 680-688.
- 36) Hanger, D. P., S. Jevons and J. T. B. Shaw. Fluconazole and Testosterone: in vivo and in vitro studies. *Antimicrobial Agents and Chemotherapy*. 32 (1988): 646-648.
- 37) Hanioka, N., K. Korzekwa and F. J. Gonzalez. Sequence requirements for cytochrome P450IIA1 and P450 IIA2 catalytic activity: evidence for both specific and non-specific substrate binding interactions through use of chimeric cDNAs and cDNA expression. *Protein Engineering*. 3 (1990): 571-575.

- 38) Herzfeld, A., and W. E. Knox. The Properties, Developmental Formation, and Estrogen Induction of Ornithine Aminotransferase in Rat Tissues. *The Journal of Biological Chemistry*. 243.12 (1968): 3327-3332.
- 39) Hunter, B. Scholey, D. & Heywood, R., 1982a. Potential tumorigenic and toxic effects in prolonged dietary administration to rats (final report). Unpublished report no.: CBG 193/8284 (test no. 78/9023) from Huntingdon research centre, Huntingdon, England. Submitted to WHO by Ciba-Geigy Ltd., Basle, Switzerland.
- 40) Hunter, B., Scholey, D. & Heywood, R., 1982b. CGA 64250 long-term feeding study in mice (final report). Unpublished report no. CBG/196/81827 d.d. October 20, 1982 from Huntingdon research centre, Huntingdon, England. Submitted to WHO by Ciba-Geigy Ltd., Basle, Switzerland.
- 41) Imaizumi, T., F. Yoshida and K. Sotoh. Regulation of CX3CL1/fractalkine expression in endothelial cells. *Journal of Atherosclerosis and Thrombosis*. 11.1 (2004): 15-21.
- 42) Imaoka, S., P. J. Wedlund, H. Ogawa, S. Kimura, F.J. Gonzalez, and H. Y. Kim. Identification of CYP2C23 expressed in rat kidney as an arachidonic acid epoxygenase. *Journal of Pharmacology and Experimental Therapeutics*. 267.2 (1993): 1012-1016.
- 43) Jackisch, B., H. Hausser, L. Schaefer, J. Kappler, H. W. Muller, and H. Kresse. Alternative Exon Usage of Rat Septins. *Biochemical and Biophysical Research Communications*. 275 (2000): 180-188.
- 44) Katsanis, N., E. M. Fisher. A novel C-terminal binding protein (CTBP2) is closely related to CTBP1, an adenovirus E1A-binding protein, and maps to human chromosome 21q21.3. *Genomics*. 47.2 (1998): 294-299.
- 45) Kellerman, G, M Luyten-Kellerman, and C. Shaw. Metabolism of polycyclic aromatic hydrocarbons in cultured human leukocytes under genetic control. *Humangenetik*. 20 (1973): 257-263. Submitted to WHO by Ciba-Geigy Ltd.
- 46) Kelloff, G. J., R. a. Lubet, R. Lieberman, K. Eisenhauer, V. E. Steele, J. A. Crowell, E. T. Hawk, C. W. Boone and C. C. Sigman. Aromatase inhibitors as potential cancer chemopreventives. *Cancer Epidemiology, Biomarkers and Prevention*. 7.1 (1998): 65-78.
- 47) Kelly, S. L., D. C. Lamb, M. Cannieux, D. Greetham, C. J. Jackson, T. Marczylo, C. Ugochukwu, and D. E. Kelly. An old activity in the cytochrome P450 superfamily (CYP51) and a new story of drugs and resistance. *Biochemical Society Transactions*. 29.2 (2001): 122-128.

- 48) Krovat, Barbara C., Julia H. Tracy, and Curtis J. Omiecinski. Fingerprinting of Cytochrome P450 and Microsomal Epoxide Hydrolase Gene Expression in Human Blood Cells. *Toxicological Sciences*. 55 (2000): 352-360.
- 49) Kuramochi, S., T. Moriguchi, K. Kuida, J. Endo, K. Semba, E. Nishida and H. Karasuyama. LOK Is a Novel Mouse STE20-like Protein Kinase That Is Expressed Predominantly in Lymphocytes. *The Journal of Biological Chemistry*. 272.36 (1997): 22679-22684.
- 50) Lamb, D.C., D.E. Kelly, N.J. Manning, and S. L. Kelly. A sterol biosynthetic pathway in Mycobacterium. *FEBS Letters* 437 (1998):142-144.
- 51) Lees-Miller, J. P. and D. M. Helfman. The molecular basis for Tropomyosin isoform diversity. *Bioessays*. 13.9 (1991): 429-37.
- 52) Liang, X. H., L. K. Kleeman, H. H. Jiang, G. Gordon, J. E. Goldman, G. Berry, B. Herman and B. Levine. Protection against fatal Sindbis virus encephalitis by beclin, a novel Bcl-2-interacting protein. *Journal of Virology*. 72.11 (1998): 8586-8596.
- 53) Livak, K.J., and T.D. Schmittgen. Analysis of Relative Gene Expression Data Using Real-Time Quantitative PCR and the $2^{-\Delta\Delta C_T}$ Method. *Methods*. 25 (2001): 402-408.
- 54) Loser, E. KWG 0519 (proposed c.n. triadimenol): Generation study on rats. Bayer AG, Wuppertal, Germany. (1984, original; 1994, supplement).
- 55) McLaughlin, S. K., P. J. McKinnon, and R. F. Margolskee. Gustducin is a taste-cell-specific G protein closely related to the transducins. *Nature*. 357 (1992): 563-9.
- 56) Millos-Santos, A., L. Milla, N. Calvo, J. Portella, L. Rallo, J. M. Casanovas, M. Pons and J. Rodes. Anastrozole as neoadjuvant therapy for patients with hormone-dependent, locally advanced breast cancer. *Anticancer Research*. 24 (2004): 1315-1318.
- 57) Morgan, H., Smith, M., Burke, Z., Carter, D. The transactivation-competent carboxyl-terminal domain of AF-9 is expressed within a sexually dimorphic transcript in rat pituitary. *The FASEB Journal*. 14 (2000): 1109–1116.
- 58) Nakashima, E., A. Oya, Y. Kubota, N. Kanada, R. Matsushita, K. Takeda, F. Ichimura, K. Kuno, N. Mukaida, K. Hiroase, I. Nakanishi, T. Ujiie, and K. Matsushima. A candidate for cancer gene therapy: MIP-1 alpha gene transfer to an adenocarcinoma cell line reduced tumorigenicity and induced protective immunity in immunoprecipitant mice. *Pharmacology Research*. 13.12 (1996): 1896-1901.

- 59) Nelson, D. R. Cytochrome P450 and the Individuality of Species. *Archives of Biochemistry and Biophysics*. 369.1 (1999): 1-10.
- 60) Nelson, N., W. R. Harvey. Vacuolar and plasma membrane proton-adenosinetriphosphatases. *Physiological Reviews*. 79.2 (1999): 361-385.
- 61) Nesnow, S., J. Ross, G. Nelson, K. Holden, G. Erexson, A. Kligerman, and R. C. Gupta. Quantitative and Temporal Relationships Between DNA Adduct Formation in Target and Surrogate Tissues: Implications for Biomonitoring. *Environmental Health Perspectives Supplements*. 101.3 (1993): 37-42.
- 62) Omiecinski, C. J., L. Aicher, R. Holubkov, and H. Checkoway. Human peripheral lymphocytes as indicators of microsomal epoxide hydrolase activity in liver and lung. *Pharmacogenetics*. 3(1993): 150-158.
- 63) Pavlovic, J., T. Zurcher, O. Haller and P. Staeheli. Resistance to influenza virus and vesicular stomatitis virus conferred by expression of human MxA protein. *Journal of Virology*. 64.7 (1990): 3370-3375.
- 64) Polakowski, T., U. Stahl, C. Lang. Over expression of a cytosolic hydroxymethylglutaryl-CoA reductase leads to squalene accumulation in yeast. *Applied Microbiology and Biotechnology*. 49(1998): 66-71.
- 65) Qi, R. Z., Y. Ching, H. Kung, and J. H. Wang. \forall -Chimerin exists in a functional complex with the Cdk5 kinase in the brain. *FEBS Letters*. 561 (2004): 177-180.
- 66) Rangasamy, D., L. Berven, P. Ridgway and D. J. Tremethick. Pericentric heterochromatin becomes enriched with H2A.Z during early mammalian development. *The EMBO Journal*. 22.7 (2003): 1599-1607.
- 67) Rasmussen, C. A., K. Hashizume, K. E. Orwig, L. Xu and M. J. Soares. Decidual prolactin-related protein: heterologous expression and characterization. *Endocrinology*. 137.12: 5558-5566.
- 68) Raychaudhuri, S. P., W. Y. Jiang and E. M. Farber. Cellular localization of fractalkine at sites of inflammation: antigen-presenting cells in psoriasis express high levels of fractalkine. *British Journal of Dermatology*. 144.6 (2001): 1105-1113.

- 69) Reddy, V. R., S. M. Gupta, and P. K. Meherji. Expression of integrin receptors on peripheral lymphocytes: correlation with endometrial receptivity. *American Journal of Reproductive Immunology*. 46.3 (Sep 2001): 188-95.
- 70) Ren, H., K. E. Thompson, J. E. Schmid and D. J. Dix. Sperm RNA Amplification for Gene Expression Profiling by DNA Microarray Technology. SOT 42nd Annual Meeting symposium, March 9th-13th, 2003, Salt Lake City, UT, USA.
- 71) Rockett, J. C. Surrogate tissue analysis for monitoring the degree and impact of exposures in agricultural workers. *AgBiotechNet*. 4 (Nov 2002): ABN 100.
- 72) Rockett, JC, Germaine Buck and Courtney Johnson. Biomarkers for Assessing Reproductive Development and Health: Part 1- Pubertal Development. Submitted 2003.
- 73) Rockett, J. C., R. J. Kavlock, C. R. Lambright, L. G. Parks, J. E. Schmid, V. S. Wilson, C. Wood, and D. J. Dix. DNA Arrays to Monitor Gene Expression in Rat Blood and Uterus following 17 β -Estradiol Exposure: Biomonitoring Environmental Effects Using Surrogate Tissues. *Toxicological Sciences*. 69 (2002): 49-59.
- 74) Ronis, M. J., M. Ingelman-Sundberg, and T. M. Badger. Induction, Suppression and inhibition of multiple hepatic cytochrome P450 isozymes in the male rat and bobwhite quail by ergosterol biosynthesis inhibiting fungicides. *Biochemical Pharmacology*. 48.10 (1994):1953-65.
- 75) Rozman, D., and M.R. Waterman. Lanosterol 14 α -Demethylase (CYP51) and Spermatogenesis. *Drug Metabolism and Disposition*. 26.12 (1998): 1199- 1201.
- 76) Sadek, C. M., A. Jimenez, A. E. Damdimopoulos, T. Keiselbach, M. Nord, J. Gustafsson, G. Spyrou, E. C. Davis, R. Oko, F. A. van der Hoorn and A. Miranda-Vizuet. Characterization of Human Thioredoxin-like 2. *The Journal of Biological Chemistry*. 278.15 (2003): 13133-13142.
- 77) Sanderson, J.T., J. Boerma, G.W.A. Lansbergen, and M. van den Berg. Induction and Inhibition of Aromatase (CYP19) Activity by Various Classes of Pesticides in H295R Human Adrenocortical Carcinoma Cells. *Toxicology and Applied Pharmacology*. 182 (2002): 44-54.
- 78) Shimizu, N., R. Itoh, Y. Hirono, H. Otera, K. Ghaedi, K. Tateishi, S. Tamura, K. Okumoto, T. Harano, S. Mukai and Y. Fujiki. The peroxin Pex14p. cDNA cloning by functional complementation on a Chinese hamster ovary cell mutant, characterization, and functional analysis. *Journal of Biological Chemistry*. 274 (1999): 12593-604.

- 79) Song, Y. H., K. Ray, S. A. Liebhaber and N. E. Cooke. Vitamin D-binding protein gene transcription is regulated by the relative abundance of hepatocyte nuclear factors 1alpha and 1beta. *Journal of Biological Chemistry*. 273.14 (1998): 28408-28418.
- 80) Spector, A. A., X. Fang, G. D. Snyder, and N. L. Weintraub. Epoxyeicosatrienoic acids (EETs): metabolism and biochemical function. *Progress in Lipid Research*. 43.1 (2004): 55-90.
- 81) Sud, I. J., and D. S. Feingold. Heterogeneity of Action Mechanisms Among Antimycotic Imidazoles. *Antimicrobial Agents and Chemotherapy*. 20.1 (1981): 71-74.
- 82) Sun, G., S. Thai, D. B. Tully, G. R. Lambert, A. K. Goetz, D. C. Wolf, D. J. Dix and S. Nesnow. Propiconazole-Induced Cytochrome P450 Gene Expression and Enzymatic Activities in Rat and Mouse Liver. *Toxicology Letters*. In Press.
- 83) Takenoshita, S., A. Mogi, M. Nagashima, K. Yang, K. Yagi, A. Hanyu, Y. Nagamachi, K. Miyazono and K. Hagiwara. Characterization of the MADH2/SMAD2 Gene, a Human Mad Homolog Responsible for the Transforming Growth Factor- β and Activin Signal Transduction Pathway. *Genomics*. 48 (1998): 1-11.
- 84) Tang, Y., A. Lu, B. J. Aronow, and F. R. Sharp. Blood Genomic Responses Differ After Stroke, Seizures, Hypoglycemia, and Hypoxia: Blood Genomic Fingerprints of Disease. *Annals of Neurology*. 50.6 (2001): 699-707.
- 85) Tully, D. B., W. Bao, H. Ren, J. E. Schmid, A. K. Goetz, C. R. Wood, G. A. Held, C. R. Blystone, R. N. Murrell, J. C. Rockett, D. S. Best, M. G. Narotsky, L. F. Strader, S. Barone Jr., L.D. White, D. C. Wolf and D. J. Dix. Gene Expression Profiling in Testis, Brain and Liver of Rats to characterize the Toxicity of Conazole Fungicides. (In Preparation). 2004.
- 86) van der Kraan, M., R. A. H. Adan, M. L. Entwistle, W. H. Gispen, J. P. H. Burbach and J. B. Tatro. Expression of Melanocortin-5 Receptor in Secretory Epithelia Supports a Functional Role in Exocrine and Endocrine Glands. *Endocrinology* 139 (1998): 2348–2355.
- 87) Vinggaard, A. M., C. Hnida, V. Breinholt and J. C. Larsen. Screening of Selected Pesticides for Inhibition of CYP19 Aromatase Activity *In Vitro*. *Toxicology in Vitro*. 14 (2000): 227-234.
- 88) Waring, J.F., R. Ciurlionis, R. A. Jolly, M. Heindel, and R. G. Ulrich. Microarray analysis of hepatotoxins in vitro reveals a correlation between gene expression profiles and mechanisms of toxicity. *Toxicology Letters*. 120 (2001): 359-368.

- 89) White, T. C., K. A. Marr, and R. A. Bowden. Clinical, Cellular, and Molecular Factors That Contribute to Antifungal Drug Resistance. *Clinical Microbiology Reviews*. 11.2 (Apr 1998): 382-402.
- 90) Witte, S., M. Villalba, K. Bi, Y. Liu, N. Isakov and A. Altman. Inhibition of the c-Jun N-terminal Kinase/AP-1 and NF- κ B Pathways by PICOT, a Novel Protein Kinase C-interacting Protein with a Thioredoxin Homology Domain. *THE Journal of Biological Chemistry*. 275.3 (2000): 1902-1909.
- 91) Xie, G., E. Ito, K. Maruyama, C. Pietruck, M. Sharma, L. Yu, and P. Pierce Palmer. An alternatively spliced transcript of the rat nociceptin receptor ORL1 gene encodes a truncated receptor. *Molecular Brain Research*. 77.1 (2000): 1-9.
- 92) Yoneda O, T. Imai, M. Nishimura, M. Miyaji, T. Mimori, T. Okazaki, N. Domae, H. Fujimoto, Y. Minami, T. Kono , E. T. Bloom, and H. Umehara. Membrane-bound form of fractalkine induces IFN-gamma production by NK cells. *European Journal of Immunology*. 33.1 (2003): 53-58.
- 93) Yoneyama, T., J. M. Brewer, K. Hatakeyama. GTP cyclohydrolase I feedback regulatory protein is a pentamer of identical subunits. Purification, cDNA cloning, and bacterial expression. *Journal of Biological Chemistry*. 272.15 (1997): 9690-9696.
- 94) Yoshida, Y., Y. Aoyama, M. Noshiro, and O. Gotoh. Sterol 14 Demethylase P450 (CYP51) Provides a Breakthrough for the Discussion on the Evolution of Cytochrome P450 Gene Superfamily. *Biochemical and Biophysical Research Communications*. 273 (2000):799-804.
- 95) Yoshida, Y., Y. Aoyama, M. Noshiro, T. Kawamoto, T. Horiuchi, and O. Gotoh. Structural and evolutionary studies on sterol 14-demethylase P450 (CYP51), the most conserved P450 monooxygenase:II. Evolutionary analysis of protein and gene structures. *Journal of Biochemistry*. 122.6 (1997): 1122-1128.
- 96) Zarn, Jürg A., Beat J Brüscheweiler, and Josef R. Schlatter. Effects of azole fungicides on mammalian steroidogenesis by inhibiting sterol 14 α -demethylase and aromatase. *Environmental Health Perspectives*. Online. Internet 30 Oct Available <http://ehpnet1.niehs.nih.gov/docs/2003/5785/abstract.html>
- 97) Zhang, W., Y. Ramamoorthy, T. Kilicarslan, H. Nolte, R. F. Tyndale and E. M. Sellers. Inhibition of Cytochromes P450 by Antifungal Imidazole Derivatives. *Drug Metabolism and Disposition*. 30.3 (2002):314-318.

- 98) Zhou, Q., G. Talaska, M. Jaeger, V. K. Bhatanagar, R. B. Hayes, T. V. Zenzer, S. K. Kashyap, V. M. Lakshmi, R. Kashyap, M. Dosemici, F. F. Hsu, D.J.Pakh, B. Davis, N. Rothman. Benzidine-DNA adduct levels in human peripheral white blood cells significantly correlate with levels in exfoliated urothelial cells. *Mutation Research*. 393 (1997): 199-205.
- 99) Zhou, Z., C. H. Shackleton, S. Pahwa, P. C. White, and P. W. Speiser. Prominent sex steroid metabolism in human lymphocytes. *Molecular and Cellular Endocrinology*. 138.1-2 (1998): 61-9.
- 100) Zhou, Z., V. R. Agarwal, N. Dixit, P. White, and P. W. Speiser. Steroid 21-hydroxylase expression and activity in human lymphocytes. *Molecular and Cellular Endocrinology*. 127.1 (1997): 11-18.
- 101) Zimmerman, P., D. Tomatis, M. Roasa, J. Grootjans, I. Leenaerts, G. Degeest, G. Reekmans, C. Coomans and G. David. Characterization of syntenin, a syndecan-binding PDZ protein, as a component of cell adhesion sites and microfilaments. *Cell*. 12.2 (2001): 339-350.

Appendix 1: Troubleshooting aRNA amplification

During the initial attempts at aRNA amplification, it became obvious that blood RNA did not amplify as successfully as tissue RNA derived from testis and liver. The inefficiency of the amplification could have been due to the presence of hemolysis degradation products being present in the blood RNA samples. The RNeasy mini kit was used to purify the samples. After the purification, the first round of amplification yielded a much higher amount of RNA, but when the Blood RNA was run on a gel, it became obvious that several blood RNA transcripts were being copied exponentially as the RNA appeared as bands, instead of the expected smear. RNA amplification was started again, this time the In Vitro Transcription incubation time was decreased from 14 hours to 8 hours in order to provide a more diverse RNA transcript pool.

While the problems of first round amplification were eliminated, the second round amplification held its own set of problems. Second round amplification was used to incorporate amino allyl UTP into the aRNA to allow for Cy Dye labeling. The use of the amino allyl UTP greatly reduced the transcription efficiency. A decision was made to amplify each sample in duplicate for the second round of amplification to ensure there would be enough resulting aRNA for use in the microarray experiments.